Measurement of event-by-event fluctuations and chemical freeze-out conditions at LHC energies

A. Kalweit, *CERN*

Many-body QCD and light flavor hadron production

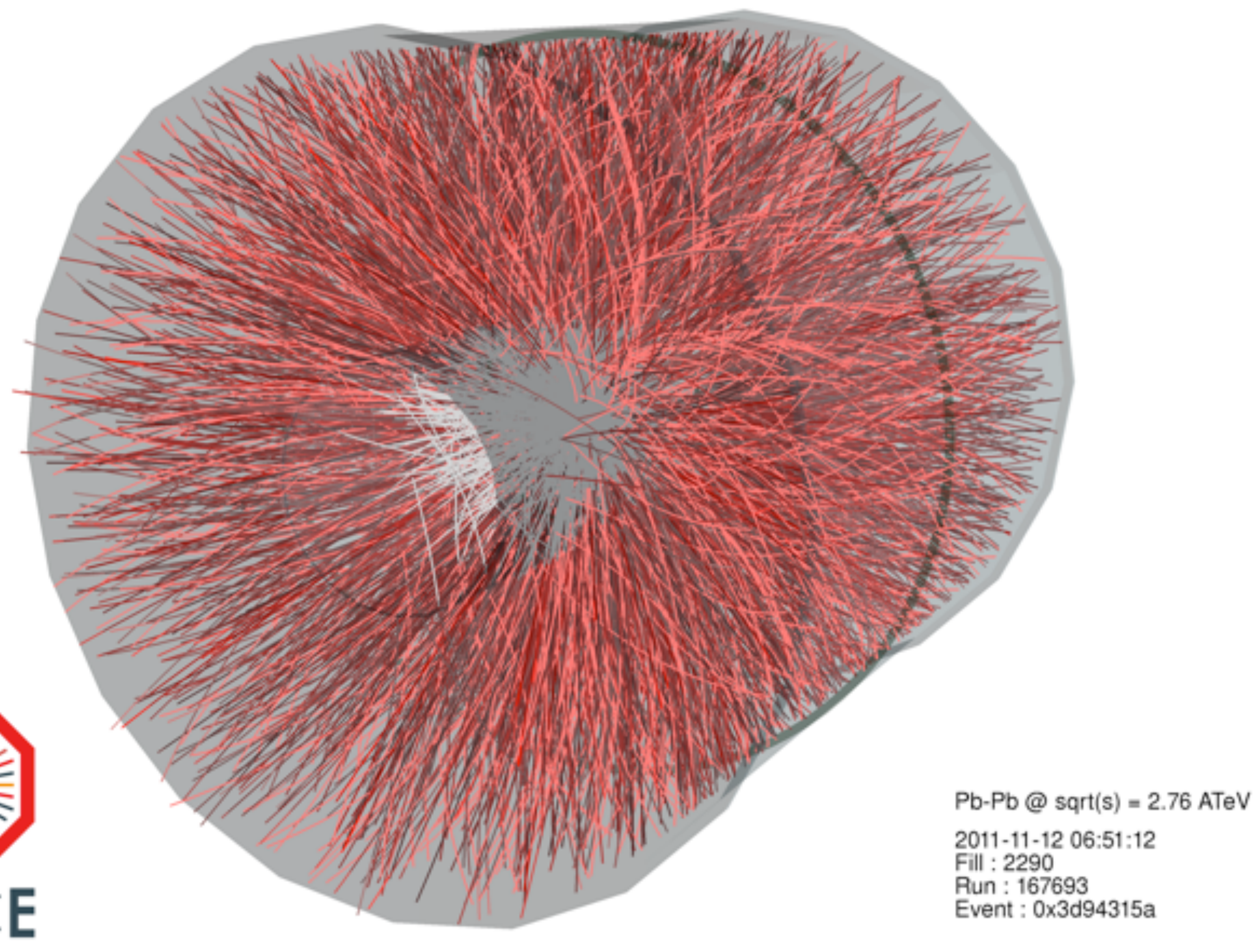

ALICE
A JOURNEY OF DISCOVERY

central (0-5%) Pb-Pb collisions (LHC): $dN_{ch}/d\eta \approx 1600$

Many-body QCD and light flavor hadron production

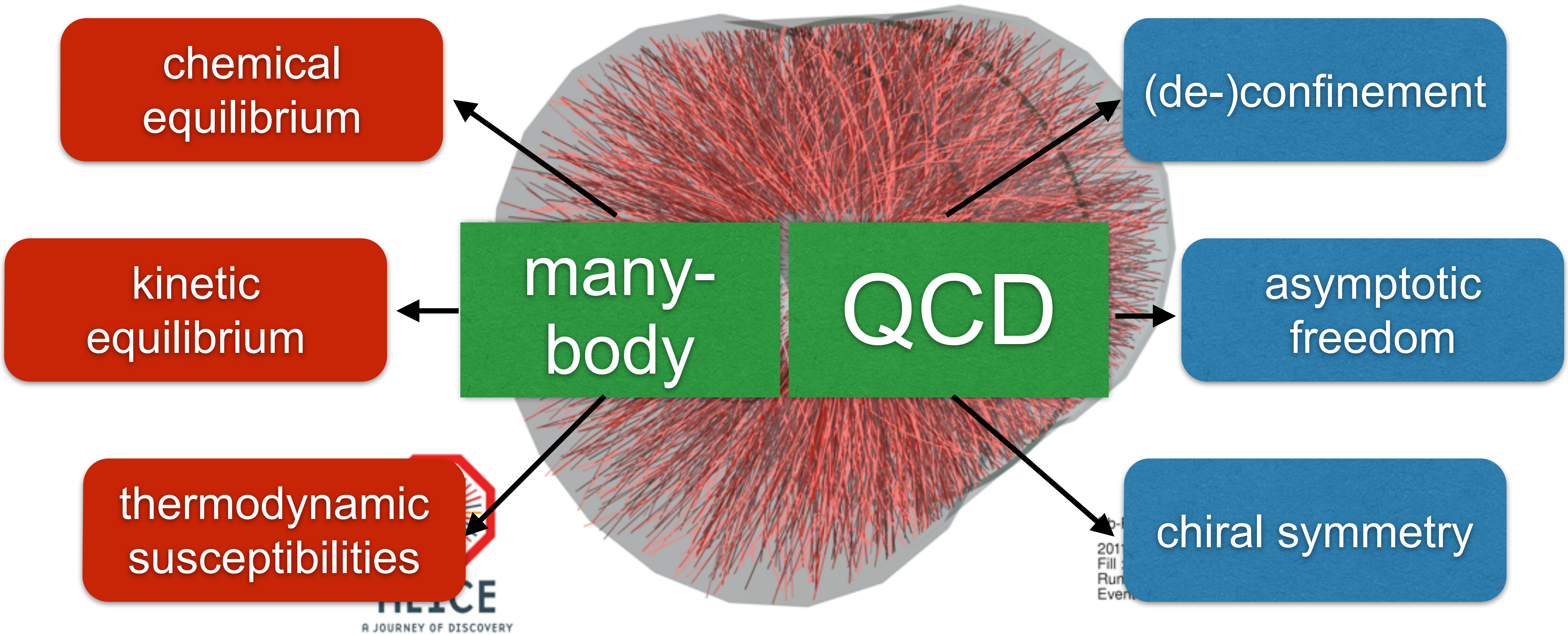

central (0-5%) Pb-Pb collisions (LHC): $dN_{ch}/d\eta \approx 1600$

Many-body QCD and light flavor hadron production

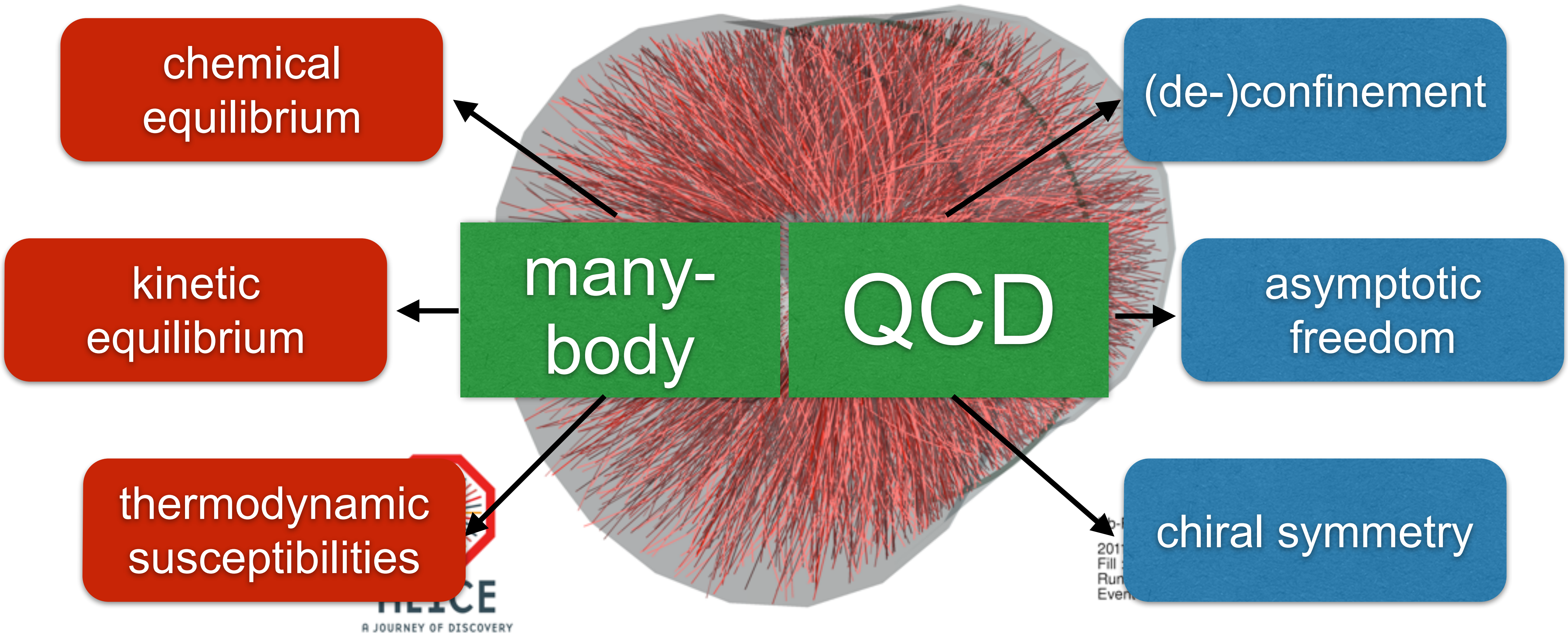

central (0-5%) Pb-Pb collisions (LHC): $dN_{ch}/d\eta \approx 1600$

Light flavor hadrons (u,d,s valence quarks) are produced in apparent chemical ($T_{chem} \approx 156$ MeV) and kinetic equilibrium ($T_{kin} \approx 100$ MeV).

Many-body QCD and light flavor hadron production

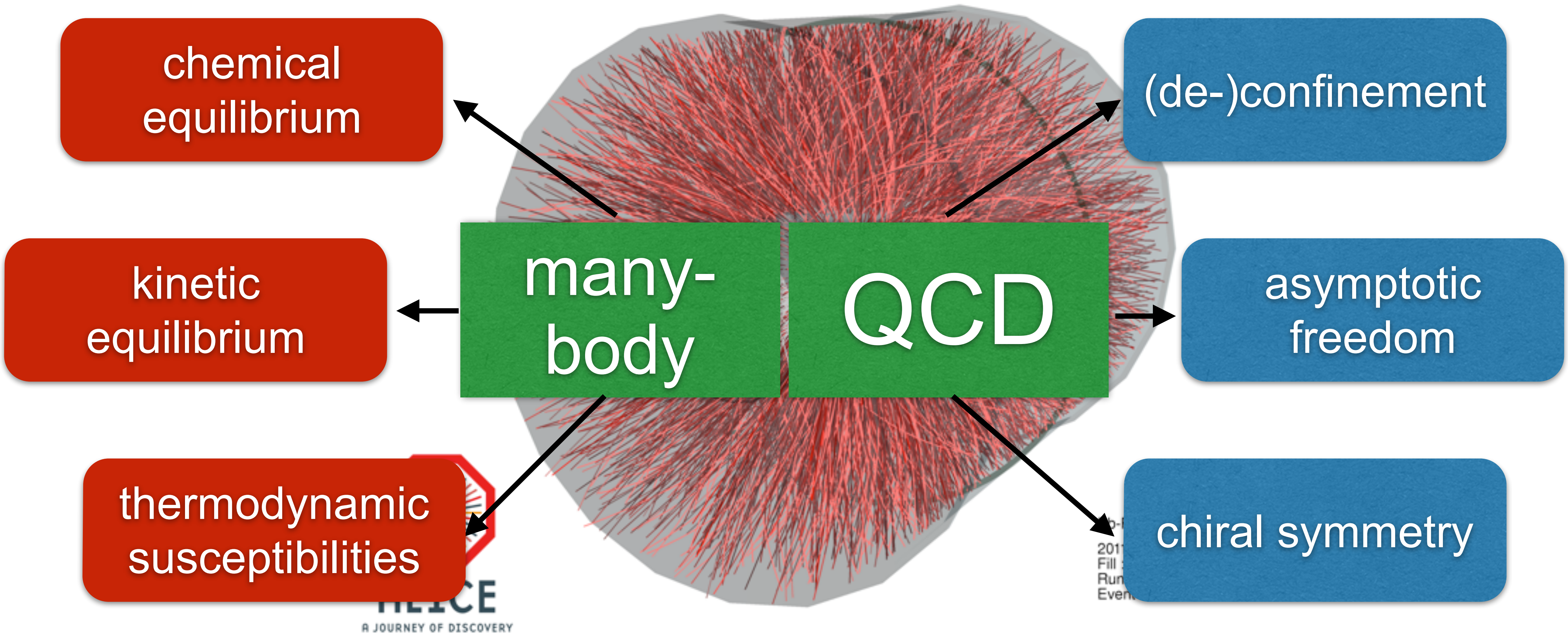

central (0-5%) Pb-Pb collisions (LHC): $dN_{ch}/d\eta \approx 1600$

Light flavor hadrons (u,d,s valence quarks) are produced in apparent chemical ($T_{chem} \approx 156$ MeV) and kinetic equilibrium ($T_{kin} \approx 100$ MeV).

98% of all particles are produced with $p_T < 2$ GeV/c → thermal particle production in a non-perturbative regime
=> **thermodynamics**
=> **LATTICE QCD** calculations

Introduction

- Measurement of the production *yields* of identified particles and chemical freeze-out conditions:
    - Hadron resonance gas approach in thermal-statistical *models*
    - Reducing the model dependence and towards ab initio approaches

- Measurement of event-by-event *fluctuations* of conserved quantities:
    - net-charge fluctuations
    - plans for future measurements
    - allows direct comparison of measurements to ab initio calculations

Introduction

- Measurement of the production *yields* of identified particles and chemical freeze-out conditions:
  - Hadron resonance gas approach in thermal-statistical *models*
  - Reducing the model dependence and towards ab initio approaches

Well measured production of particles **integrated over many events**. Beautifully established picture from experimental and theoretical side.

- Measurement of event-by-event *fluctuations* of conserved quantities:
  - net-charge fluctuations
  - plans for future measurements
  - allows direct comparison of measurements to ab initio calculations

Introduction

- Measurement of the production *yields* of identified particles and chemical freeze-out conditions:
  - Hadron resonance gas approach in thermal-statistical *models*
  - Reducing the model dependence and towards ab initio approaches

Well measured production of particles **integrated over many events**. Beautifully established picture from experimental and theoretical side.

But no (or little) sensitivity to critical behavior…

- Measurement of event-by-event *fluctuations* of conserved quantities:
  - net-charge fluctuations
  - plans for future measurements
  - allows direct comparison of measurements to ab initio calculations

Introduction

- Measurement of the production *yields* of identified particles and chemical freeze-out conditions:
  - Hadron resonance gas approach in thermal-statistical *models*
  - Reducing the model dependence and towards ab initio approaches

Well measured production of particles **integrated over many events**. Beautifully established picture from experimental and theoretical side.

But no (or little) sensitivity to critical behavior…

- Measurement of event-by-event *fluctuations* of conserved quantities:
  - net-charge fluctuations
  - plans for future measurements
  - allows direct comparison of measurements to ab initio calculations

Very sensitive to critical behavior.

Introduction

- Measurement of the production *yields* of identified particles and chemical freeze-out conditions:
  - Hadron resonance gas approach in thermal-statistical *models*
  - Reducing the model dependence and towards ab initio approaches

Well measured production of particles **integrated over many events**. Beautifully established picture from experimental and theoretical side.

But no (or little) sensitivity to critical behavior…

- Measurement of event-by-event *fluctuations* of conserved quantities:
  - net-charge fluctuations
  - plans for future measurements
  - allows direct comparison of measurements to ab initio calculations

Very sensitive to critical behavior.

Still a lot of work to do at LHC energies.. Many questions are still open.

The ALICE detector

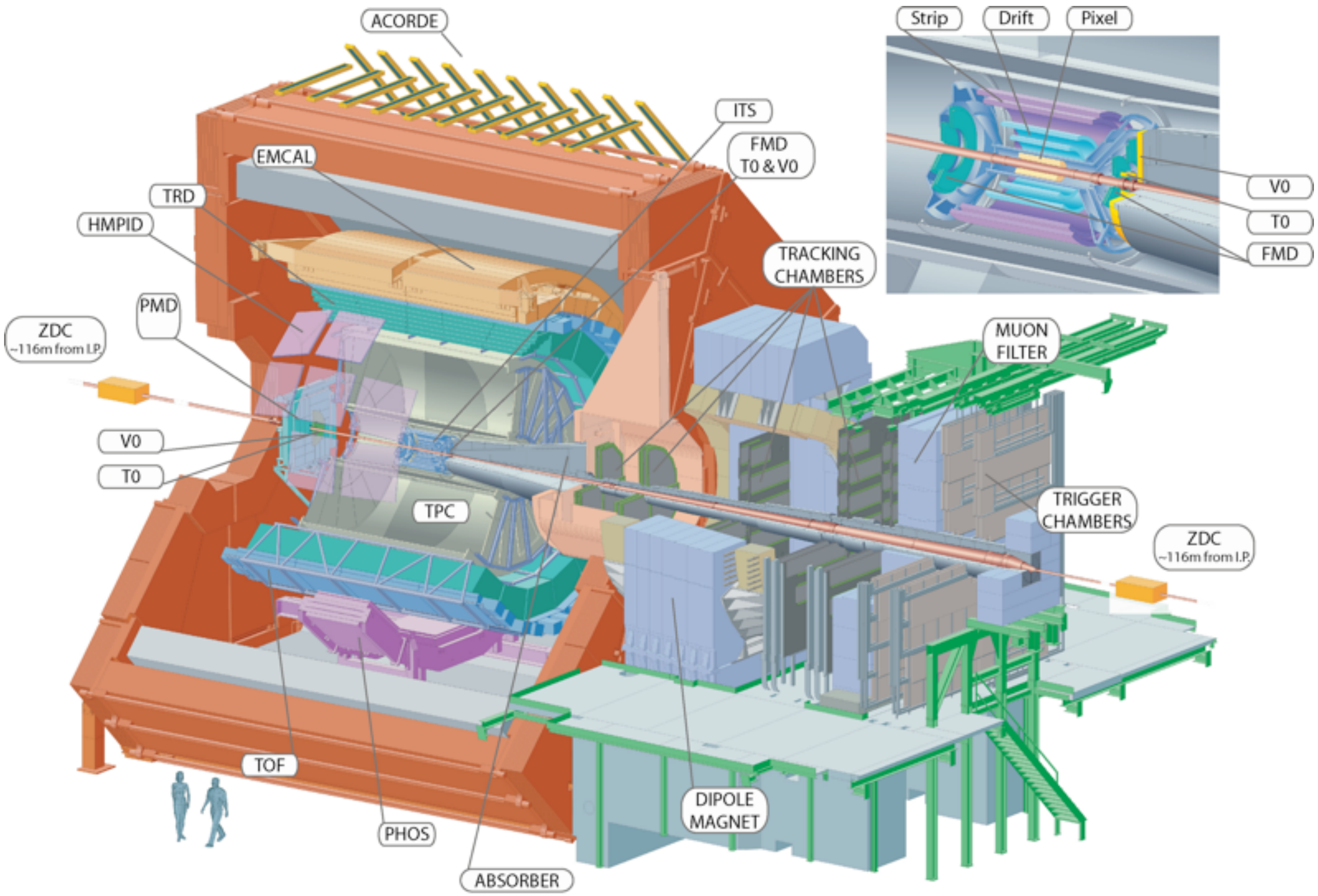

The ALICE detector

ITS+TPC+TRD: excellent track reconstruction capabilities in a high track density environment.

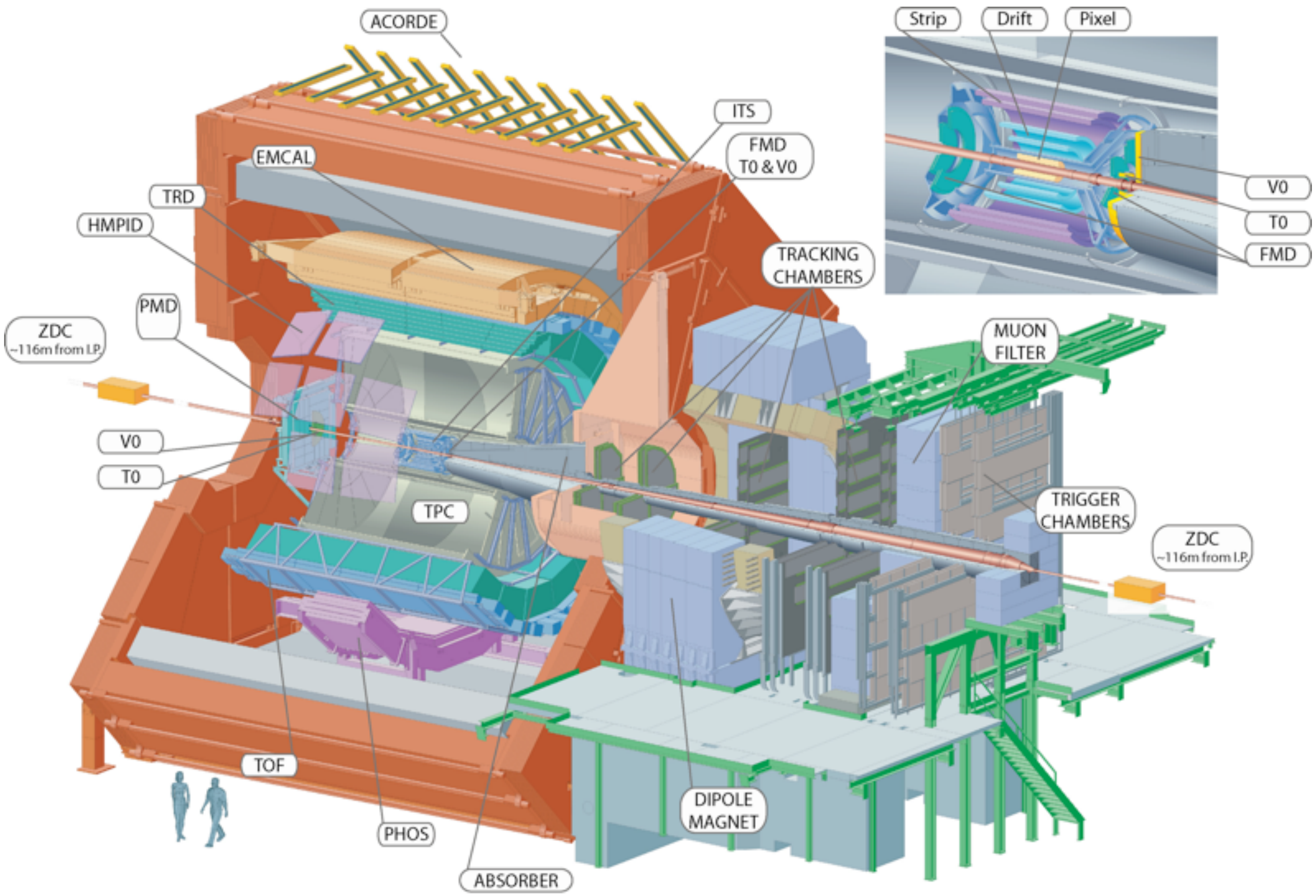

The ALICE detector

ITS+TPC+TRD: excellent track reconstruction capabilities in a high track density environment.

ITS: precise separation of primary particles and those from weak decays of strange particles or knock-out from material.

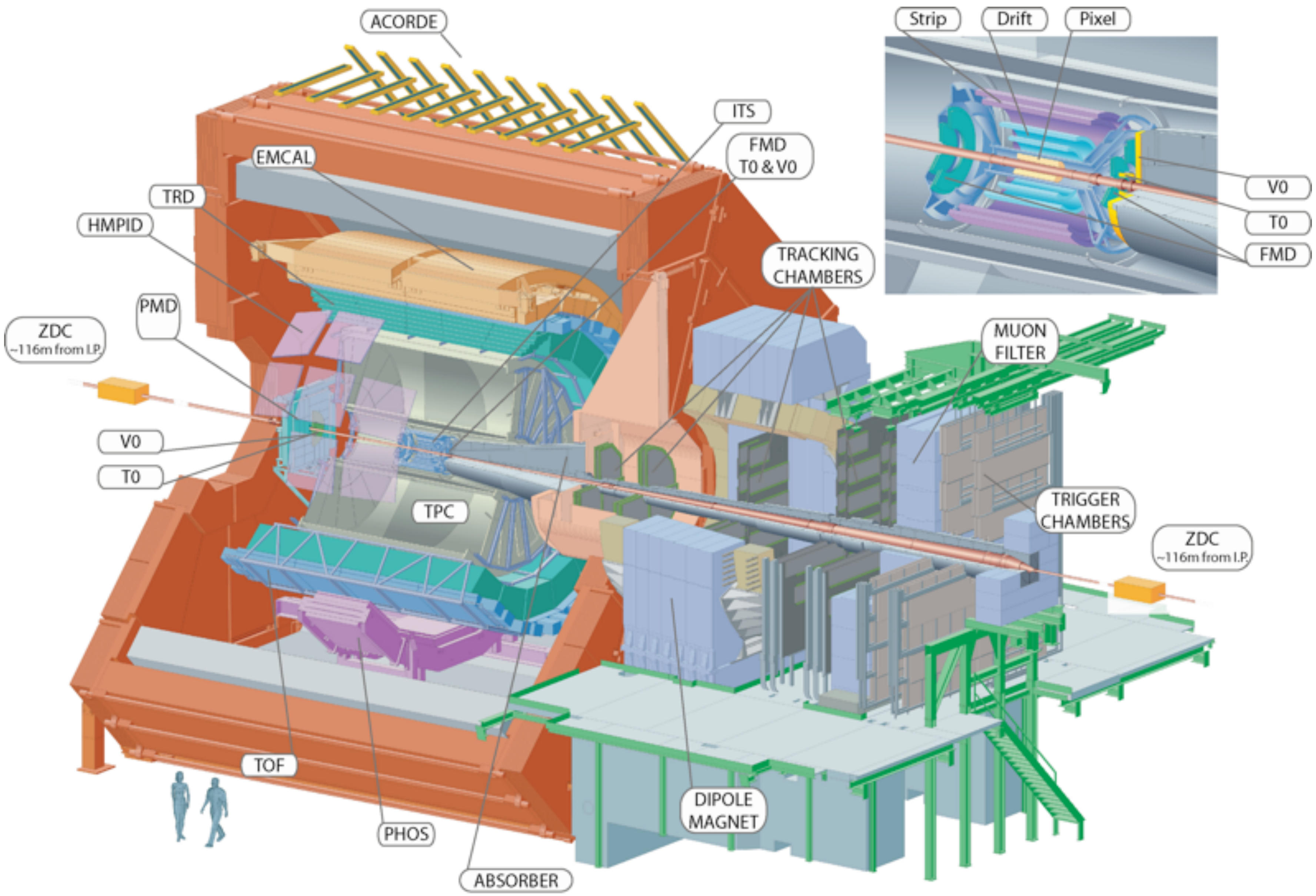

The ALICE detector

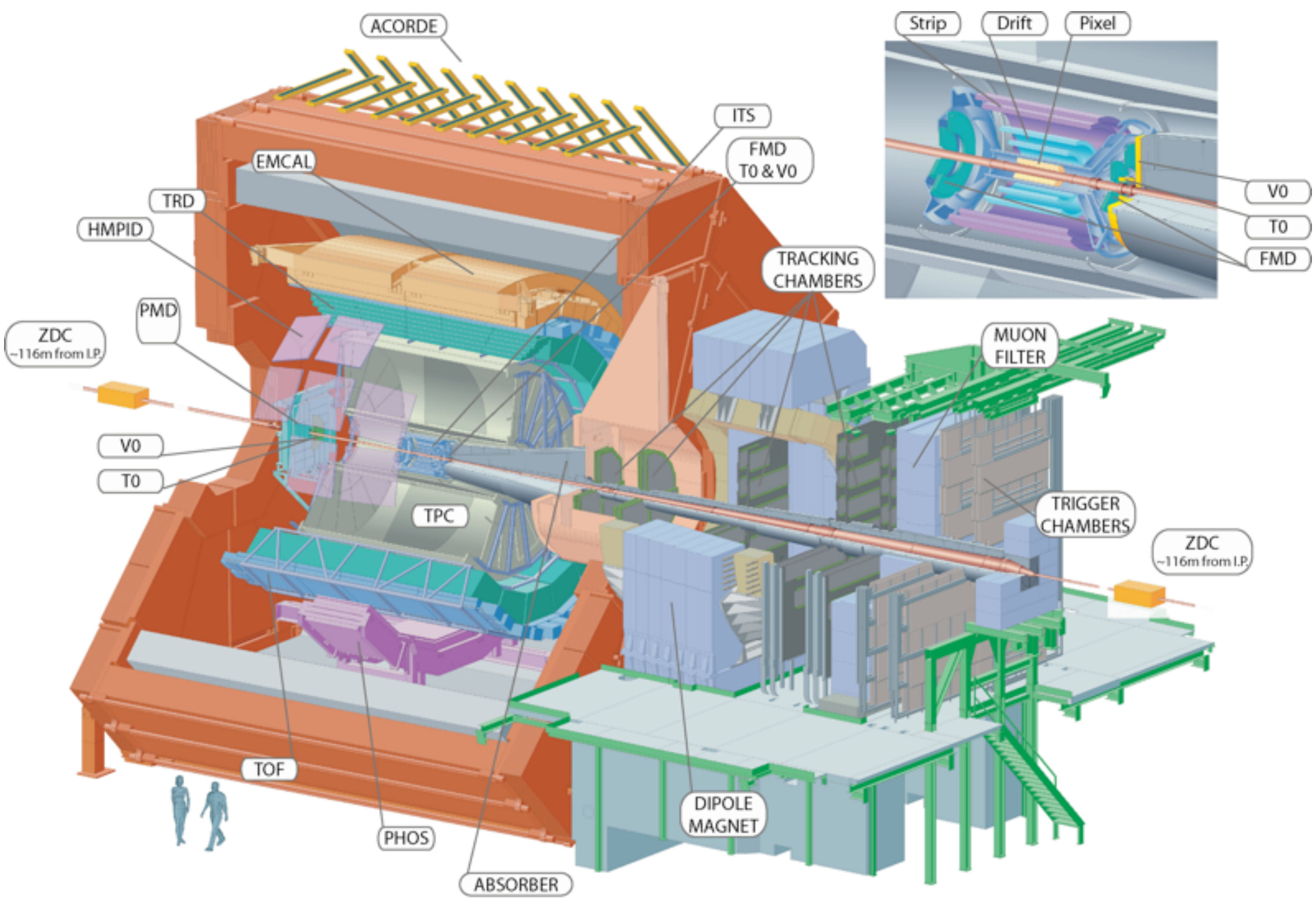

ITS+TPC+TRD: excellent track reconstruction capabilities in a high track density environment.

ITS: precise separation of primary particles and those from weak decays of strange particles or knock-out from material.

TPC: particle identification via d*E*/dx (allows also separation of charges).

The ALICE detector

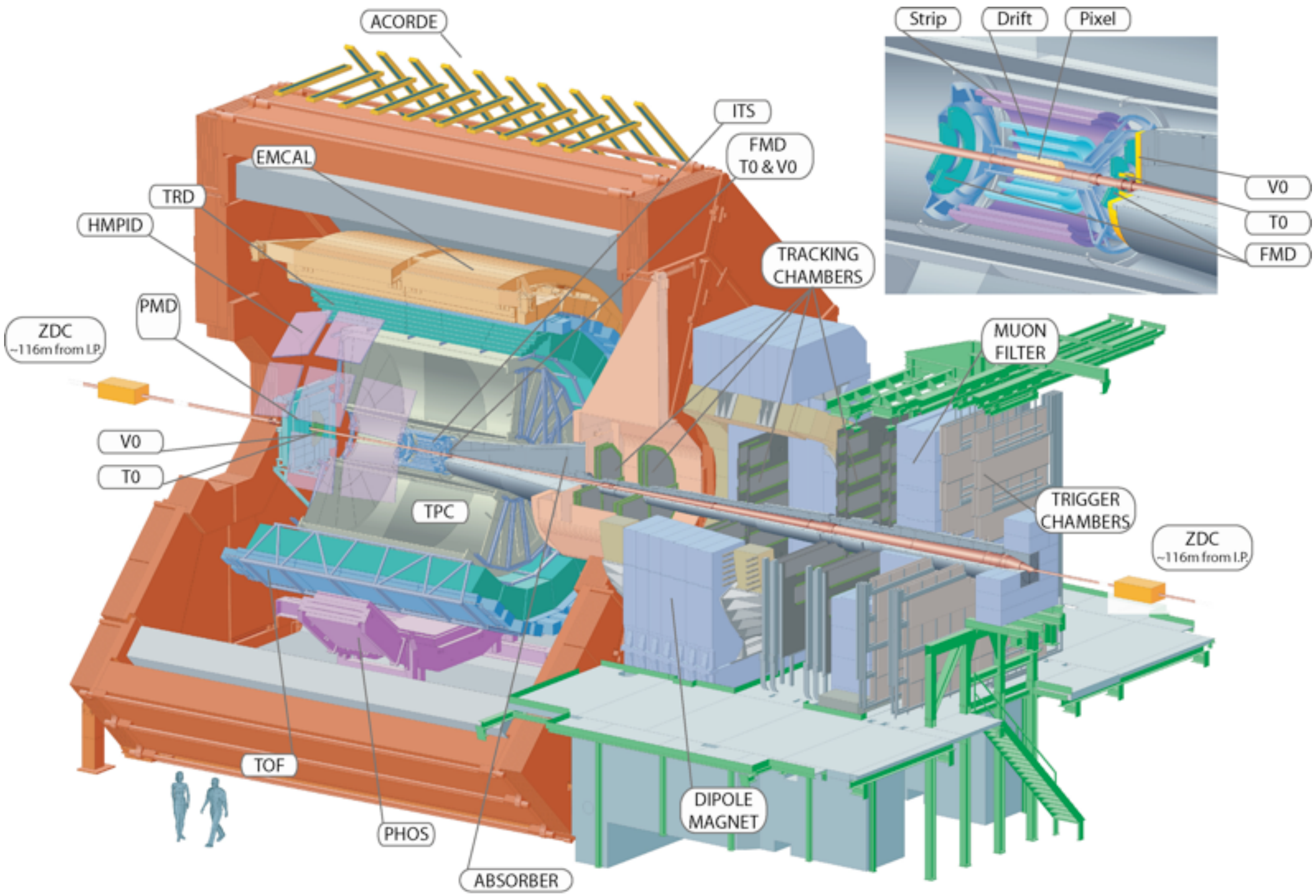

ITS+TPC+TRD: excellent track reconstruction capabilities in a high track density environment.

ITS: precise separation of primary particles and those from weak decays of strange particles or knock-out from material.

TPC: particle identification via d*E*/dx (allows also separation of charges).

TOF: particle identification via time-of-flight.

The ALICE detector

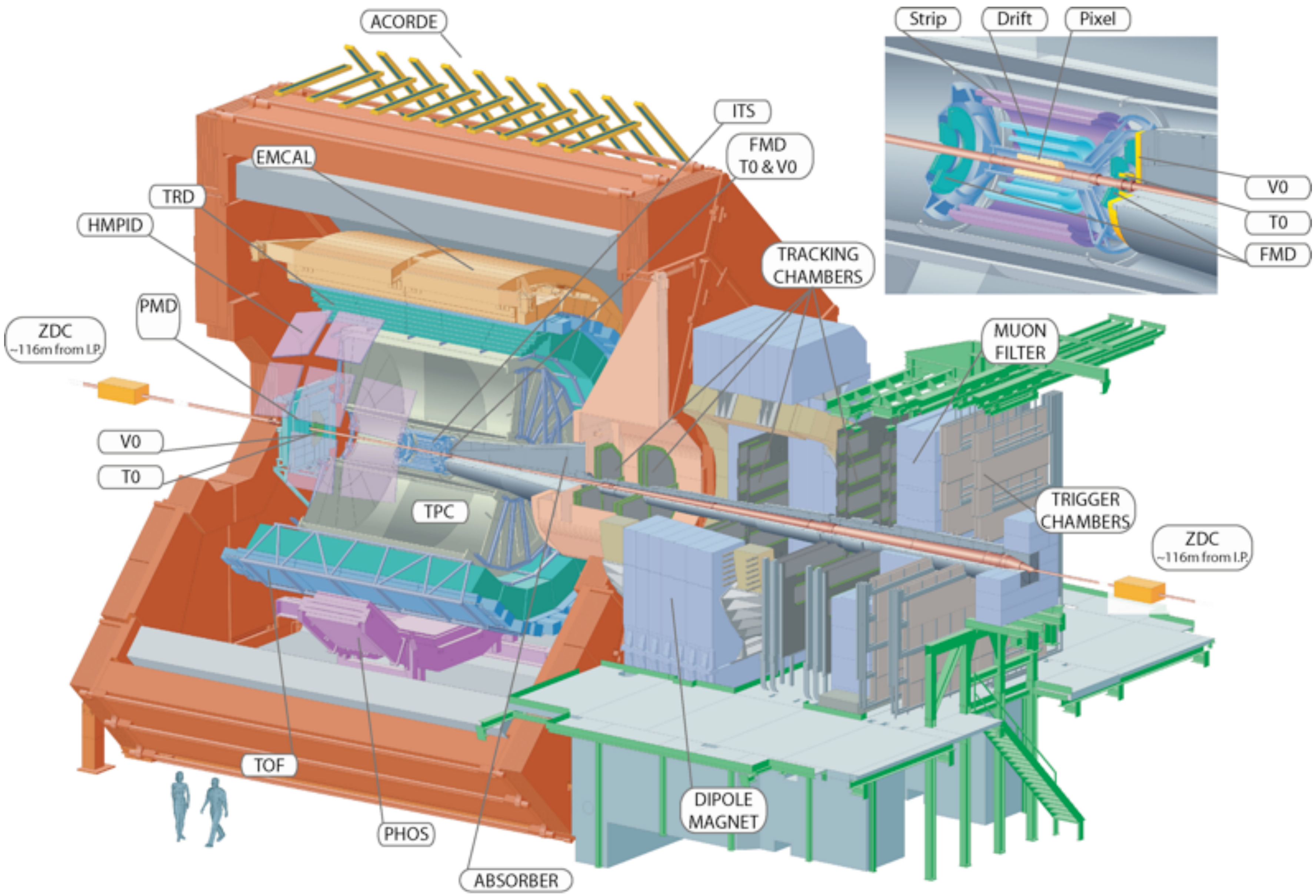

ITS+TPC+TRD: excellent track reconstruction capabilities in a high track density environment.

ITS: precise separation of primary particles and those from weak decays of strange particles or knock-out from material.

TPC: particle identification via d*E*/dx (allows also separation of charges).

TOF: particle identification via time-of-flight.

Excellent particle identification over a wide momentum range (≈ 0.1 GeV/*c* to ≈ 30 GeV/*c*).

The ALICE detector

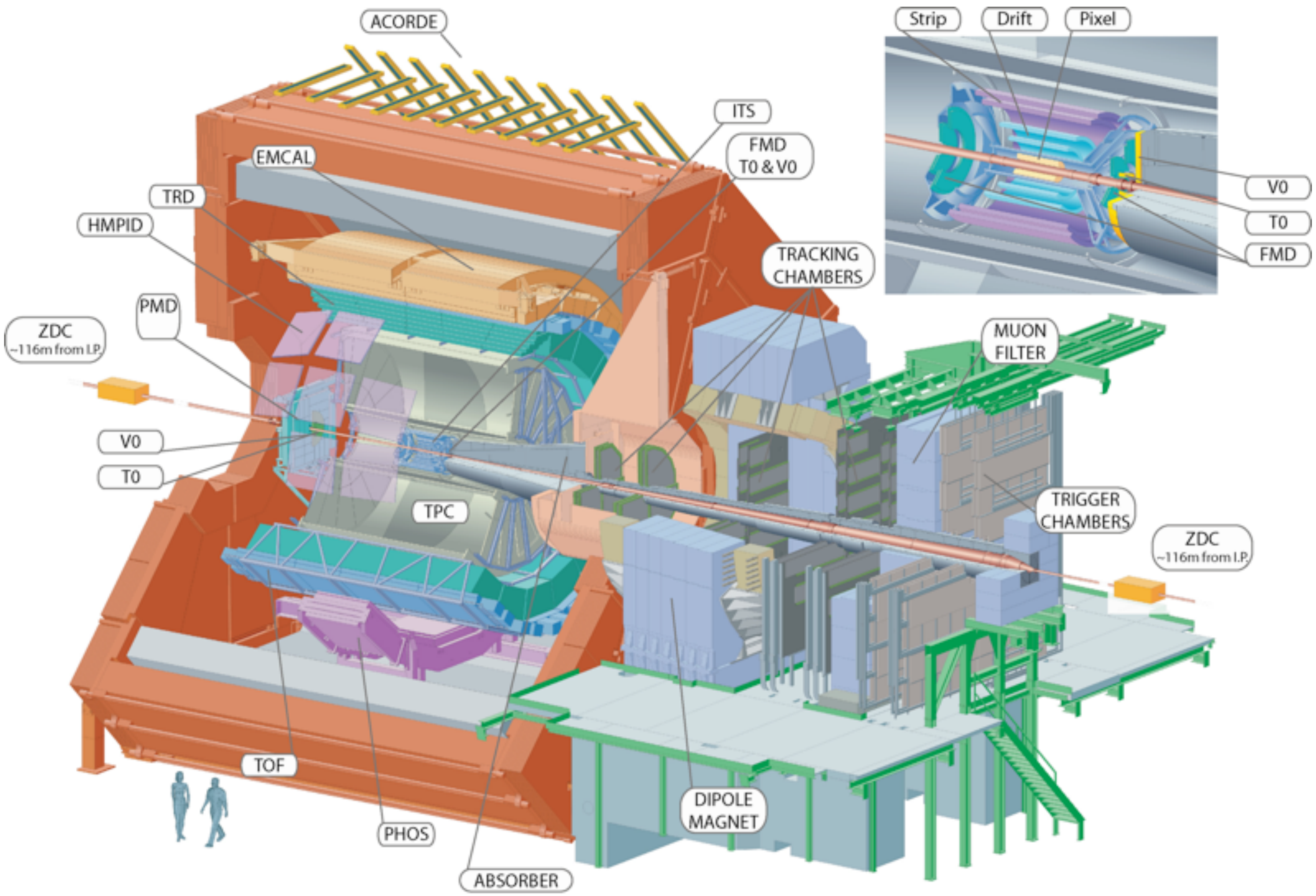

ITS+TPC+TRD: excellent track reconstruction capabilities in a high track density environment.

ITS: precise separation of primary particles and those from weak decays of strange particles or knock-out from material.

TPC: particle identification via d*E*/dx (allows also separation of charges).

TOF: particle identification via time-of-flight.

Excellent particle identification over a wide momentum range (≈ 0.1 GeV/*c* to ≈ 30 GeV/*c*).

ALICE is ideally suited for the measurement of light flavor hadrons on an event-by-event basis.

Bulk particle production

- Investigate matter in local thermal equilibrium => Look at the hadrons made up of the most abundantly produced quarks: u,d,s.

  π, K, p, Λ, Ξ, Ω, Φ, K^{*0}, d, ^{3}He, $^{3}_{\Lambda}$H, ^{4}He

- Decays of strange particles feed into the states with lower mass and need to be carefully subtracted for consistent data ↔ model comparisons:

  Λ → p π (63.9 %)
  Ξ → Λ π (99.87 %)

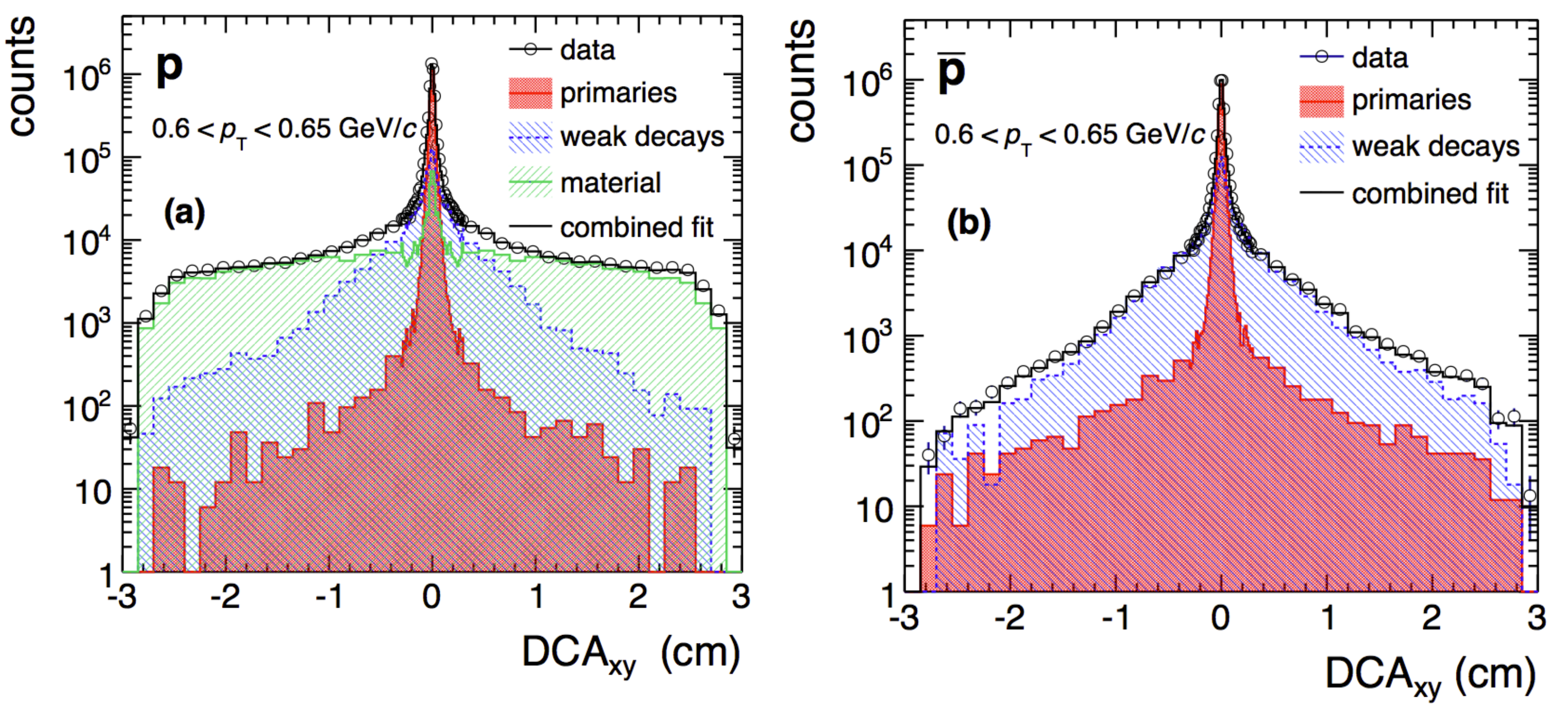

[Phys. Rev. C 88, 044910 (2013)]

Bulk particle production

- Investigate matter in local thermal equilibrium => Look at the hadrons made up of the most abundantly produced quarks: u,d,s.

π, K, p, Λ, Ξ, Ω, Φ, K^{*0}, d, ^{3}He, $^{3}_{\Lambda}$H, ^{4}He

- Decays of strange particles feed into the states with lower mass and need to be carefully subtracted for consistent data ↔ model comparisons:

$\Lambda \to p\,\pi$ (63.9 %)
$\Xi \to \Lambda\,\pi$ (99.87 %)

(ALICE Definition) *Primary particles* are defined as prompt particles produced in the collision including all decay products, except products from weak decays of light flavor hadrons and of muons.

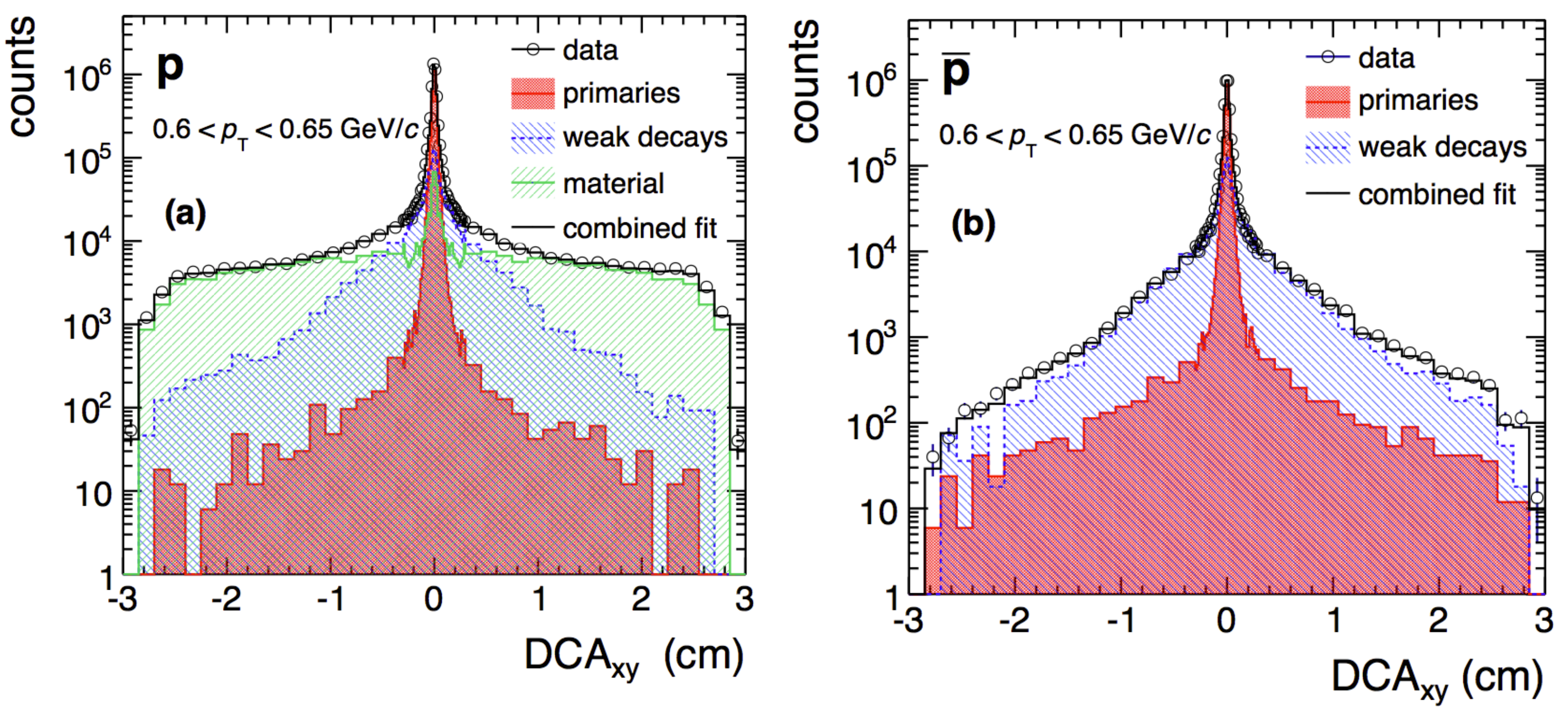

[Phys. Rev. C 88, 044910 (2013)]

Chemical freeze-out and thermal model calculations

Pb-Pb: Thermal fits to ALICE data

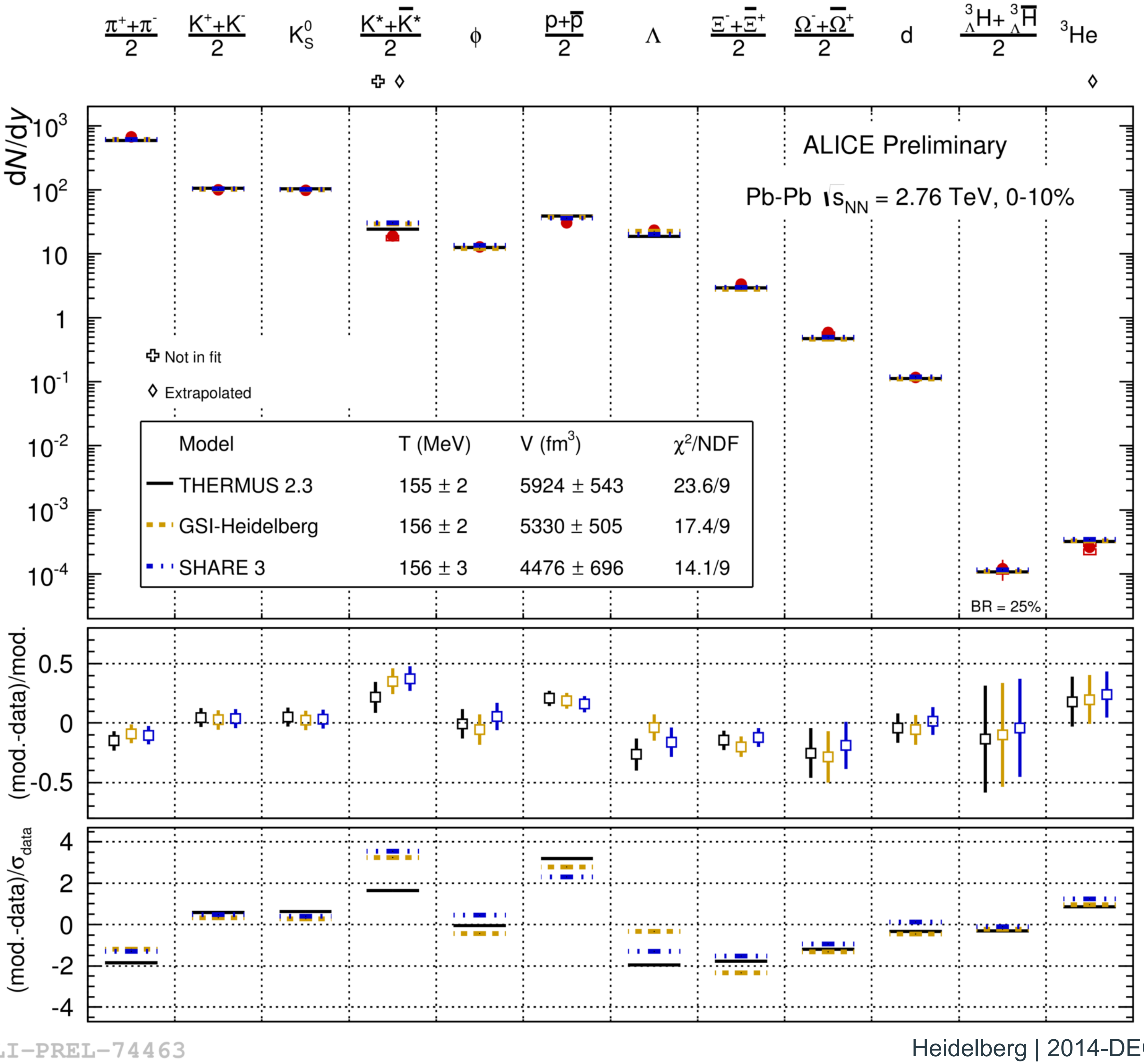

[Wheaton et al, Comput.Phys.Commun, 180 84]
[Petran et al, arXiv:1310.5108]
[Andronic et al, PLB 673 142]

Pb-Pb: Thermal fits to ALICE data

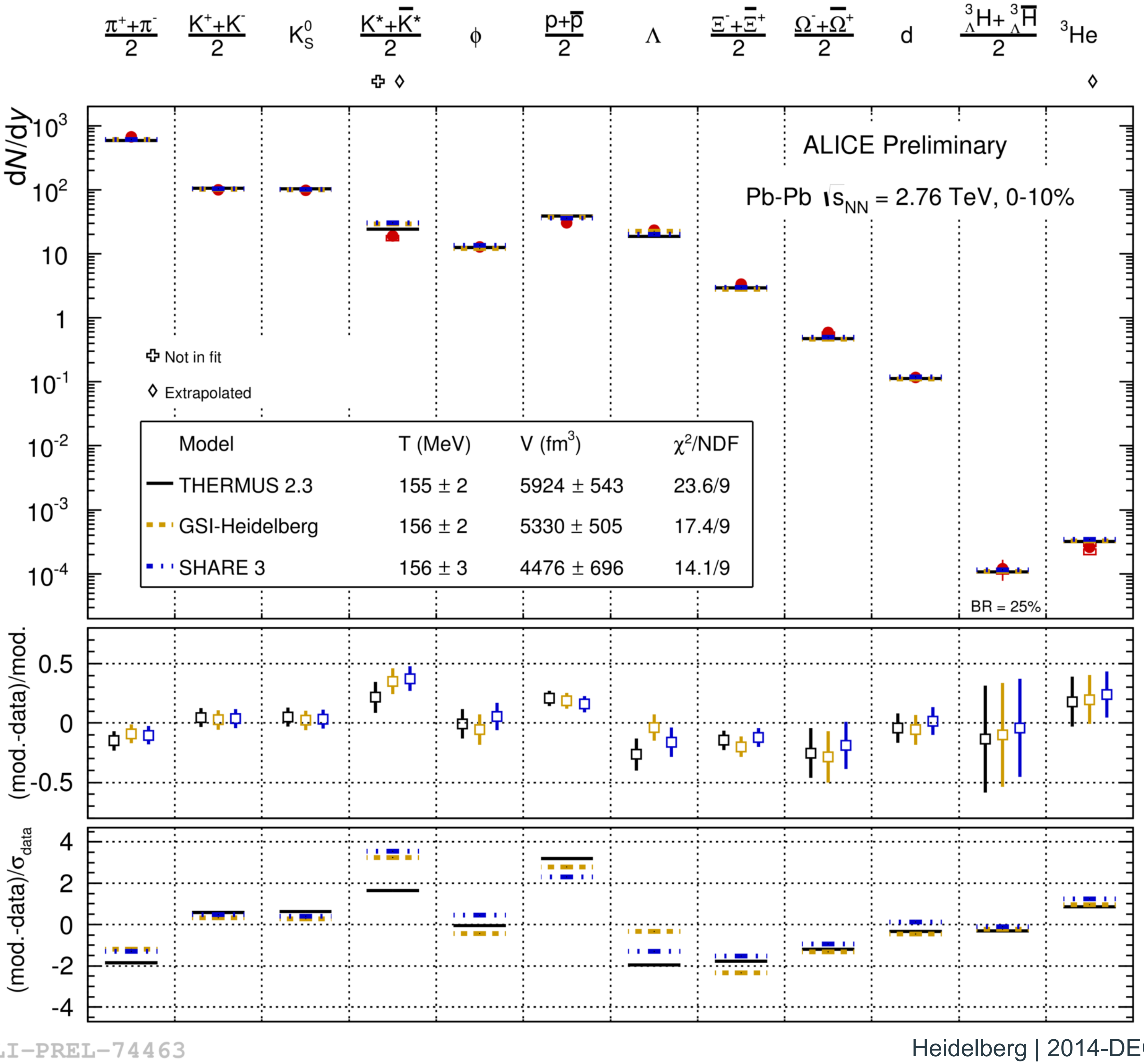

Particle yields of light flavor hadrons are described over 7 orders of magnitude within 20% (except K^{*0}) with a common chemical freeze-out temperature of $T_{ch} \approx 156$ MeV (prediction from RHIC extrapolation was ≈ 164 MeV).

[Wheaton et al, Comput.Phys.Commun, 180 84]
[Petran et al, arXiv:1310.5108]
[Andronic et al, PLB 673 142]

Pb-Pb: Thermal fits to ALICE data

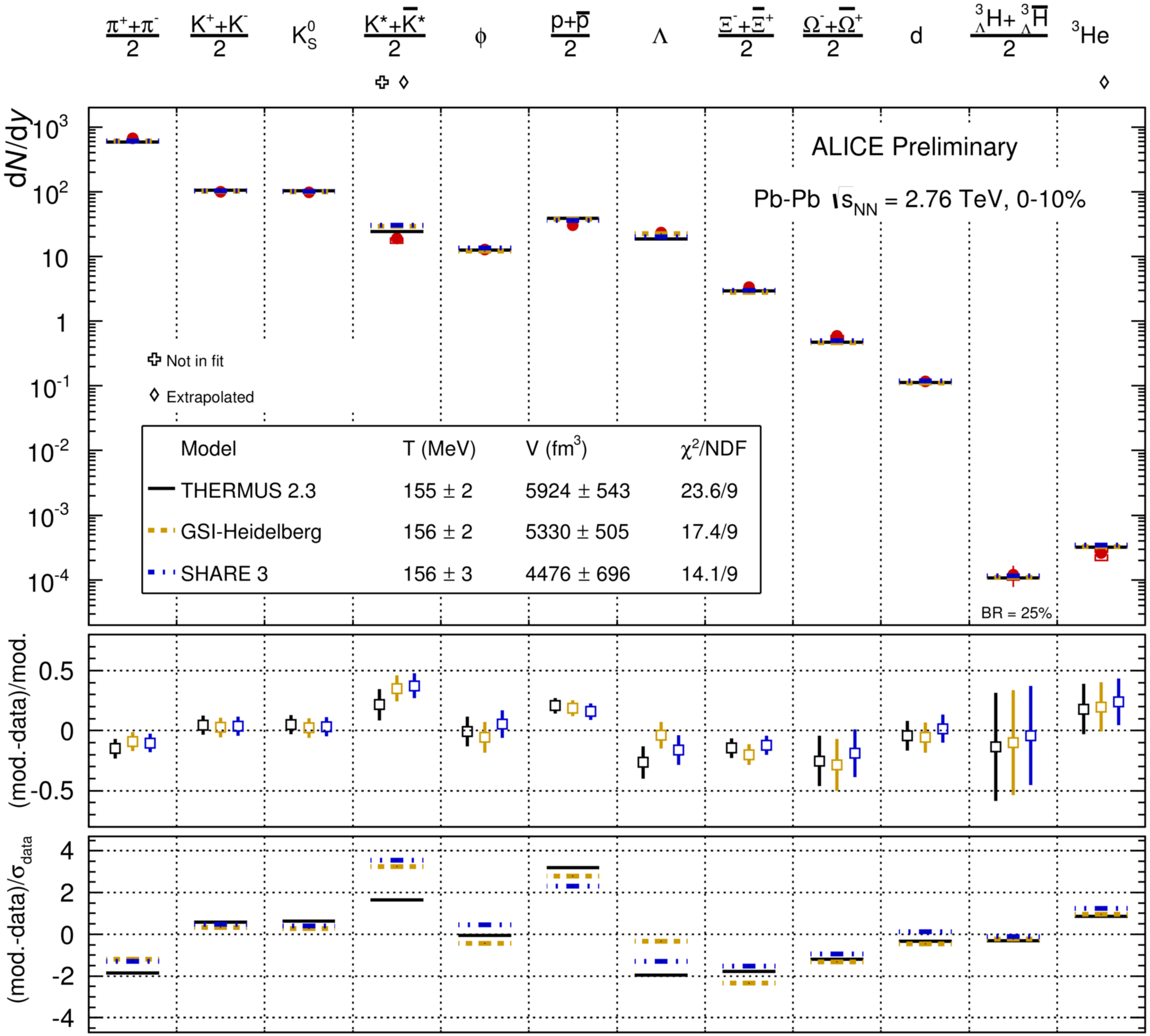

Model	T (MeV)	V (fm^3)	χ^2/NDF
THERMUS 2.3	155 ± 2	5924 ± 543	23.6/9
GSI-Heidelberg	156 ± 2	5330 ± 505	17.4/9
SHARE 3	156 ± 3	4476 ± 696	14.1/9

Particle yields of light flavor hadrons are described over 7 orders of magnitude within 20% (except K^{*0}) with a common chemical freeze-out temperature of $T_{ch} \approx 156$ MeV (prediction from RHIC extrapolation was ≈ 164 MeV).

Hadrons are produced in apparent chemical equilibrium in Pb-Pb collisions at LHC energies.

[Wheaton et al, Comput.Phys.Commun, 180 84]
[Petran et al, arXiv:1310.5108]
[Andronic et al, PLB 673 142]

Pb-Pb: Thermal fits to ALICE data

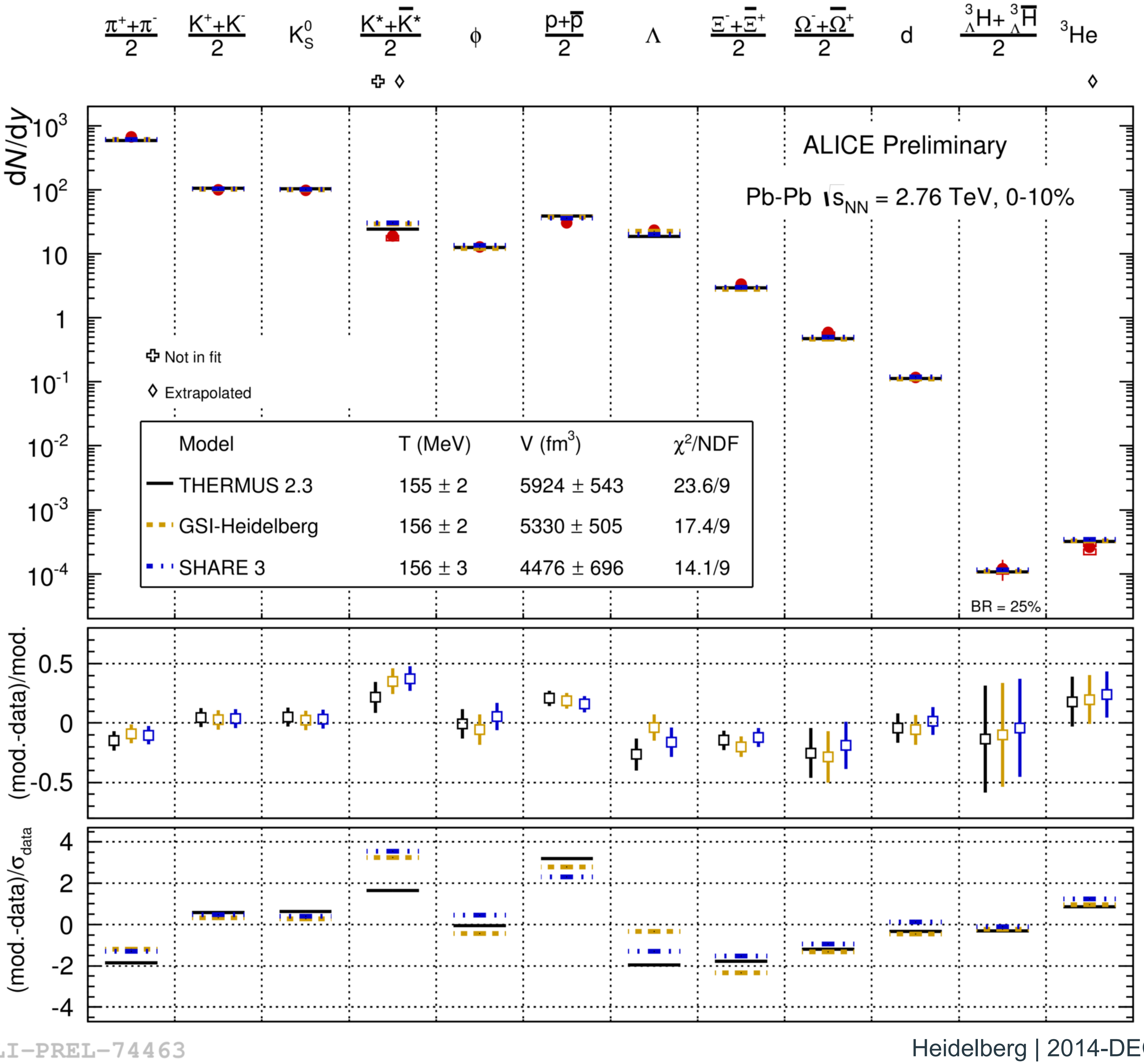

Particle yields of light flavor hadrons are described over 7 orders of magnitude within 20% (except K^{*0}) with a common chemical freeze-out temperature of T_{ch} ≈ 156 MeV (prediction from RHIC extrapolation was ≈ 164 MeV).

Hadrons are produced in apparent chemical equilibrium in Pb-Pb collisions at LHC energies.

Largest deviations observed for **protons** (incomplete hadron spectrum, baryon annihilation in hadronic phase,..?) and for **K^{*0}**.

[Wheaton et al, Comput.Phys.Commun, 180 84]
[Petran et al, arXiv:1310.5108]
[Andronic et al, PLB 673 142]

Pb-Pb: Thermal fits to ALICE data

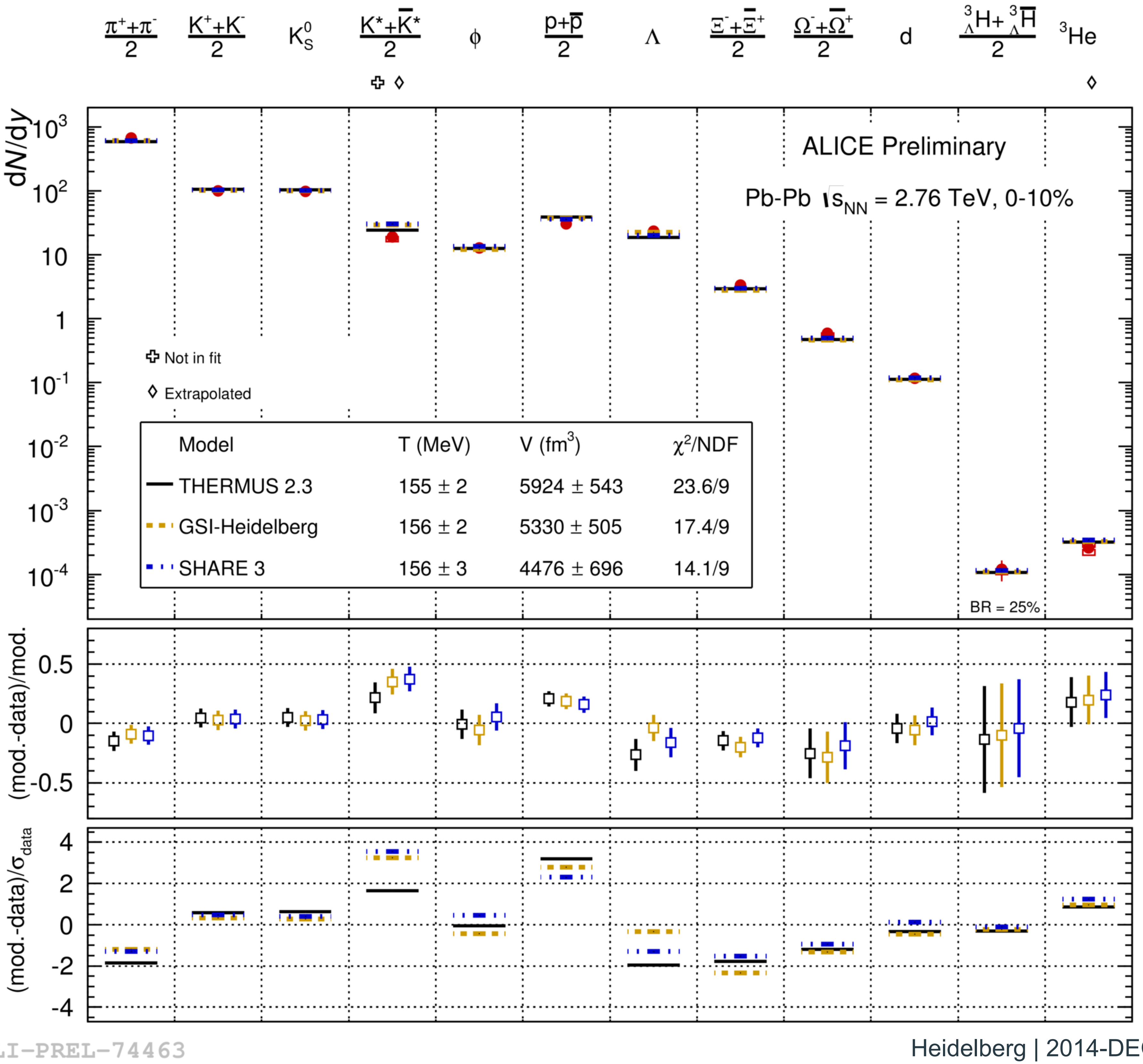

Particle yields of light flavor hadrons are described over 7 orders of magnitude within 20% (except K^{*0}) with a common chemical freeze-out temperature of $T_{ch} \approx 156$ MeV (prediction from RHIC extrapolation was ≈ 164 MeV).

Hadrons are produced in apparent chemical equilibrium in Pb-Pb collisions at LHC energies.

Largest deviations observed for **protons** (incomplete hadron spectrum, baryon annihilation in hadronic phase,..?) and for **K*^{0}**.

Three different versions of thermal model implementations give similar results.

[Wheaton et al, Comput.Phys.Commun, 180 84]
[Petran et al, arXiv:1310.5108]
[Andronic et al, PLB 673 142]

The importance of (anti-)nuclei

- Also for nuclei, it is a priori not clear that they can be described in a thermal picture:
  - The binding energy of the deuteron is E_B = 2.2 MeV.. In principle, they should immediately dissociate in a medium with $T_{ch} \approx$ 160 MeV and be suppressed by a large factor.
  - However, it is the entropy per baryon which determines their production yield and this is fixed at chemical freeze-out [1].

- The model gives a very good description of the data. Nuclei yields are very sensitive to the freeze-out temperature due to their large mass: yield ~ $\exp(-m/T_{ch})$

- Predictions from non-equilibrium models cannot describe the data (disagree up to a factor of five).

[1] P. Siemens and J. I. Kapusta, Phys.Rev.Lett. 43, 1486 (1979)

Anti-alpha

- Studies of light (anti-)nuclei production in ALICE have recently been extended to the anti-alpha.
- Also in this case the yield is found to be in agreement with thermal model expectations.

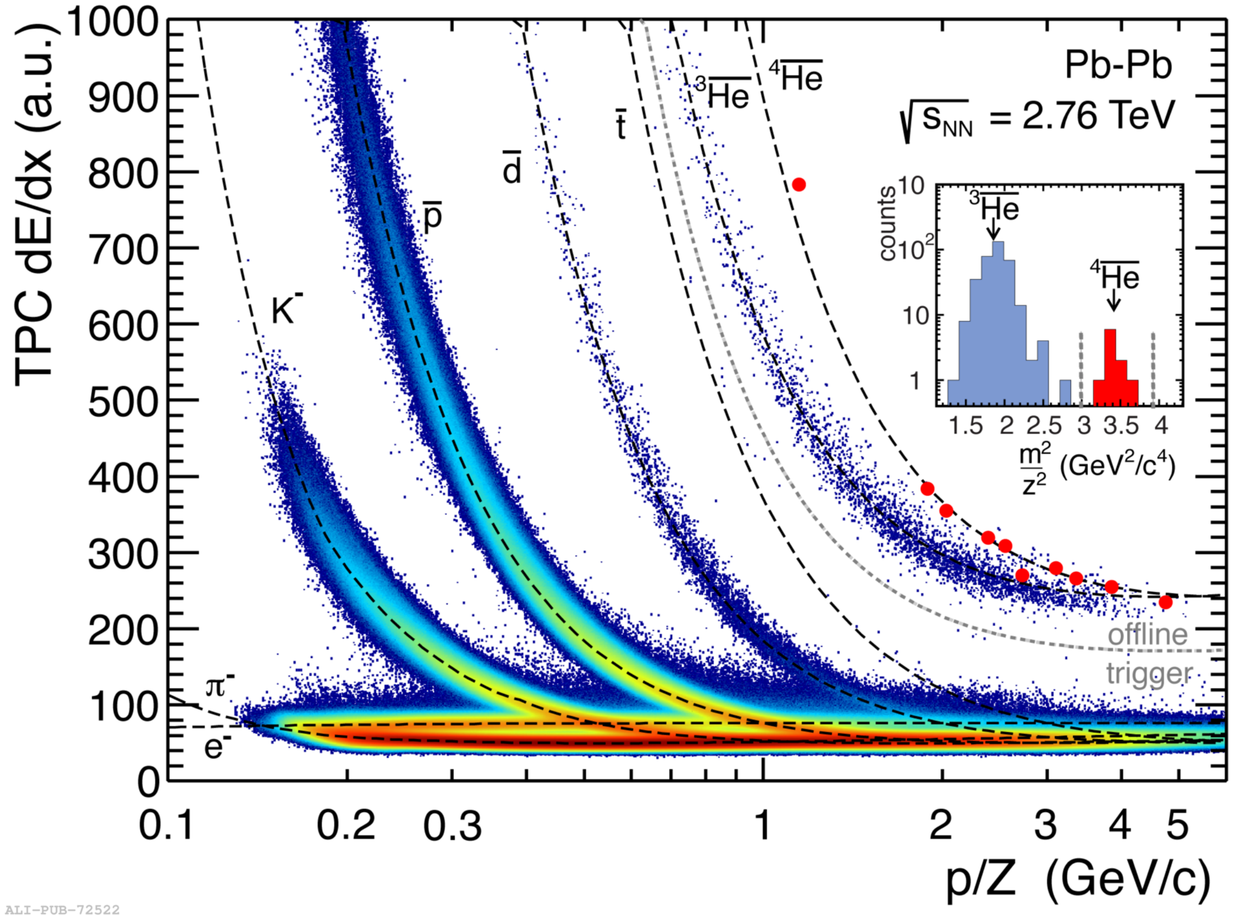

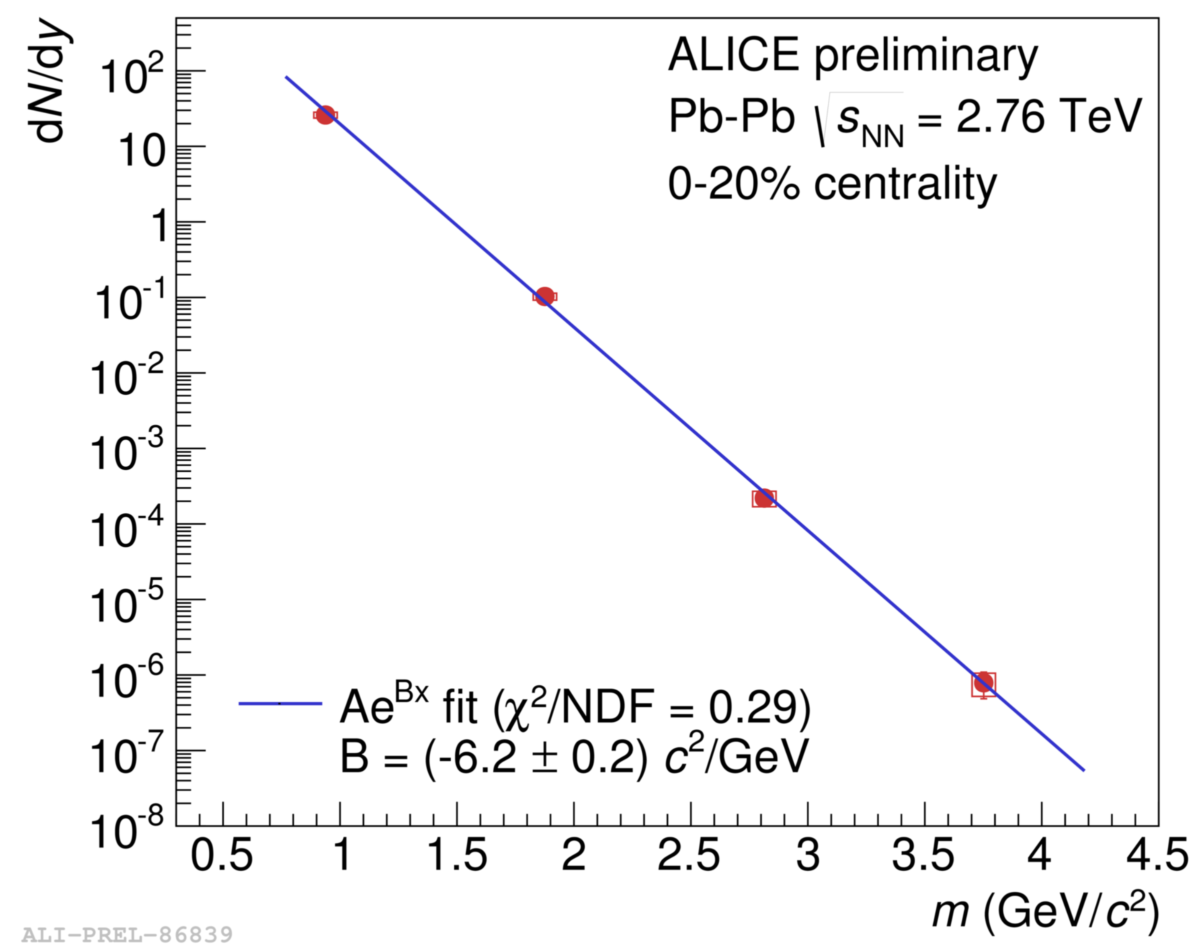

Light nuclei and resonance feed-down

$$\langle N_i \rangle = V \cdot \left(n_i^{th}(T, \vec{\mu}) + \sum_K \Gamma_{K \to i} n_i^{th-Res.}(T, \vec{\mu}) \right)$$

[A. Andronic, P.Braun-Munzinger, J. Stachel]

[1407.5003]

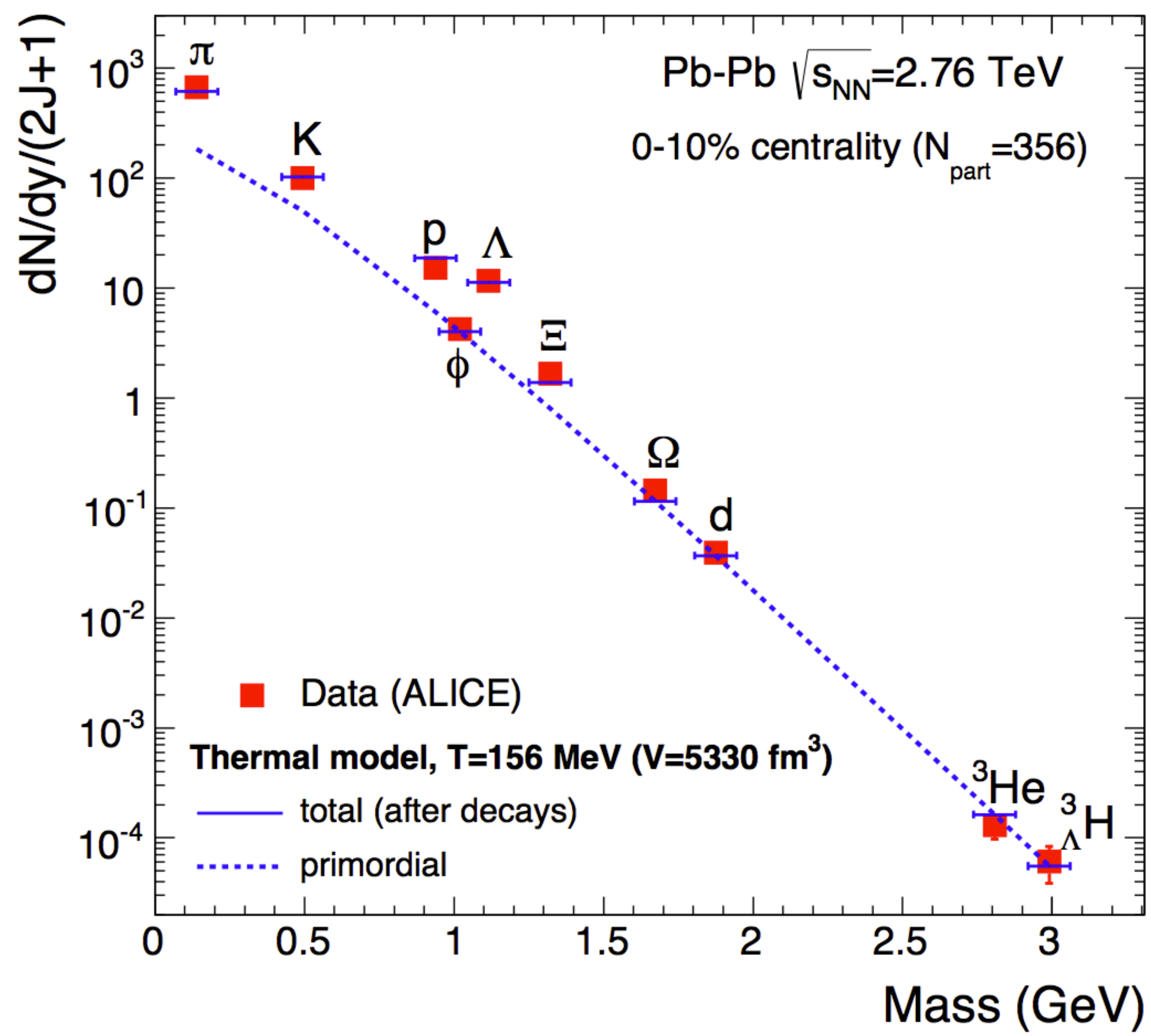

- In a thermal model approach, the production of light (anti-)nuclei is not affected by feed-down from (maybe unknown) resonances.
- Thermal-statistical analysis of light (anti-)nuclei yields reduces the model dependence!
- Can we go even further and use Lattice QCD calculations to deduce the particle yields?
  → **No.** But see talk by Krzysztof for what can be done in this respect.

Event-by-event fluctuations of conserved quantities

Thermodynamic susceptibilities (1)

- Event-by-event fluctuations of the conserved quantities in QCD (*charge Q*, *baryon number B*, *strangeness S*) correspond to thermodynamic susceptibilities χ of the system which can be directly calculated in Lattice QCD or in the Hadron Resonance Gas (HRG) model:

$$\chi_{lmn}^{BSQ} = \frac{\partial^{l+m+n}(P/T^4)}{\partial(\mu_B/T)^l\,\partial(\mu_S/T)^m\,\partial(\mu_S/T)^n}$$

- Statistical distribution of conserved quantities are quantified by their (central) moments or cumulants.

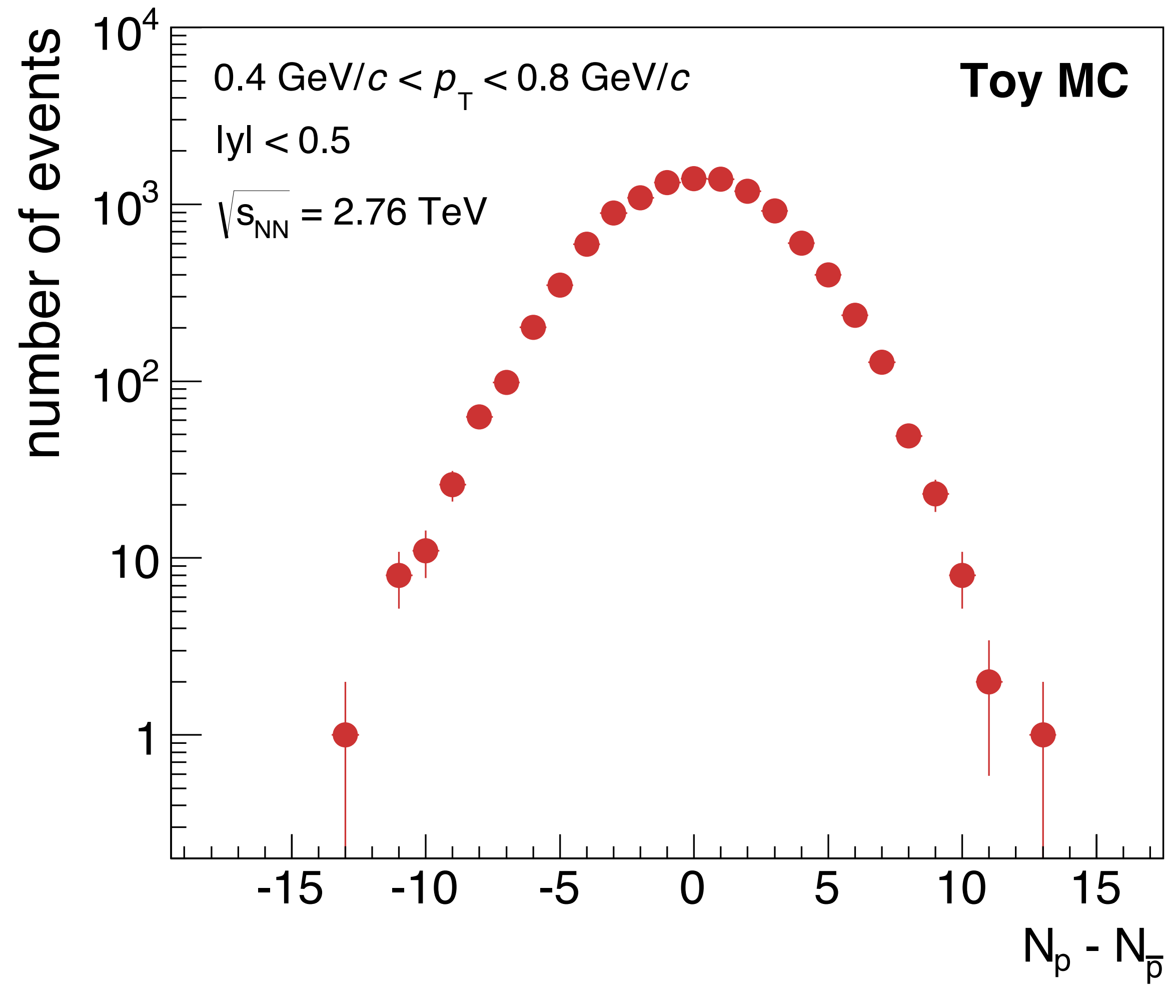

Thermodynamic susceptibilities (1)

- Event-by-event fluctuations of the conserved quantities in QCD (*charge Q*, *baryon number B*, *strangeness S*) correspond to thermodynamic susceptibilities χ of the system which can be directly calculated in Lattice QCD or in the Hadron Resonance Gas (HRG) model:

$$\chi_{lmn}^{BSQ} = \frac{\partial^{l+m+n}(P/T^4)}{\partial(\mu_B/T)^l\,\partial(\mu_S/T)^m\,\partial(\mu_S/T)^n}$$

- Statistical distribution of conserved quantities are quantified by their (central) moments or cumulants.

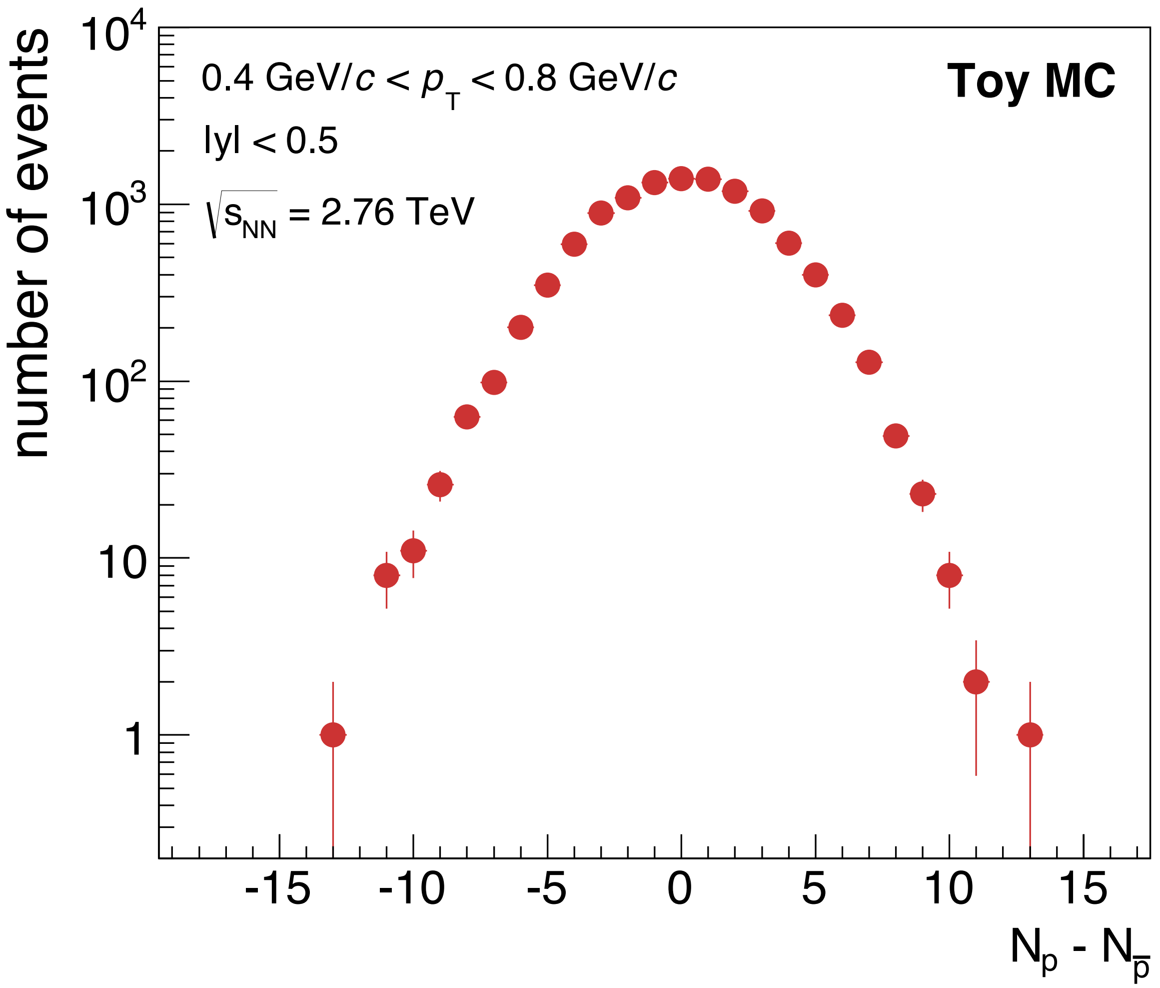

LHC (ALICE) data allows the most direct comparison to Lattice QCD calculations which correspond to $\mu_B = 0$. No extrapolation needed at LHC energies!

Thermodynamic susceptibilities (1)

- Event-by-event fluctuations of the conserved quantities in QCD (*charge Q*, *baryon number B*, *strangeness S*) correspond to thermodynamic susceptibilities χ of the system which can be directly calculated in Lattice QCD or in the Hadron Resonance Gas (HRG) model:

$$\chi_{lmn}^{BSQ} = \frac{\partial^{l+m+n}(P/T^4)}{\partial(\mu_B/T)^l\,\partial(\mu_S/T)^m\,\partial(\mu_S/T)^n}$$

- Statistical distribution of conserved quantities are quantified by their (central) moments or cumulants.

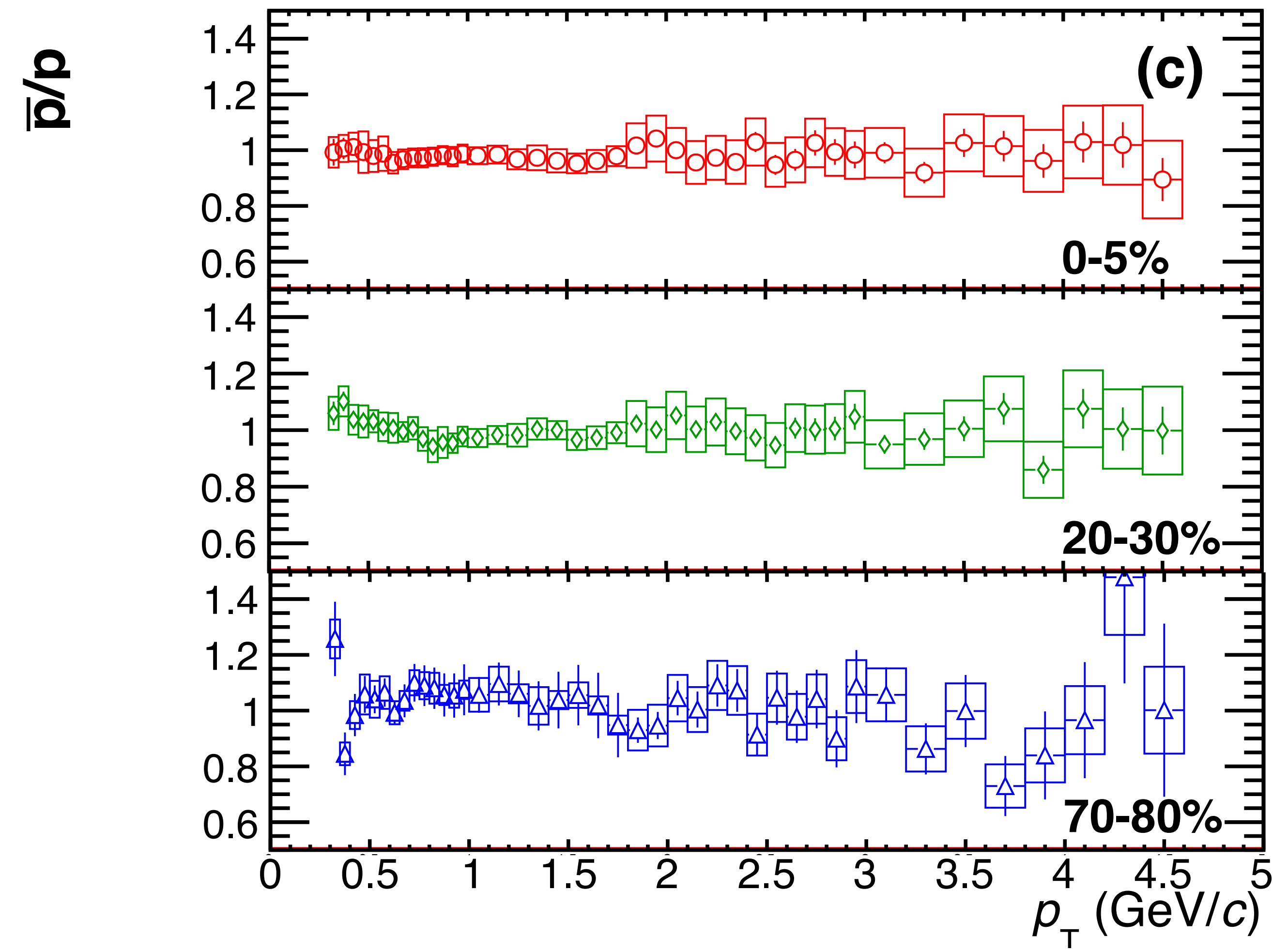

LHC (ALICE) data allows the most direct comparison to Lattice QCD calculations which correspond to $\mu_B = 0$. No extrapolation needed at LHC energies!

Thermodynamic susceptibilities (2)

- Moments μ and cumulants K:

$$
\begin{array}{ccccccccc}
M & = & K_1 & = & \mu & = & \langle N \rangle & = & VT^3 \cdot \chi_1 \\
\sigma^2 & = & K_2 & = & \mu_2 & = & \langle (\delta N)^2 \rangle & = & VT^3 \cdot \chi_2 \\
S & = & K_3/\sigma^3 & = & \mu_3/\sigma^3 & = & \langle (\delta N)^3 \rangle/\sigma^3 & = & VT^3 \cdot \chi_3/(VT^3 \cdot \chi_2)^{3/2} \\
\kappa & = & K_4/\sigma^4 & = & (\mu_4 - 3\mu_2^2)/\mu_2^2 & = & \langle (\delta N)^4 \rangle/\sigma^4 - 3 & = & (VT^3 \cdot \chi_4)/(VT^3 \cdot \chi_2)^2
\end{array}
$$

- In ratios of cumulants, the volume dependence cancels:

$$
\begin{array}{ccccccc}
\chi_2/\chi_1 & = & K_2/K_1 & = & \mu_2/\mu & = & \sigma^2/M \\
\chi_3/\chi_1 & = & K_3/K_1 & = & \mu_3/\mu & = & S \cdot \sigma^2/M \\
\chi_3/\chi_2 & = & K_3/K_2 & = & \mu_3/\mu_2 & = & S \cdot \sigma \\
\chi_4/\chi_2 & = & K_4/K_2 & = & (\mu_4 - 3\mu_2^2)/\mu_2 & = & \kappa \cdot \sigma^2 \\
\chi_6/\chi_2 & = & K_6/K_2 & = & (\mu_6 - 15\mu_4\mu_2 - 10\mu_3^2 + 30\mu_2^3)/\mu_2 & & .
\end{array}
$$

Fluctuations and lattice QCD

- Thermodynamic susceptibilities at $\mu_B = 0$ can be directly calculated in lattice QCD.

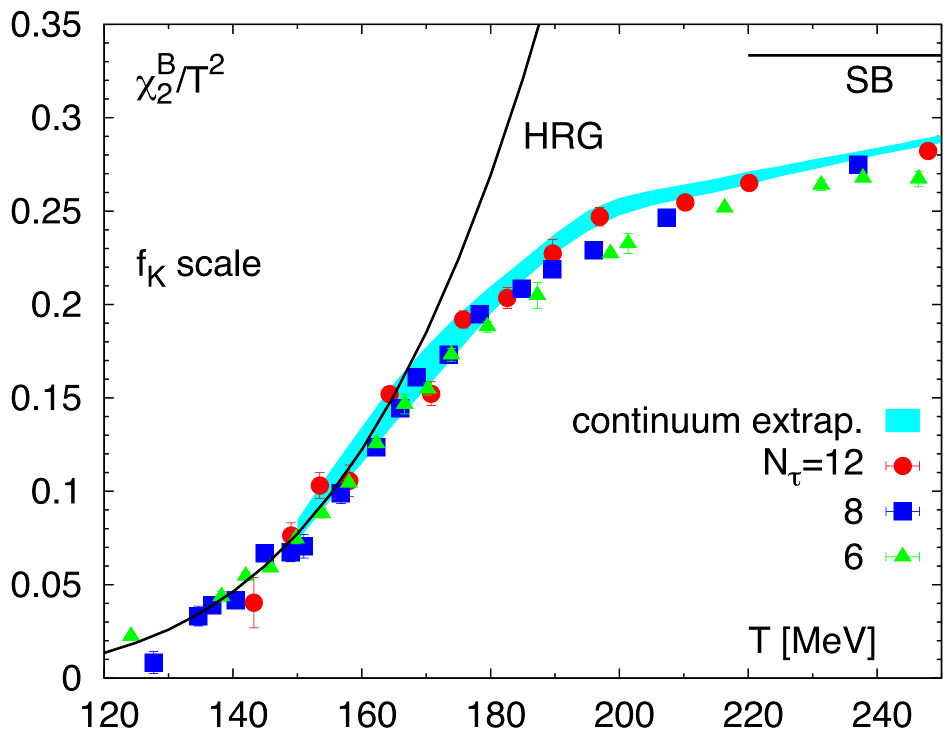

[1203.0784]

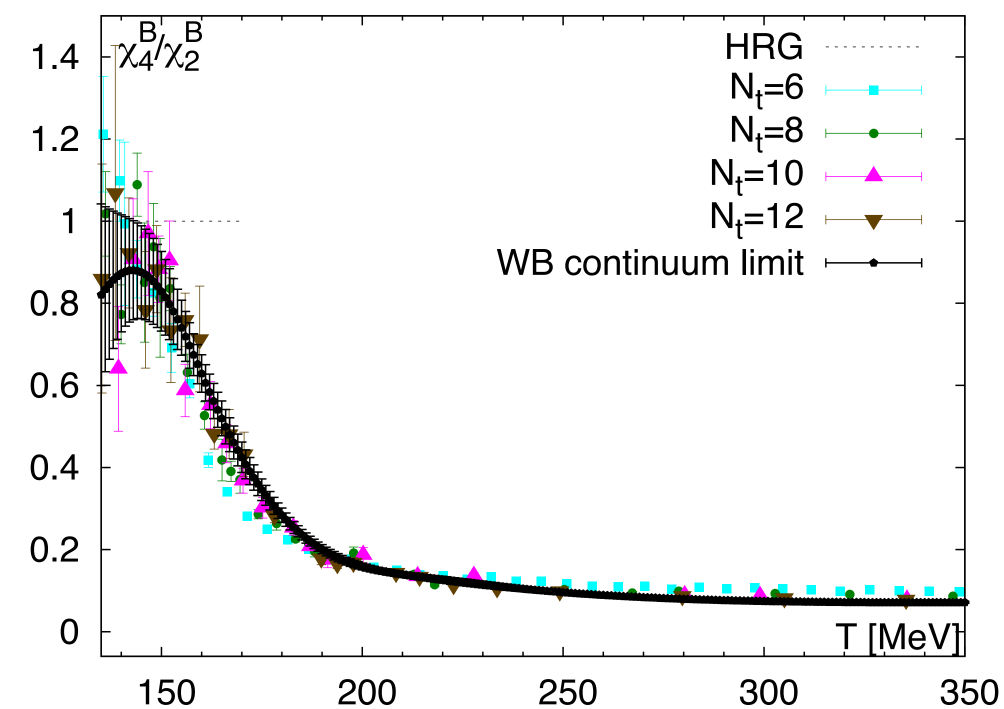

[1305.5161]

- The HRG is a very good approximation below T_c, but significant deviations at T_c are expected with increasing order of the moments due to remnants of the critical chiral behavior:
  $\chi_6/\chi_2 < 0$ at T_c in Lattice QCD and $\chi_6/\chi_2 = 1$ in HRG

Towards a measurement of net-baryon number at LHC… (1)

- The measurement is experimentally very challenging:
  - Correction for detector efficiency (N.B.: efficiencies differ for protons and anti-protons due to absorption).
  - Auto-correlations with centrality estimator.
  - Contamination from protons from material.
  - Contamination from weak decays:
    - Does the inclusion of them bring us closer to the total baryon number *B*?
    - Can one separate cleanly χ_B and χ_S?
  - Misidentified particles.

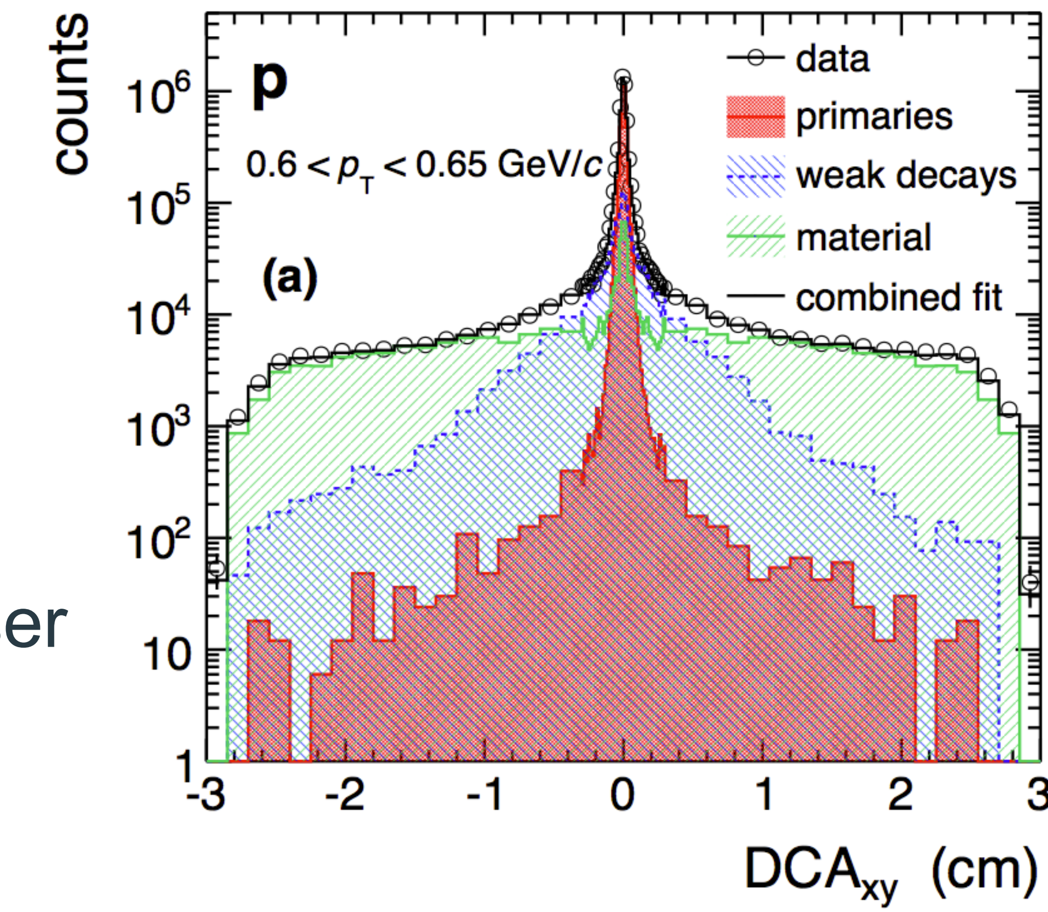

Detector efficiencies

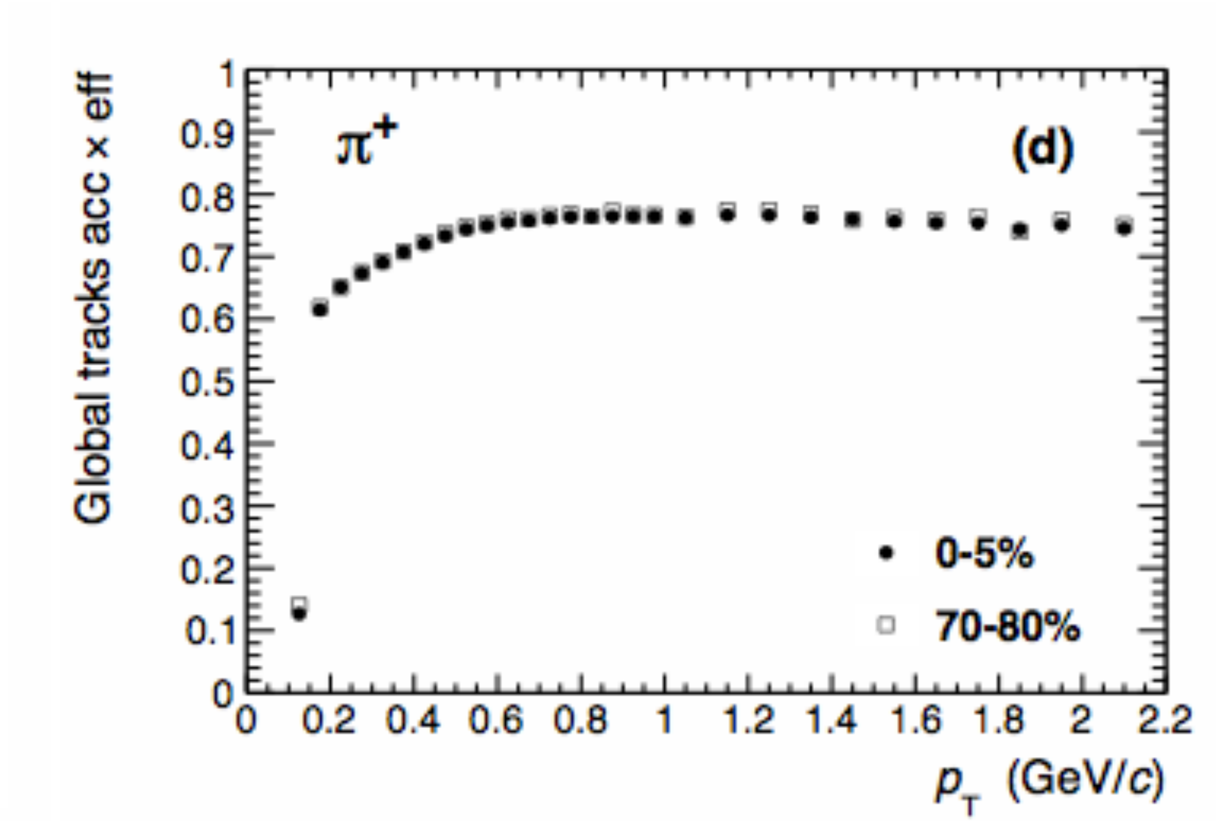

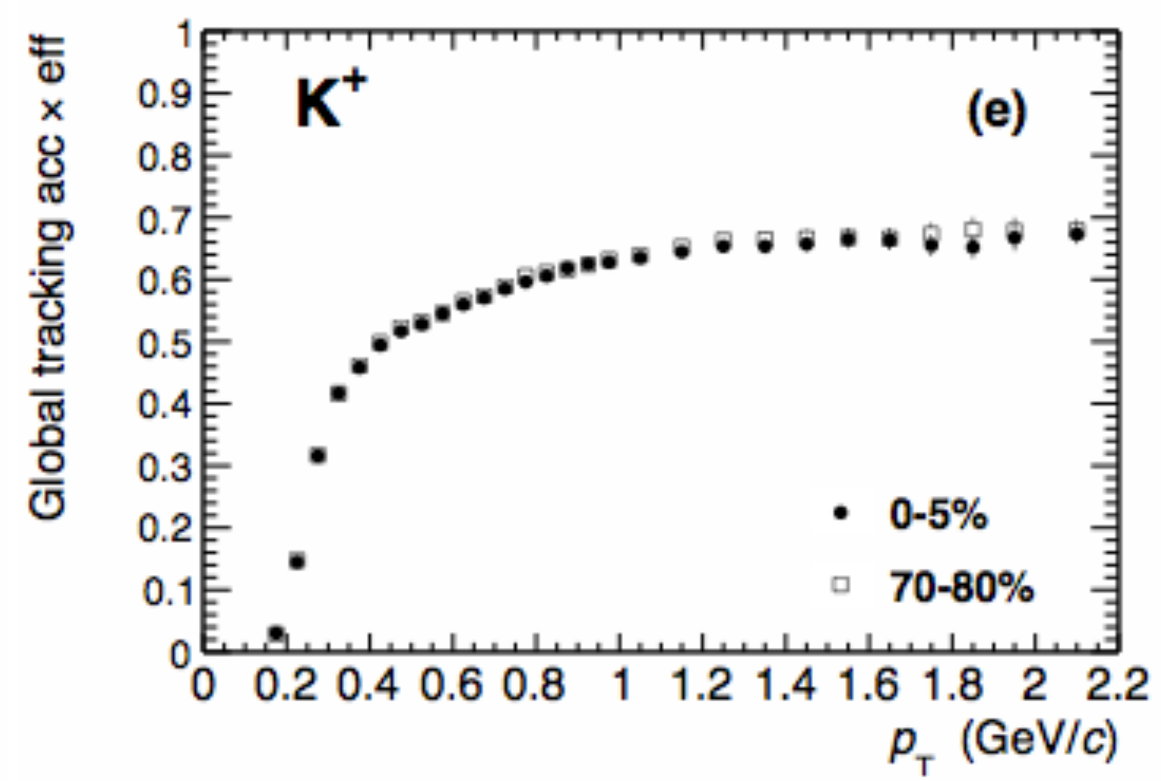

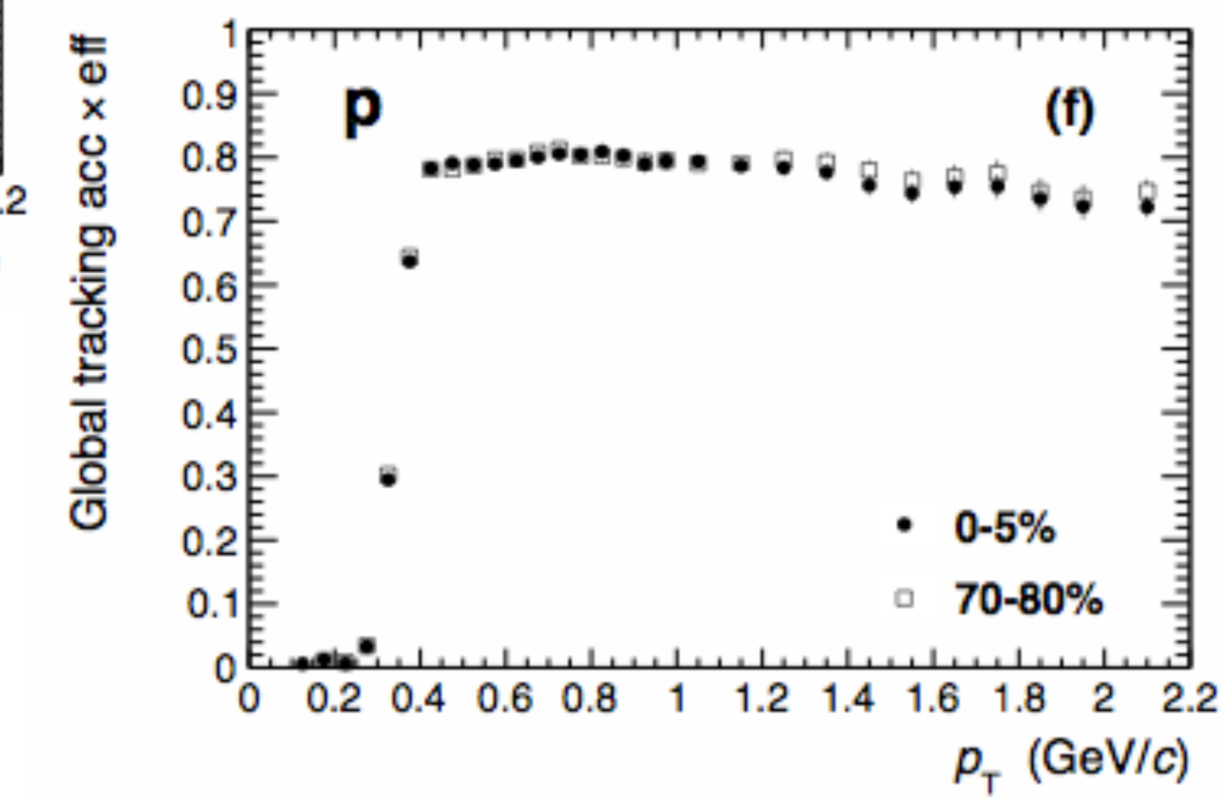

Towards a measurement of net-baryon number at LHC… (2)

- The choice of the rapidity and momentum window is crucial:
  - It needs to be systematically studied (see recent STAR results): larger than typical correlation length, but small enough that requirements of a grand-canonical ensemble are still fulfilled (global conservation of conserved quantity suppresses the signal).
  - The statistic requirements depend crucially on the maximum window. Assuming a Skellam-Distribution, we obtain in the delta-theorem that

$$\Delta K_6 \propto \sigma^4 \propto (\langle N_p \rangle + \langle N_{p^-} \rangle)^2$$

  - Current estimates indicate that between 10^8 and 10^{10} central events are needed to measure sixth order moments depending on the acceptance window and the size of the expected effect.

Net charge fluctuations

Net charge fluctuations — introduction

- So far, only a net-charge measurements corresponding has been finalized at LHC energies: **[Phys. Rev. Lett. 110, 152301]**.
- Simplified picture:

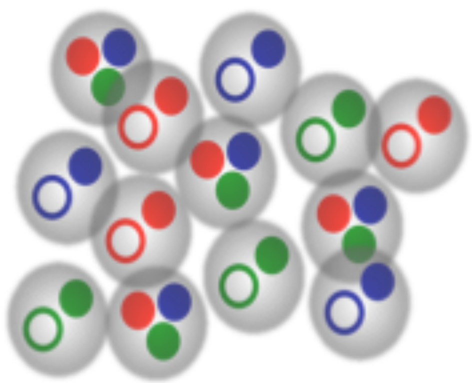

Hadronic phase:
q =±1
=> q^2 =±1

Partonic phase:
q =±(2/3),±(1/3)
=> q^2 =±(4/9),±(1/9)

- ν_{dyn} as robust variable to quantify dynamical fluctuations and to identify relevant charge carriers:

$$\nu_{(+-,dyn.)} = \frac{\langle N_+(N_+ - 1)\rangle}{\langle N_+\rangle^2} + \frac{\langle N_-(N_- - 1)\rangle}{\langle N_-\rangle^2} - 2\frac{\langle N_+ N_-\rangle}{\langle N_+\rangle\langle N_-\rangle}$$

Net charge fluctuations — introduction

- So far, only a net-charge measurements corresponding has been finalized at LHC energies: **[Phys. Rev. Lett. 110, 152301]**.
- Simplified picture:

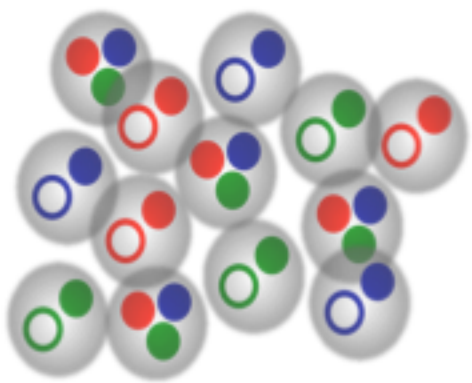

Hadronic phase:
q =±1
=> q^2 =±1

Partonic phase:
q =±(2/3),±(1/3)
=> q^2 =±(4/9),±(1/9)

Substantially smaller value of the correlation function is expected in the QGP phase than in the hadronic phase.

- ν_{dyn} as robust variable to quantify dynamical fluctuations and to identify relevant charge carriers:

$$\nu_{(+-,dyn.)} = \frac{\langle N_+(N_+-1)\rangle}{\langle N_+\rangle^2} + \frac{\langle N_-(N_--1)\rangle}{\langle N_-\rangle^2} - 2\frac{\langle N_+N_-\rangle}{\langle N_+\rangle\langle N_-\rangle}$$

D-measure of net-charge fluctuations

- ν_{dyn} can be connected to the entropy of the system via the D-measure in order to relate it to theoretical expectations (corrected for acceptance and global charge conservation):

$$D = \langle N_{ch} \rangle \langle \delta R^2 \rangle$$

$$D \approx 4 \frac{\langle \delta Q^2 \rangle}{\langle N_{ch} \rangle} \approx \begin{cases} 3 & \text{HRG} \\ 1-1.5 & \text{QGP} \end{cases}$$

$$D - 4 \approx \langle N_{ch} \rangle \nu^{corr}_{(+-,dyn)}$$

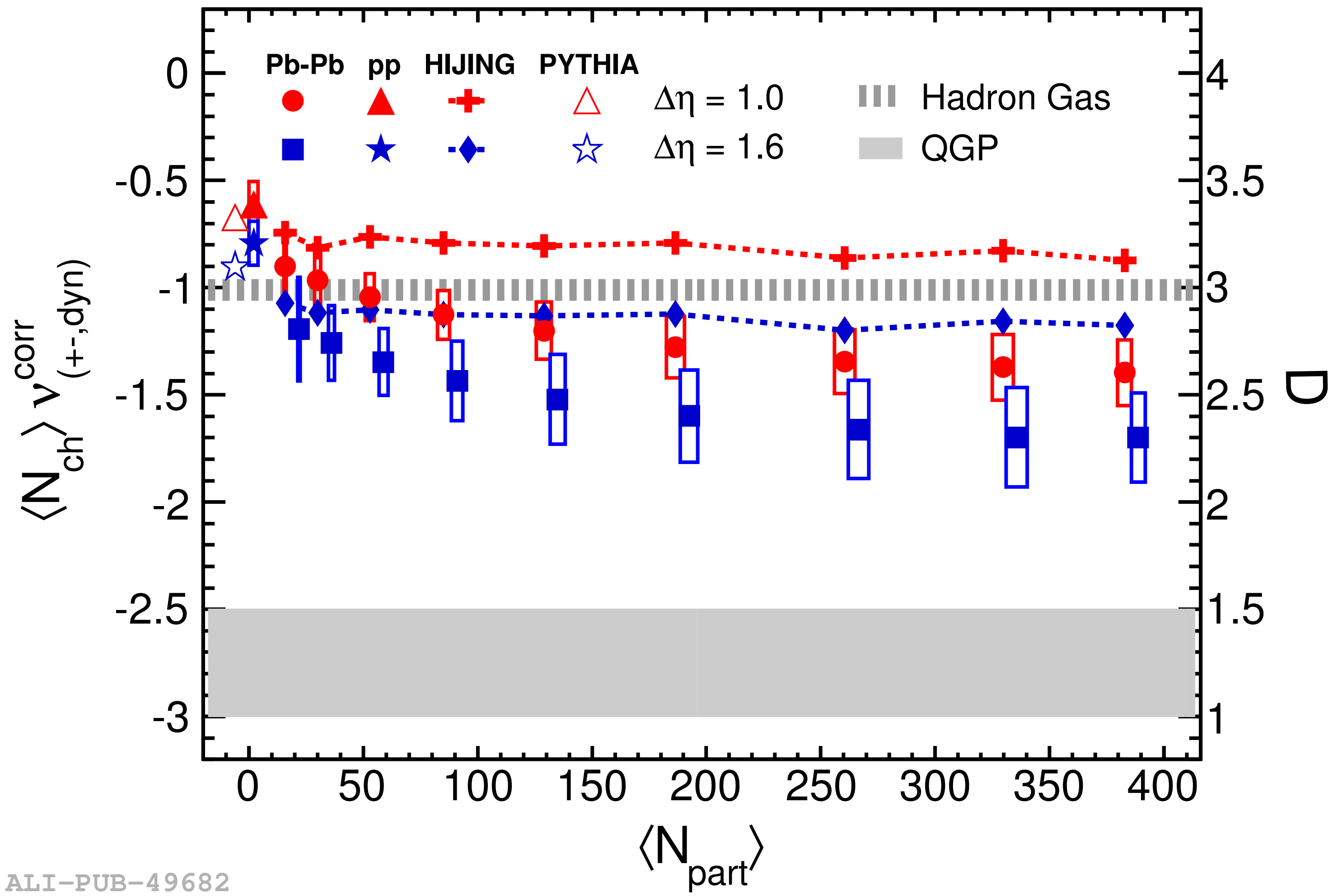

ALI-PUB-49682

D-measure of net-charge fluctuations

- ν_{dyn} can be connected to the entropy of the system via the D-measure in order to relate it to theoretical expectations (corrected for acceptance and global charge conservation):

$$D = \langle N_{ch} \rangle \langle \delta R^2 \rangle$$

$$D \approx 4 \frac{\langle \delta Q^2 \rangle}{\langle N_{ch} \rangle} \approx \begin{cases} 3 & \text{HRG} \\ 1-1.5 & \text{QGP} \end{cases}$$

$$D - 4 \approx \langle N_{ch} \rangle \nu^{corr}_{(+-,dyn)}$$

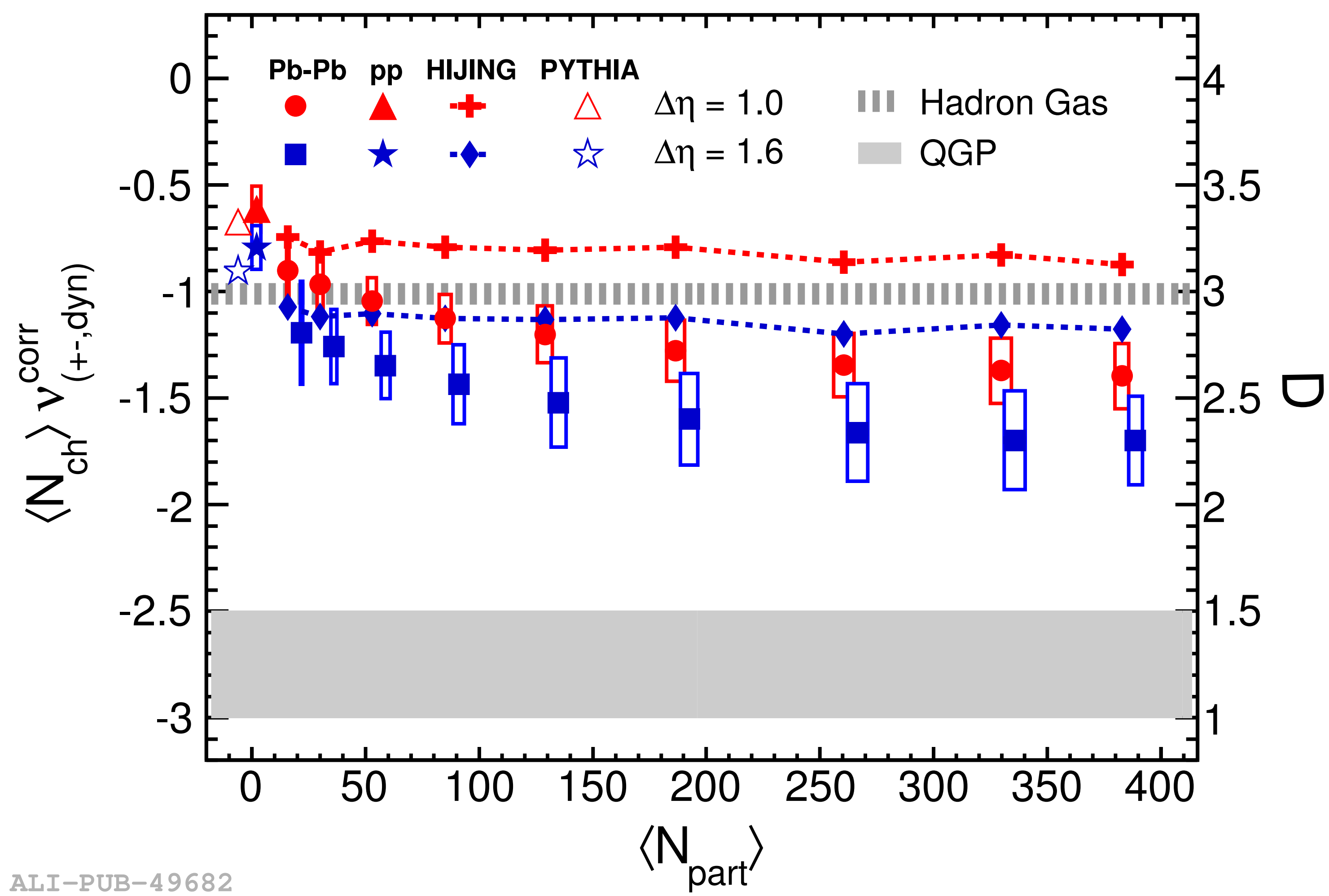

D decreases slightly with centrality and shows values between HRG and QGP expectation.

D-measure of net-charge fluctuations

- ν_{dyn} can be connected to the entropy of the system via the D-measure in order to relate it to theoretical expectations (corrected for acceptance and global charge conservation):

$$D = \langle N_{ch} \rangle \langle \delta R^2 \rangle$$

$$D \approx 4 \frac{\langle \delta Q^2 \rangle}{\langle N_{ch} \rangle} \approx \begin{cases} 3 & \text{HRG} \\ 1-1.5 & \text{QGP} \end{cases}$$

$$D - 4 \approx \langle N_{ch} \rangle \nu^{corr}_{(+-,dyn)}$$

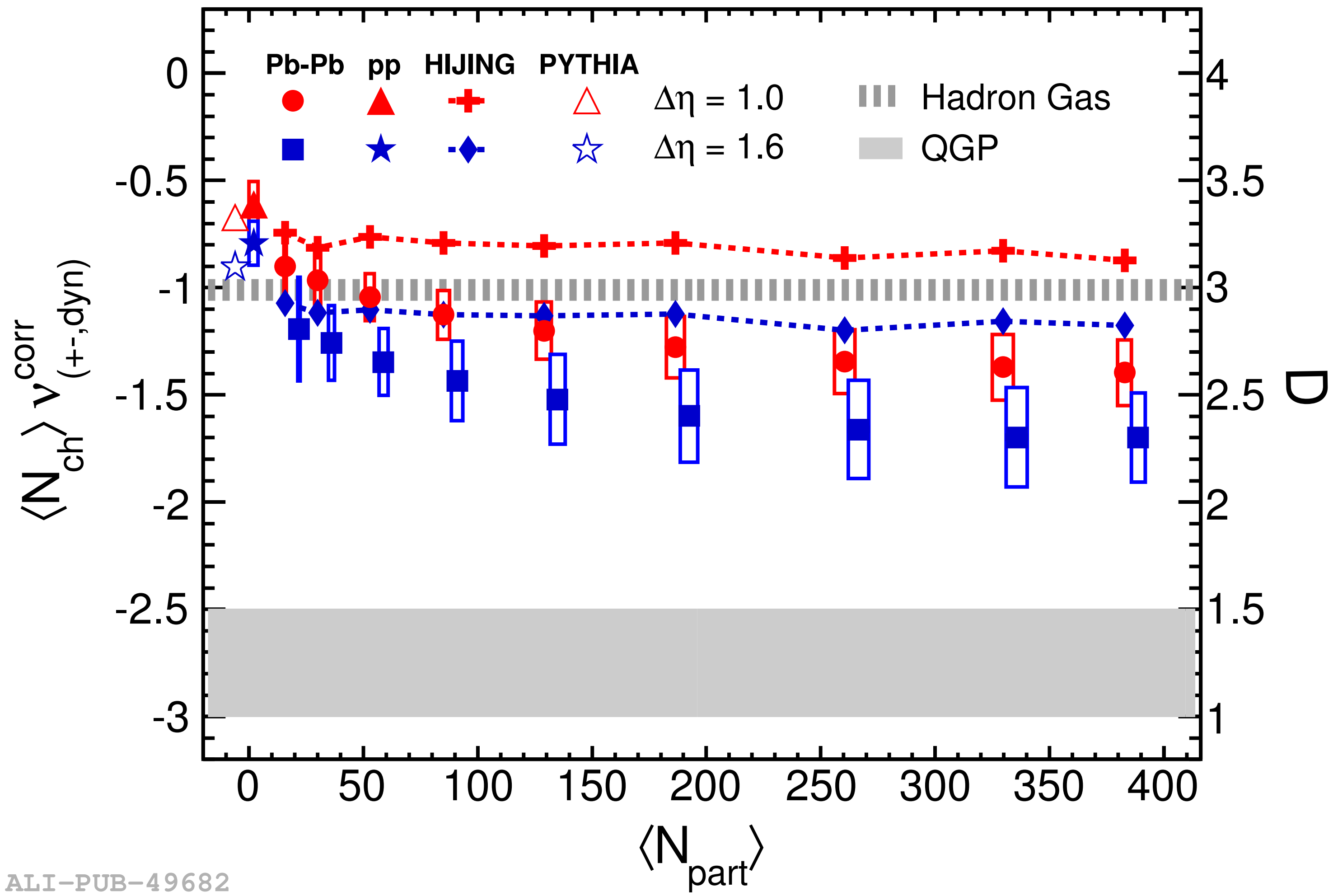

D decreases slightly with centrality and shows values between HRG and QGP expectation.

HIJING shows no centrality dependence and larger values than the data.

Energy and rapidity window dependence

- Results are shown for 0-5% most central collisions.
- Decreasing trend with increasing center-of-mass energy is observed.
- ALICE values significantly lower than the hadron gas expectation while RHIC measurements are still compatible.
- Strong dependence on rapidity window observed which saturates above $\Delta\eta \approx 2.3$. Initial fluctuations are diluted by final state interactions and limited experimental acceptance.

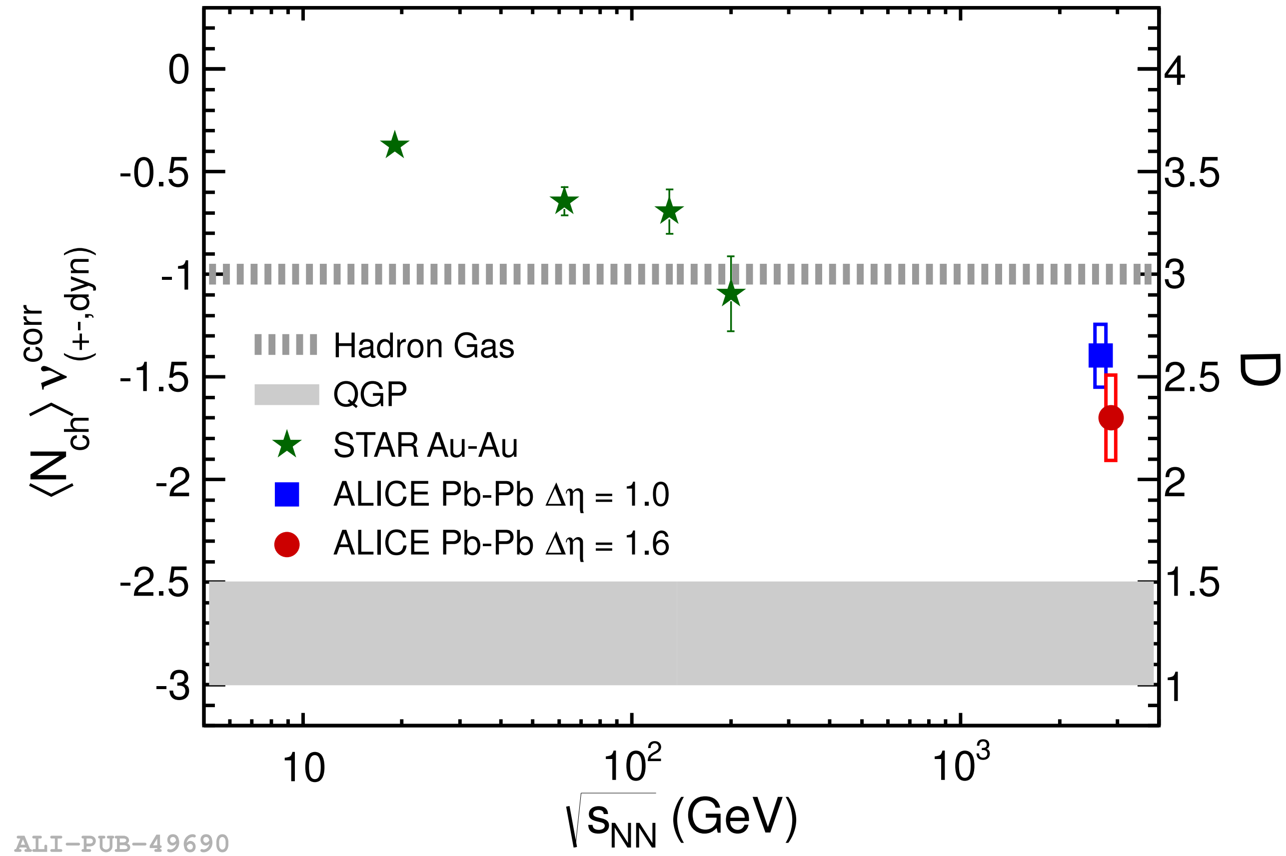

ALI-PUB-49690

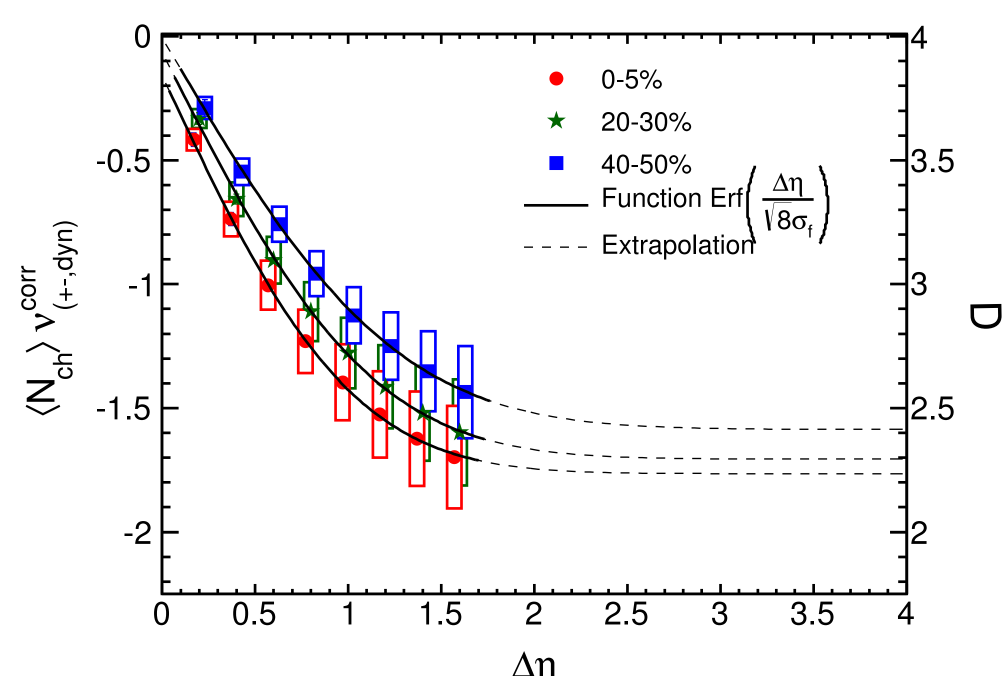

ALI-PUB-49686

Summary & conclusion

Summary and conclusions

- Light flavor hadron yields at LHC energies can be described in a thermal fit based on the hadron resonance gas model with a chemical freeze-out temperature of T_{chem} = 156 MeV.
- Production of light (anti-)nuclei is found to be in agreement with this temperature. Within thermal-statistical models, their yield is independent of feed-down from (unknown) resonances.
- In order to find deviations from HRG, the measurements of event-by-event fluctuations of conserved quantities (charge, baryon number, strangeness) are on their way…
- Measurements of net-charge fluctuations indicate a reduction of fluctuations from RHIC to LHC (as expected), but also emphasize the importance of systematic studies w.r.t. to the acceptance window etc.

SUPPORTING SLIDES

Missing strange resonances (Lattice QCD)

[1404.6511]

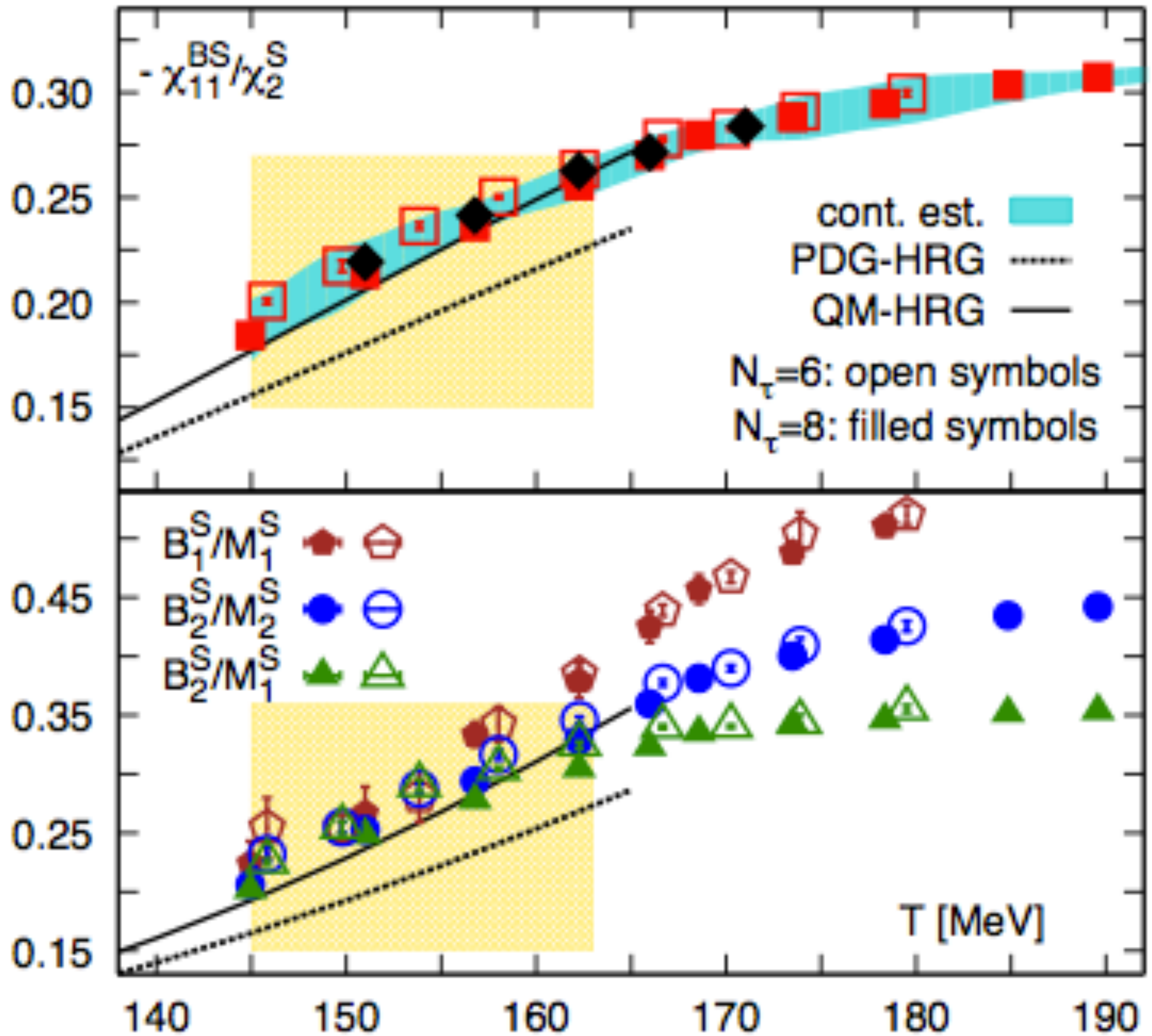

Nuclei and non-equilibrium models

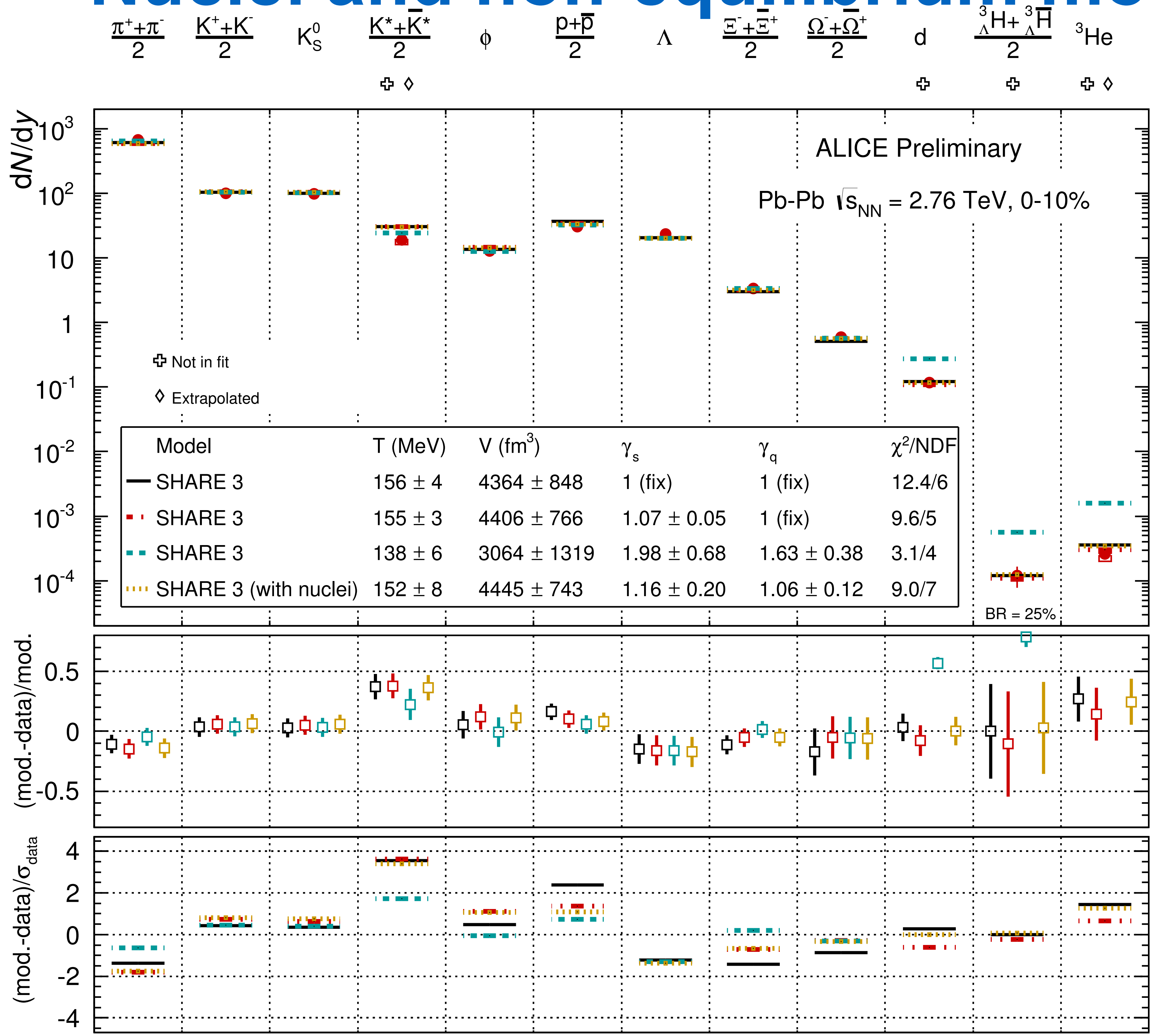

Nuclei and non-equilibrium models

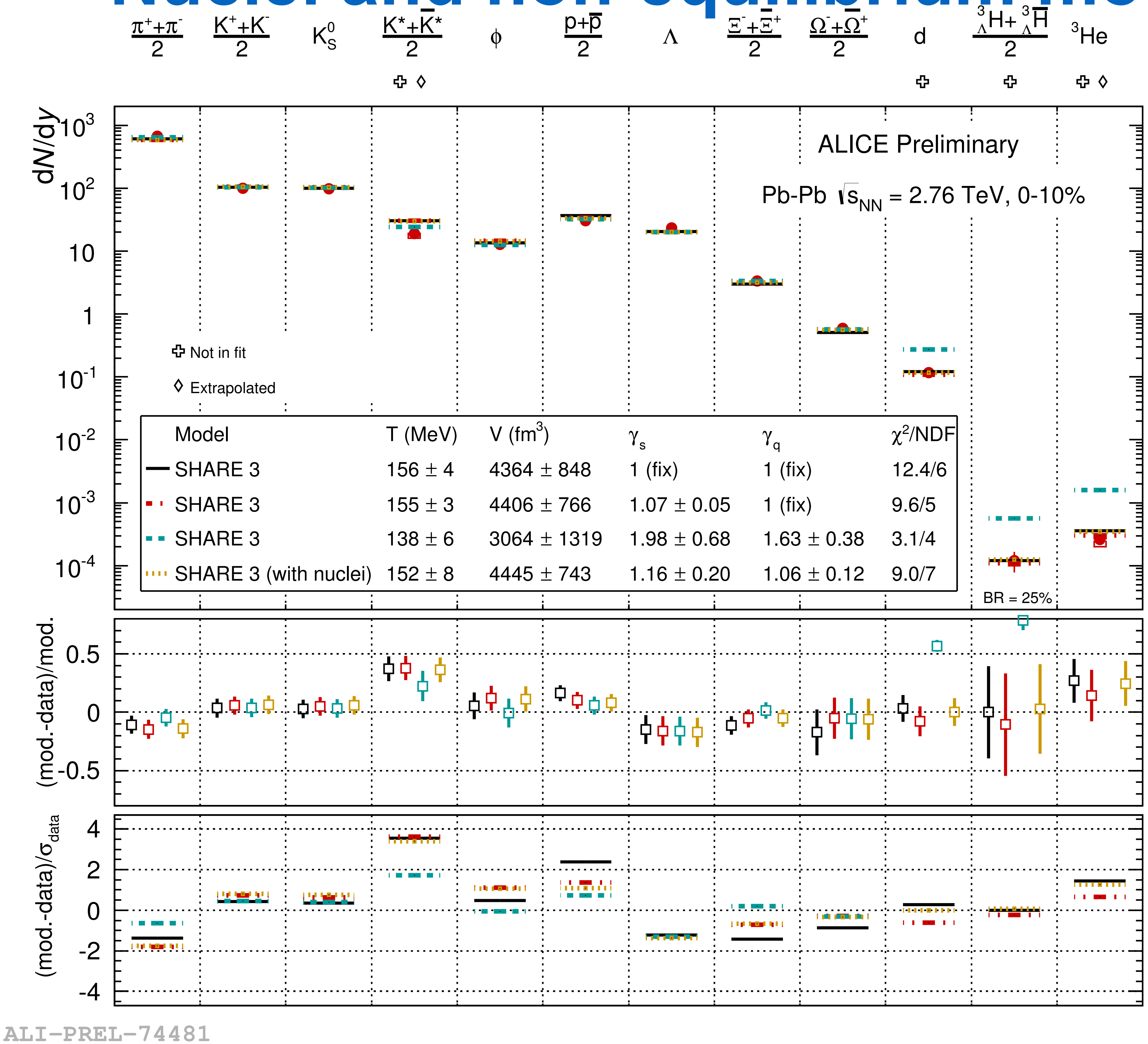

SHARE performs a thermal fit in an equilibrium mode (γ_q=γ_s=1) or in a non-equilibrium mode (γ_q and γ_s free).

Nuclei and non-equilibrium models

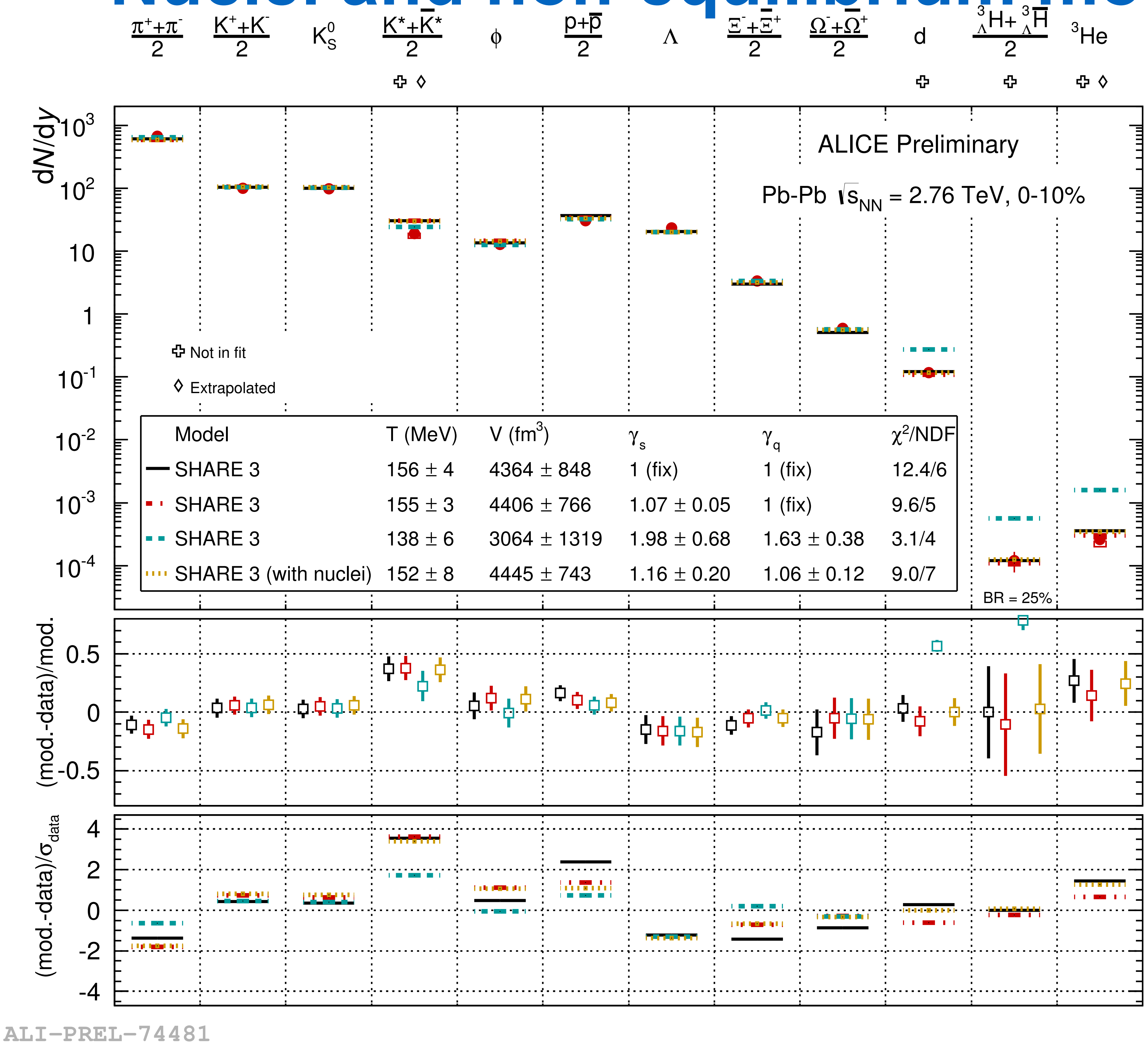

SHARE performs a thermal fit in an equilibrium mode ($\gamma_q=\gamma_s=1$) or in a non-equilibrium mode (γ_q and γ_s free).

In equilibrium mode, the model describes the nuclei yields.

Nuclei and non-equilibrium models

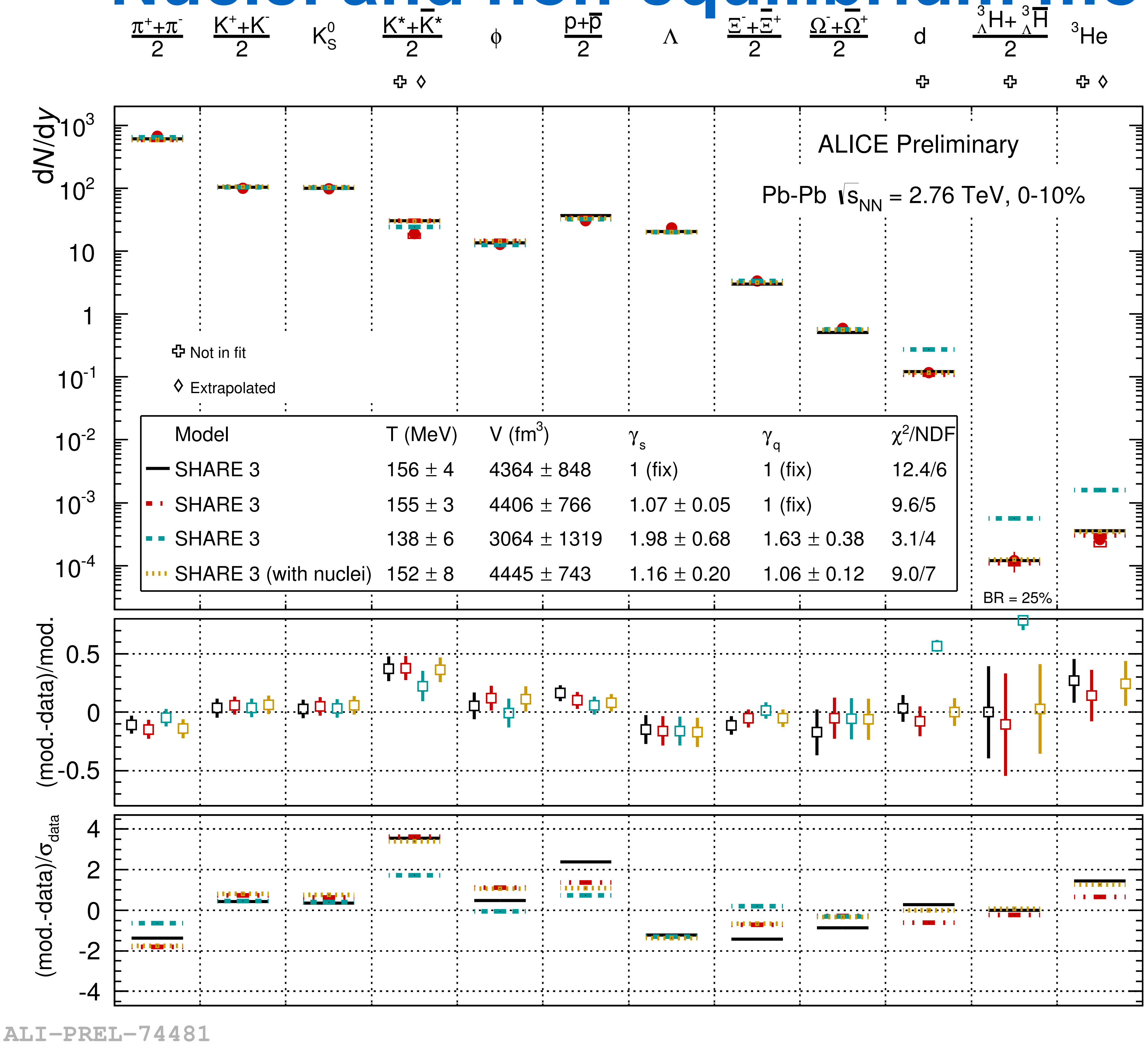

SHARE performs a thermal fit in an equilibrium mode ($\gamma_q = \gamma_s = 1$) or in a non-equilibrium mode (γ_q and γ_s free).

In equilibrium mode, the model describes the nuclei yields.

In non-equilibrium mode and *if nuclei are not included*, the model converges to values of γ_q and γ_s which are significantly different from 1 and yields a slightly better description for protons and Ξs.

Nuclei and non-equilibrium models

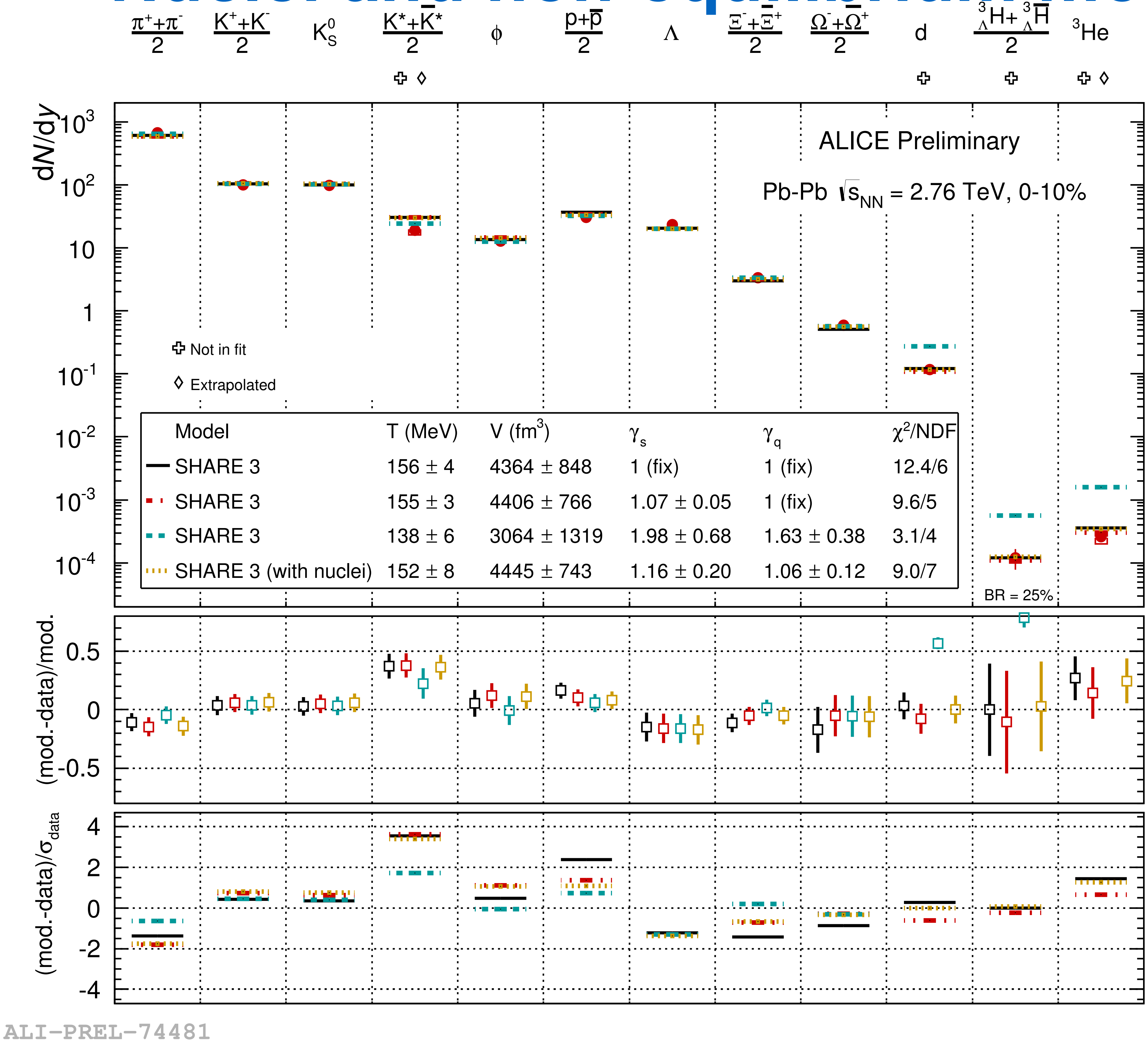

SHARE performs a thermal fit in an equilibrium mode (γ_q=γ_s=1) or in a non-equilibrium mode (γ_q and γ_s free).

In equilibrium mode, the model describes the nuclei yields.

In non-equilibrium mode and *if nuclei are not included*, the model converges to values of γ_q and γ_s which are significantly different from 1 and yields a slightly better description for protons and Ξs.

In non-equilibrium mode and *if nuclei are included*, the model converges to values of γ_q and γ_s which are in agreement with 1.

Radial flow in Pb-Pb

- Mass ordering

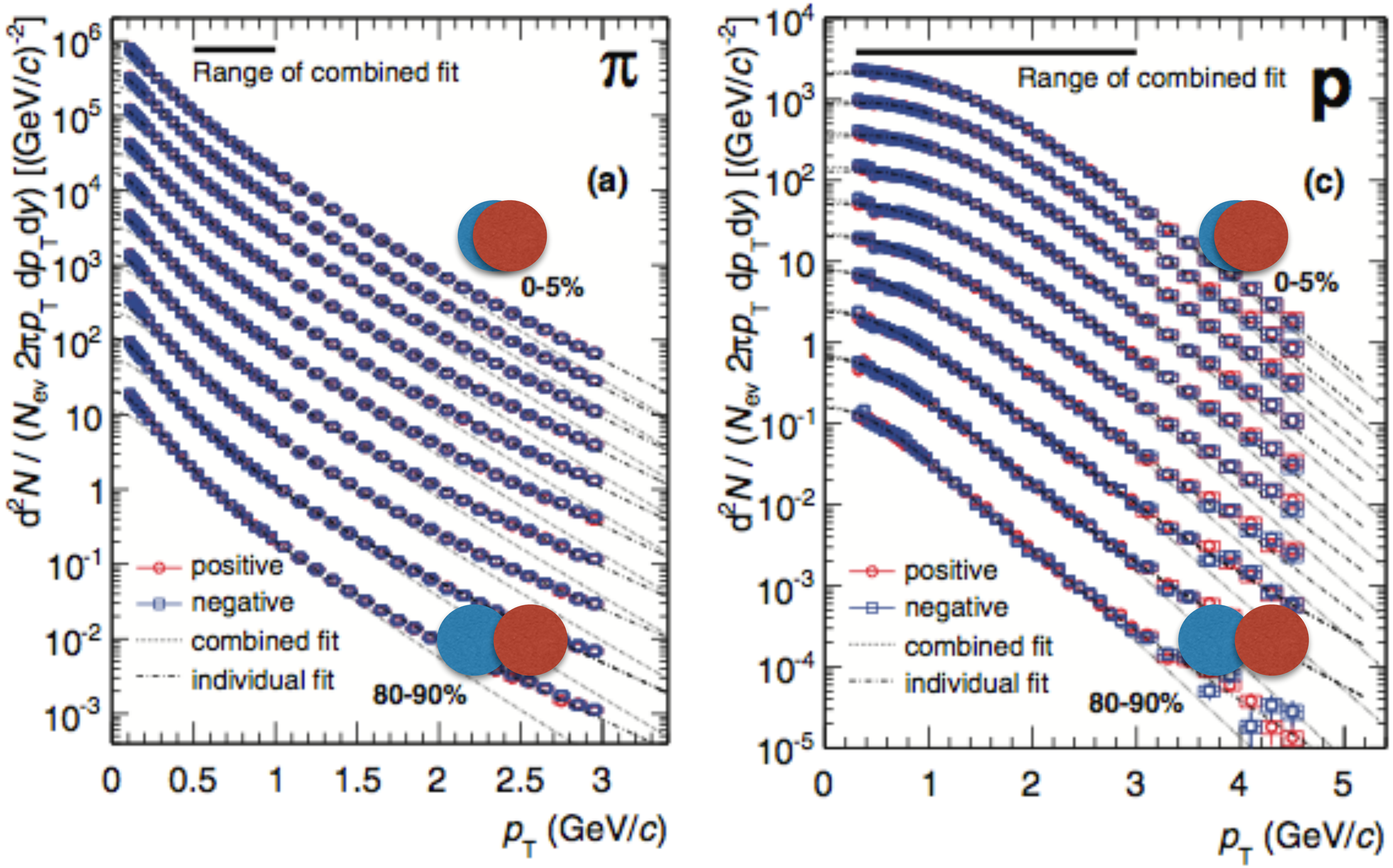

[Phys. Rev. C 88, 044910 (2013)]

Radial flow in Pb-Pb

- Mass ordering

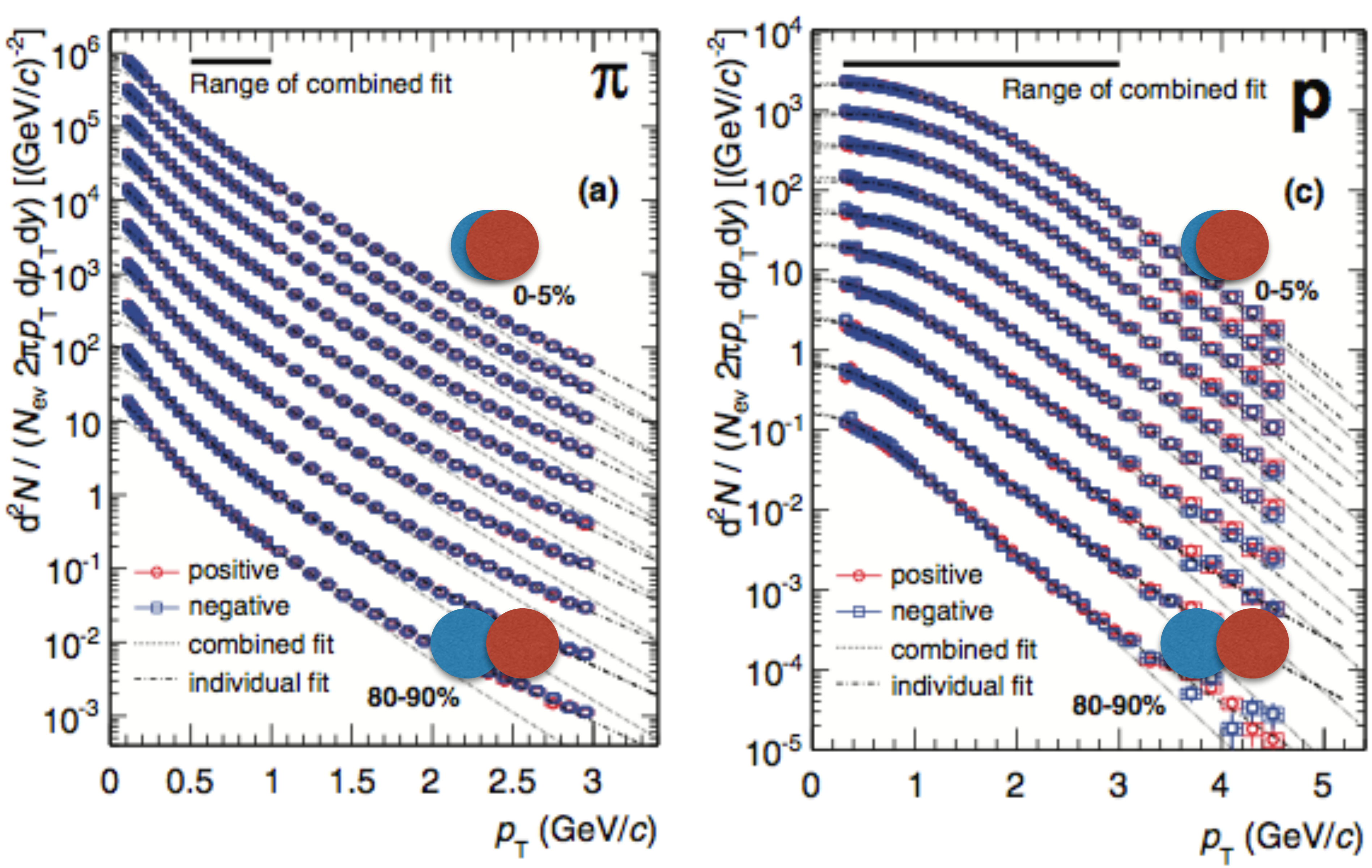

[Phys. Rev. C 88, 044910 (2013)]

Characteristic hardening of the spectrum with increasing centrality. It is more pronounced for the heavier protons than for pions.
→ *Mass ordering* as expected from hydrodynamics.

Radial flow in Pb-Pb

- Mass ordering

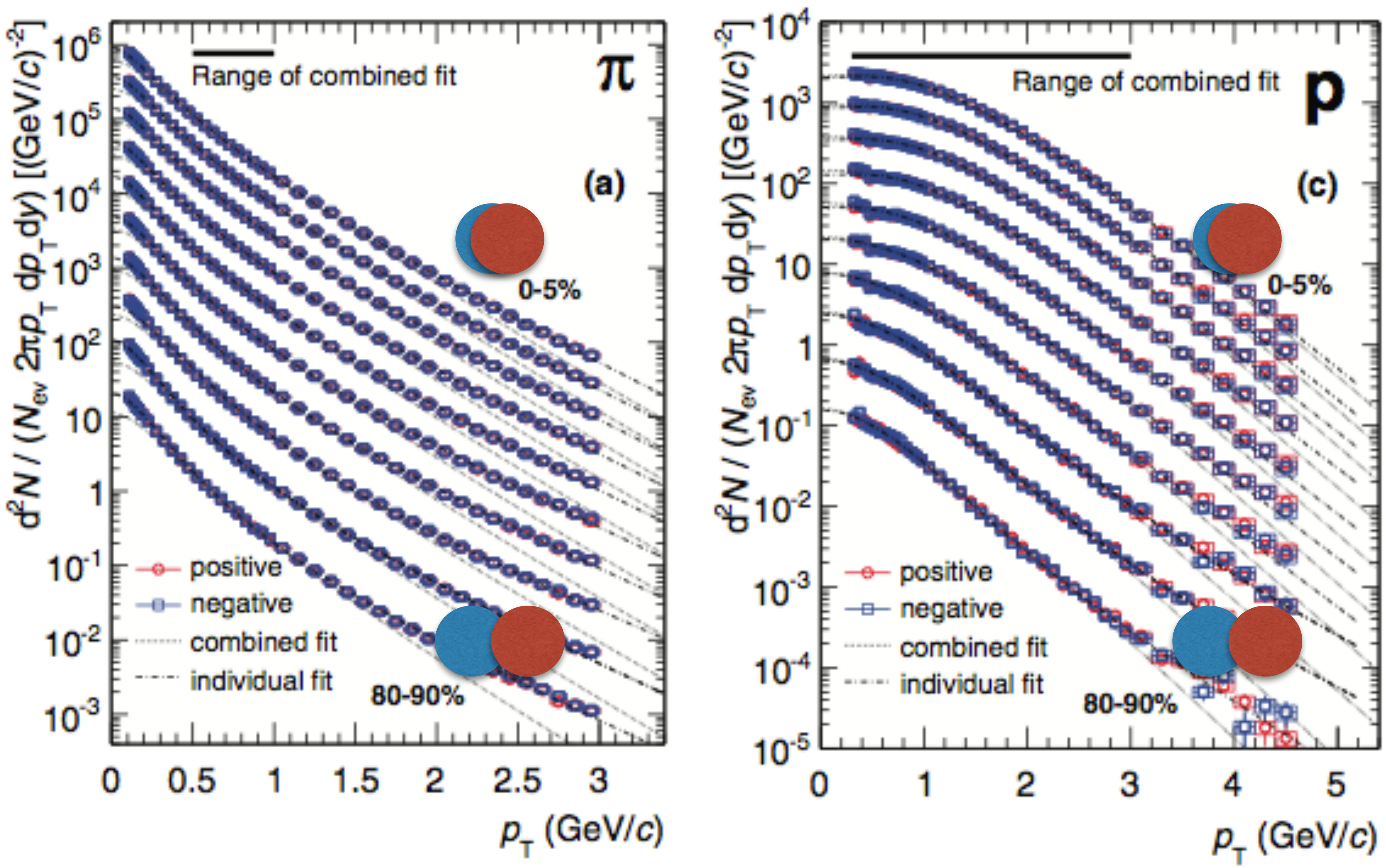

[Phys. Rev. C 88, 044910 (2013)]

Characteristic hardening of the spectrum with increasing centrality. It is more pronounced for the heavier protons than for pions. → *Mass ordering* as expected from hydrodynamics.

Very clean signature of radial flow in Pb-Pb collisions.

Radial flow in Pb-Pb

- Mass ordering

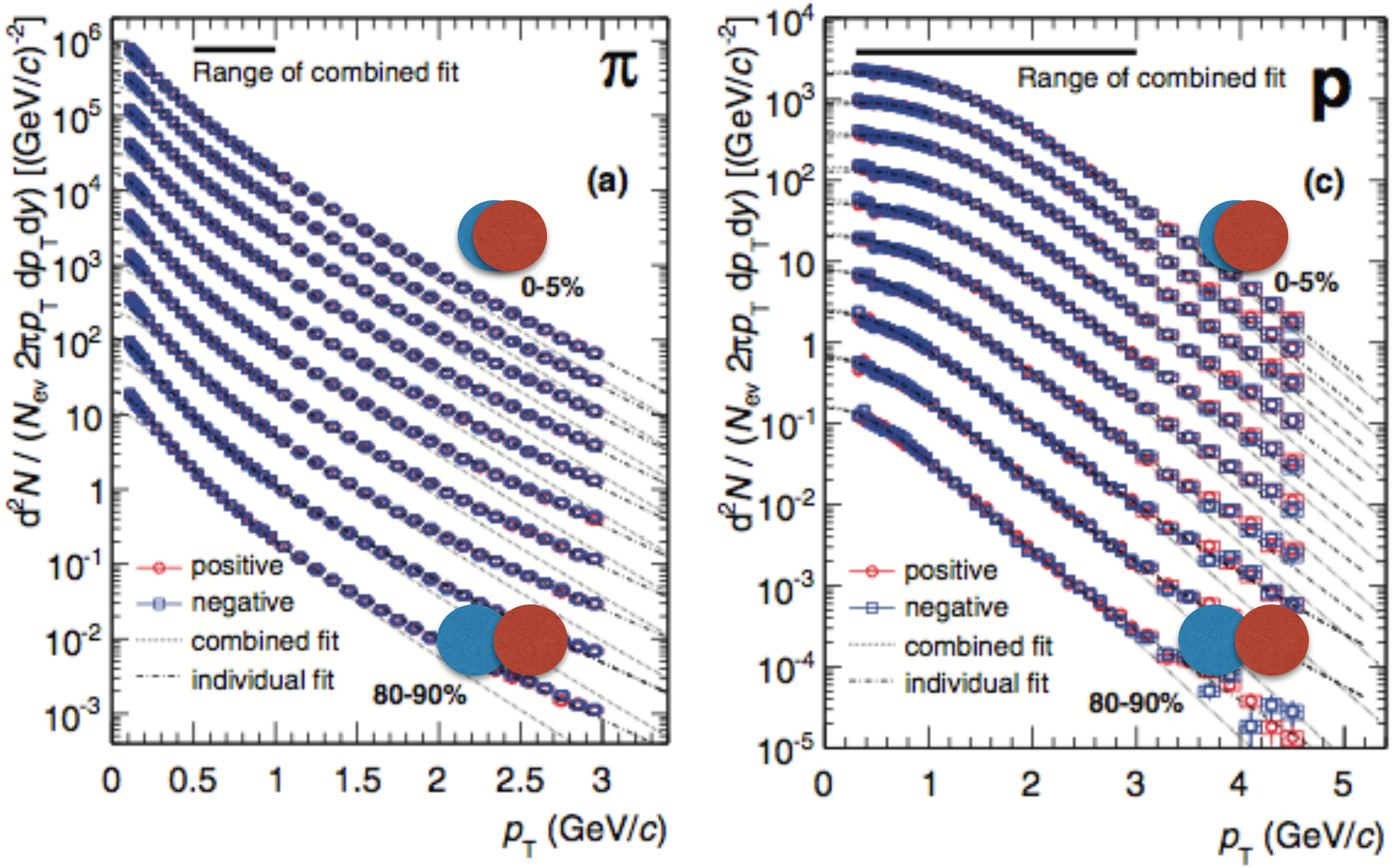

[Phys. Rev. C 88, 044910 (2013)]

Characteristic hardening of the spectrum with increasing centrality. It is more pronounced for the heavier protons than for pions. → *Mass ordering* as expected from hydrodynamics.

Very clean signature of radial flow in Pb-Pb collisions.

Full hydro models describe spectra fairly well.

Radial flow in Pb-Pb

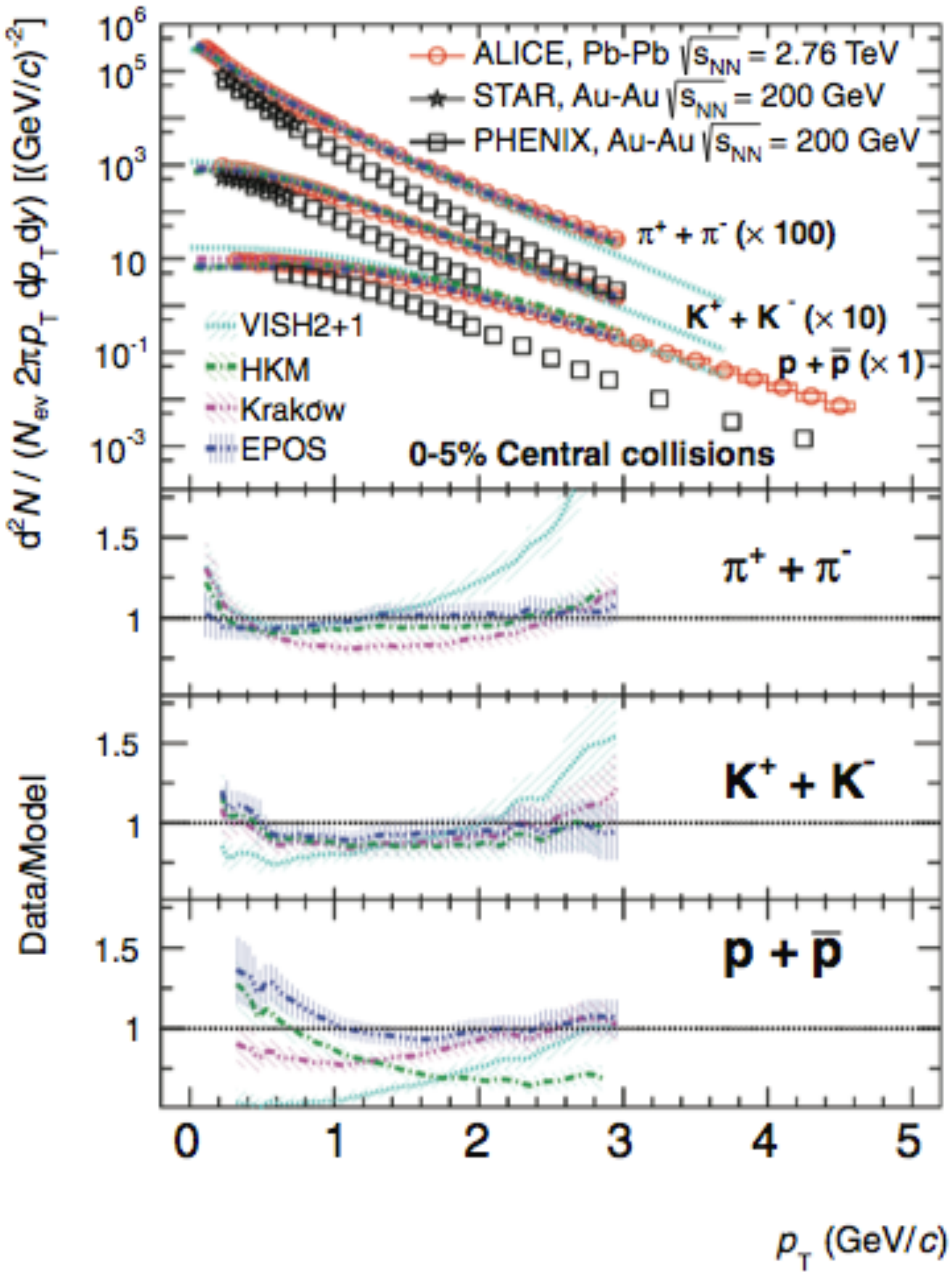

Characteristic hardening of the spectrum with increasing centrality. It is more pronounced for the heavier protons than for pions.
→ *Mass ordering* as expected from hydrodynamics.

Very clean signature of radial flow in Pb-Pb collisions.

Full hydro models describe spectra fairly well.

Radial flow in Pb-Pb

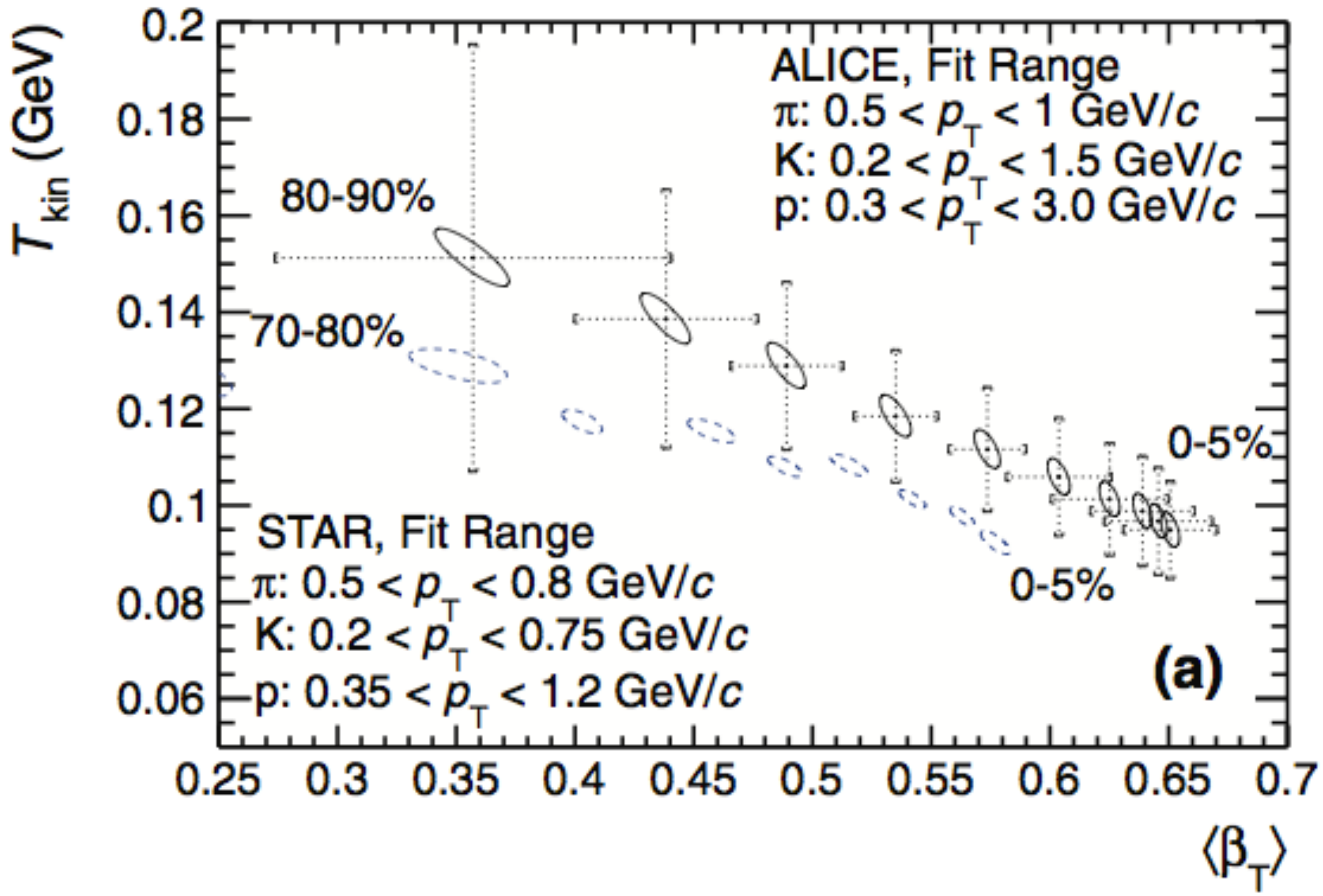

Characteristic hardening of the spectrum with increasing centrality. It is more pronounced for the heavier protons than for pions. → *Mass ordering* as expected from hydrodynamics.

Very clean signature of radial flow in Pb-Pb collisions.

Full hydro models describe spectra fairly well.

Radial flow in Pb-Pb

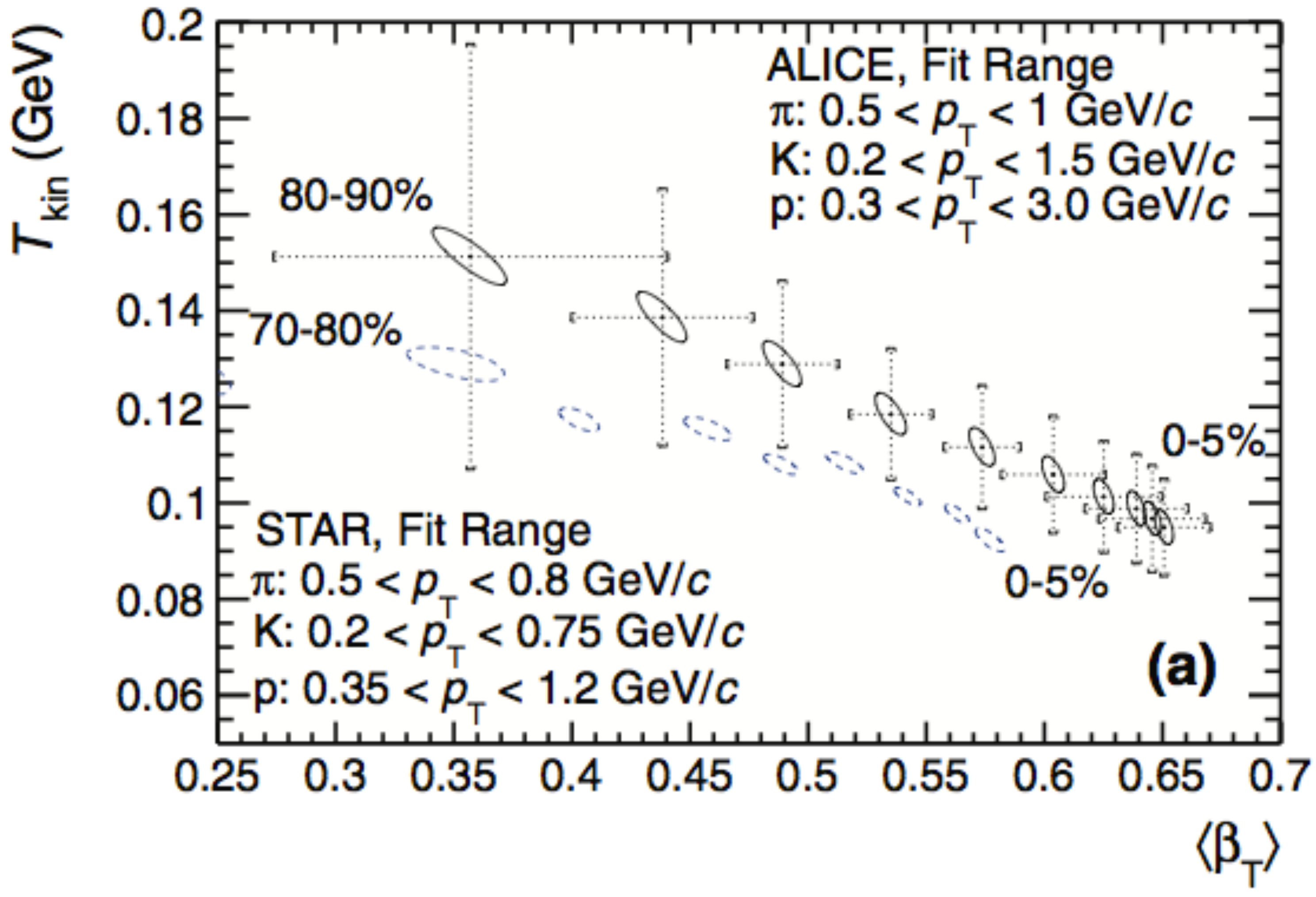

Characteristic hardening of the spectrum with increasing centrality. It is more pronounced for the heavier protons than for pions. → *Mass ordering* as expected from hydrodynamics.

Very clean signature of radial flow in Pb-Pb collisions.

Full hydro models describe spectra fairly well.

A combined blast-wave fit to the data (**simplified hydro model** → T_{kin}, β) gives also a reasonable description allowing a systematic study of the evolution of the spectral shape versus centrality.

Radial flow in Pb-Pb

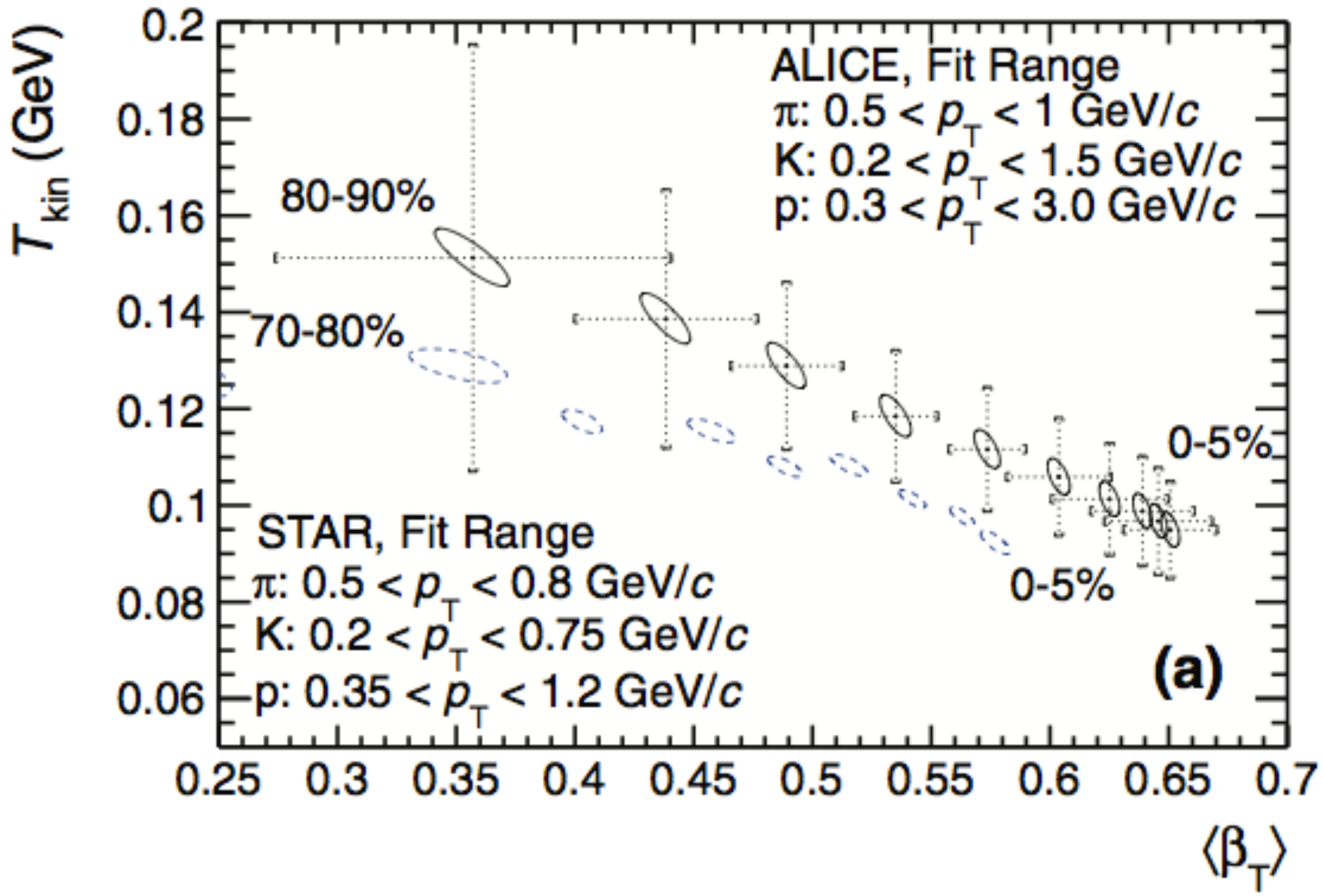

Characteristic hardening of the spectrum with increasing centrality. It is more pronounced for the heavier protons than for pions. → *Mass ordering* as expected from hydrodynamics.

Very clean signature of radial flow in Pb-Pb collisions.

Full hydro models describe spectra fairly well.

A combined blast-wave fit to the data (**simplified hydro model** → T_{kin}, β) gives also a reasonable description allowing a systematic study of the evolution of the spectral shape versus centrality.

Within the severe limitations of the blast-wave model one finds: $T_{kin} \approx 100$ MeV significantly smaller than $T_{chem} \approx 156$ MeV and an average transverse expansion velocity around $<\beta_T>$ 0.65 for most central Pb-Pb collisions.

Φ/π and Φ/p ratios

- The mass ordering can be best validated by looking simultaneously at Φ-mesons and protons, because of their similar mass.

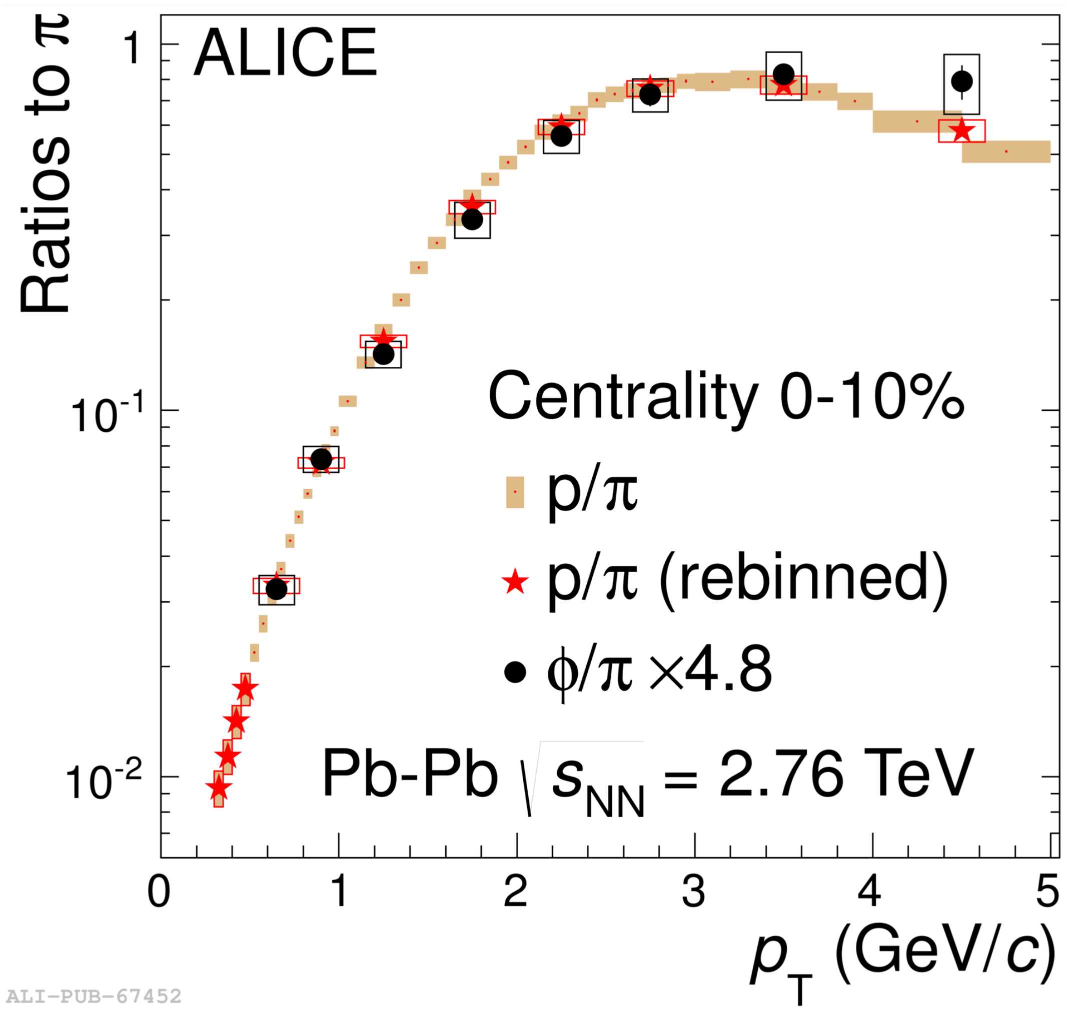

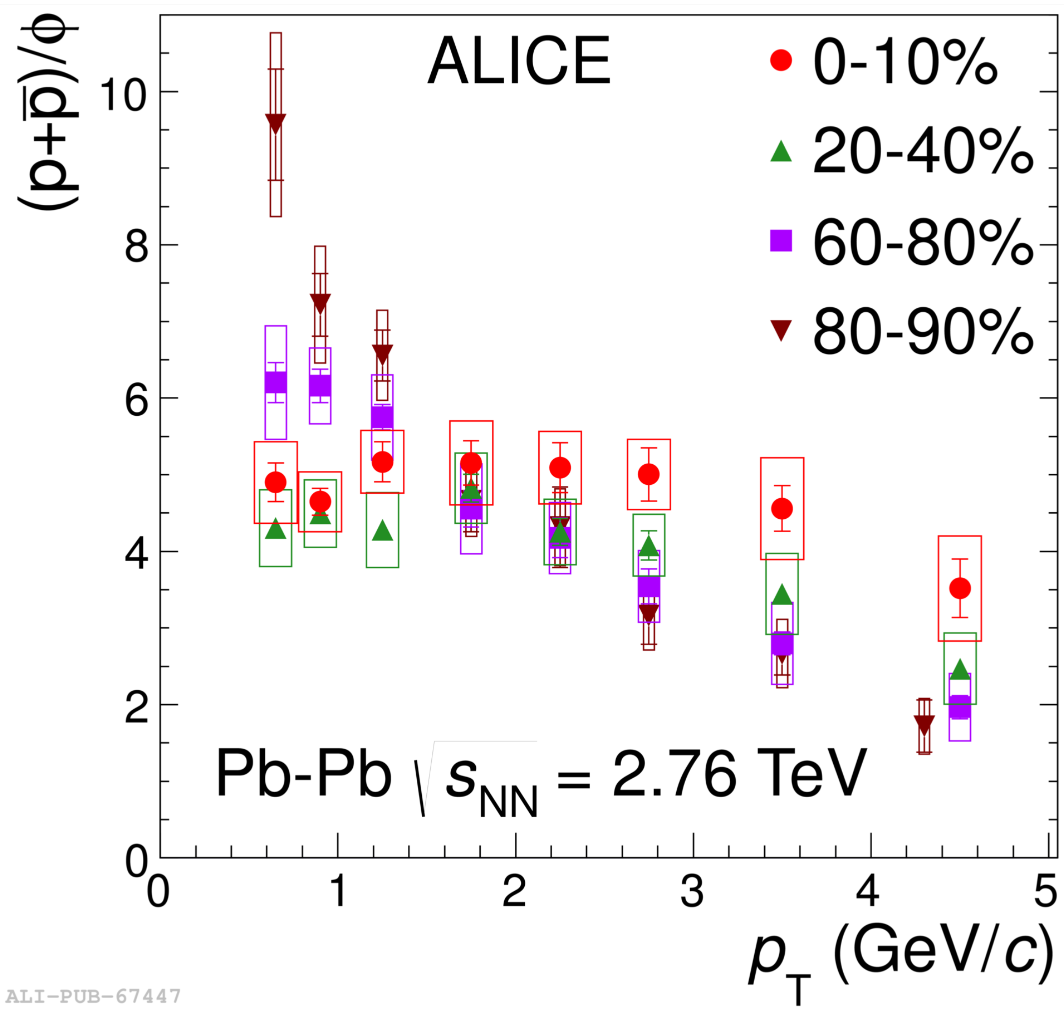

[1404.0495]

Φ/π and Φ/p ratios

- The mass ordering can be best validated by looking simultaneously at Φ-mesons and protons, because of their similar mass.

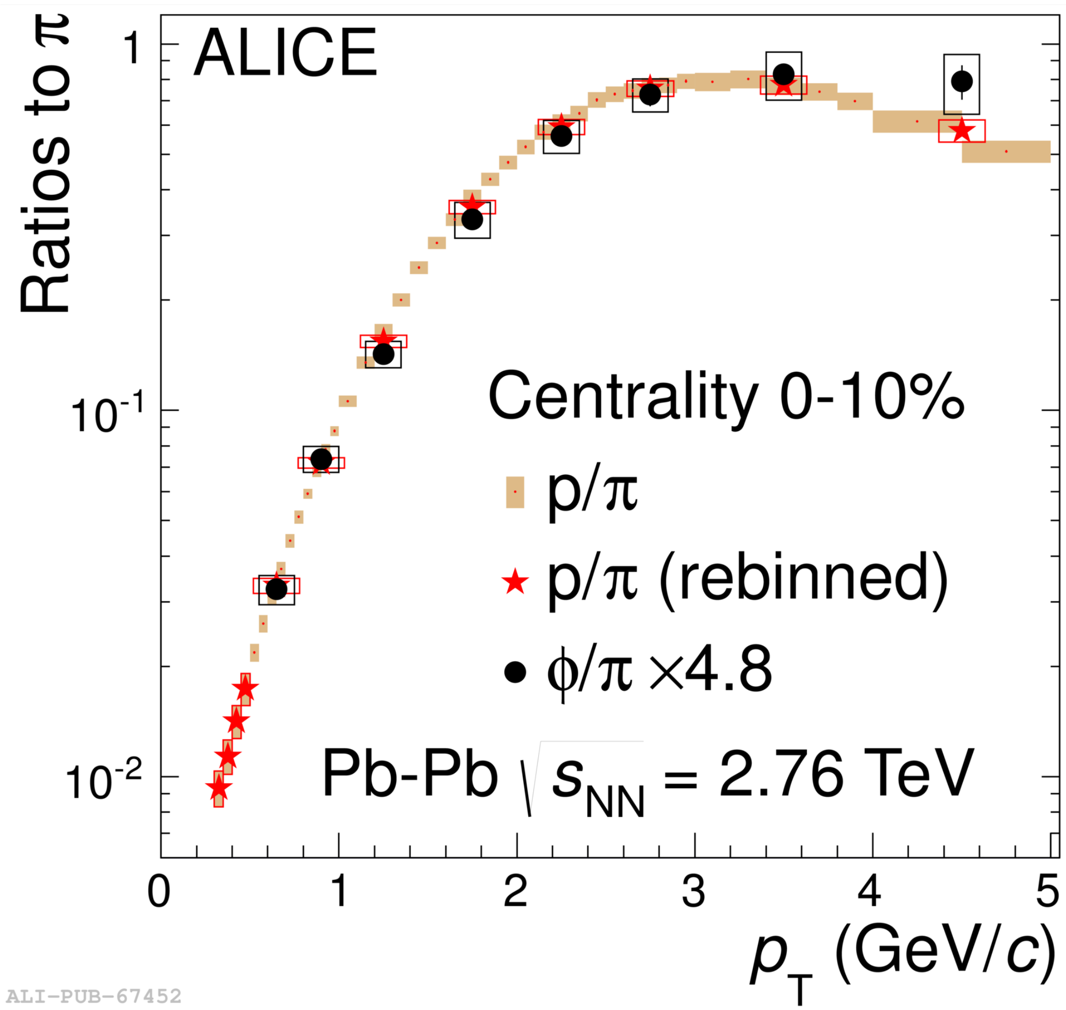

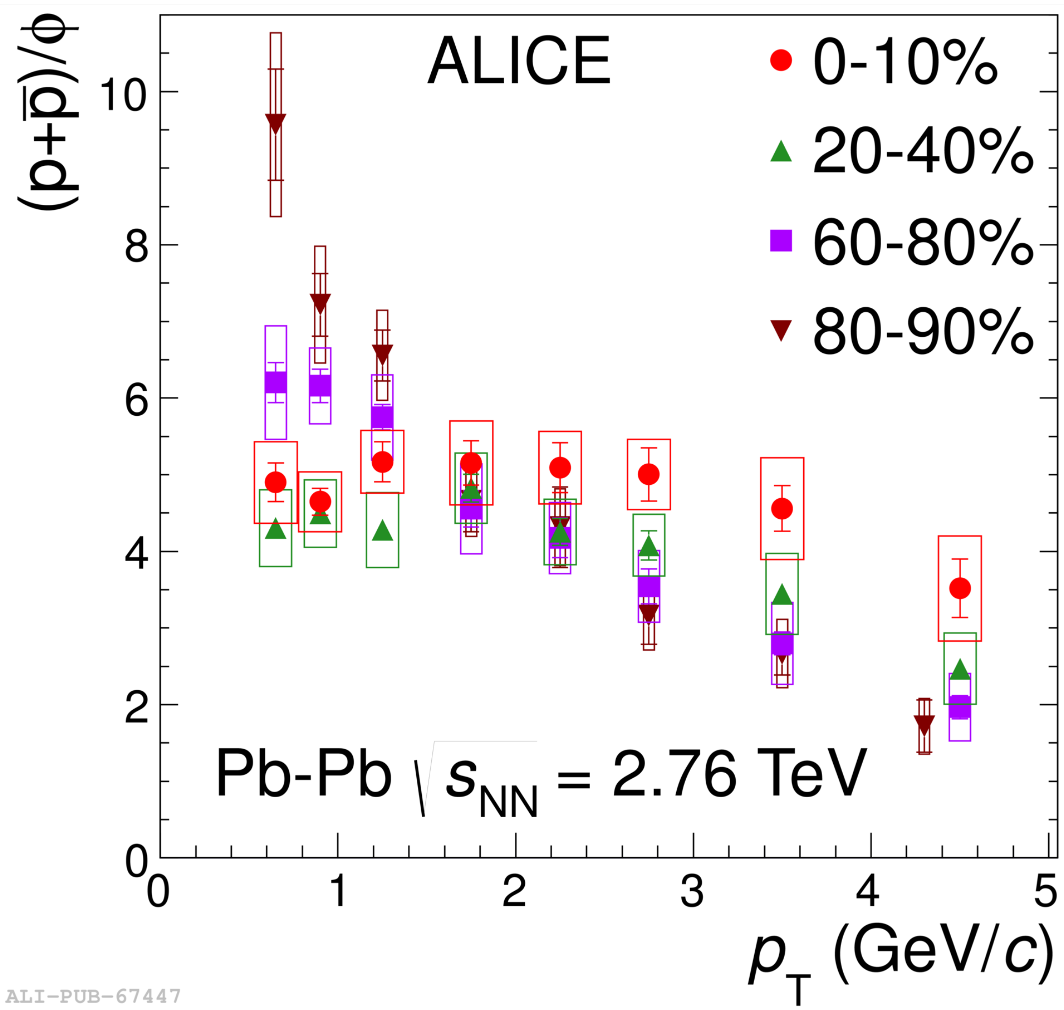

[1404.0495]

Baryon-to-meson and meson-to-meson have similar shapes in central Pb-Pb if the masses of the baryon and the meson are similar: p/Φ is flat as a function of p_T for p_T < 3-4 GeV/c.

Φ/π and Φ/p ratios

- The mass ordering can be best validated by looking simultaneously at Φ-mesons and protons, because of their similar mass.

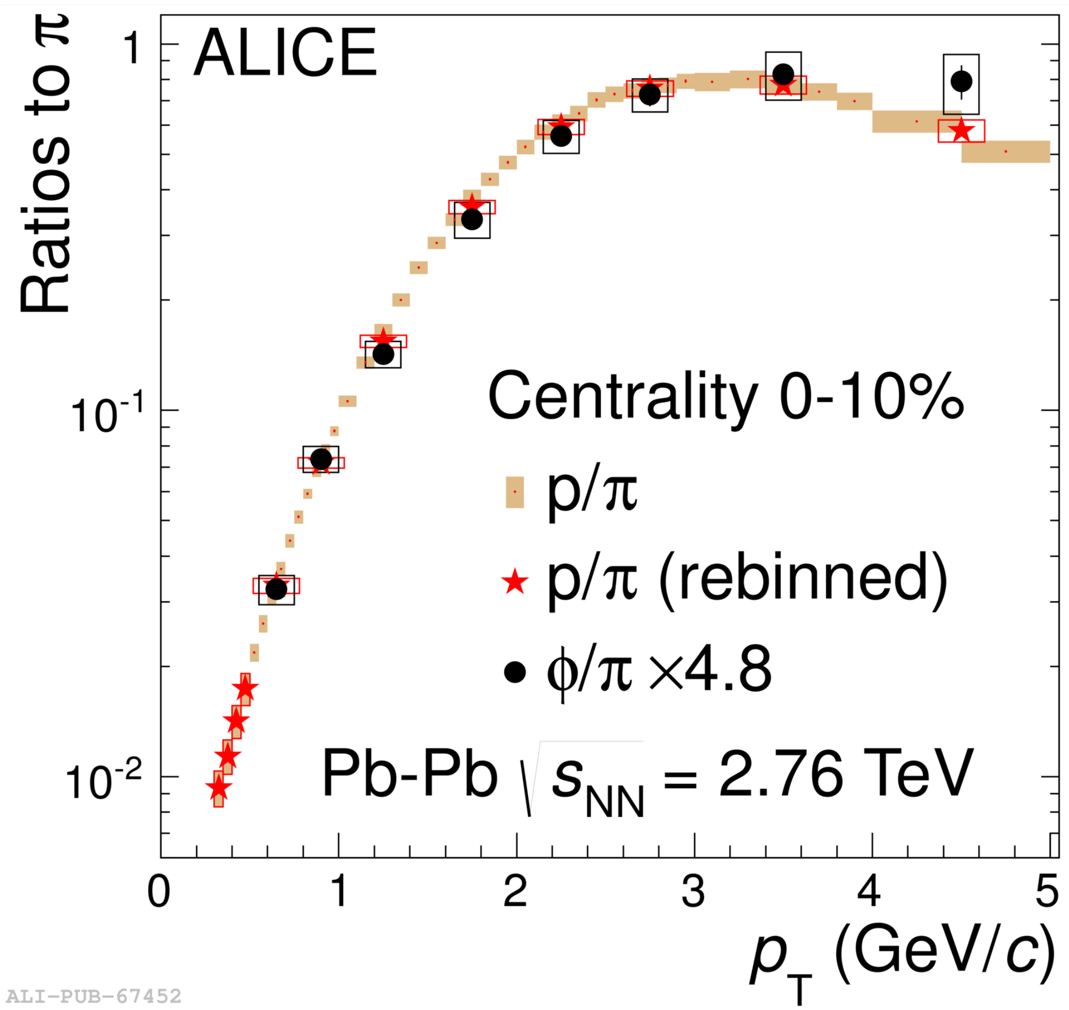

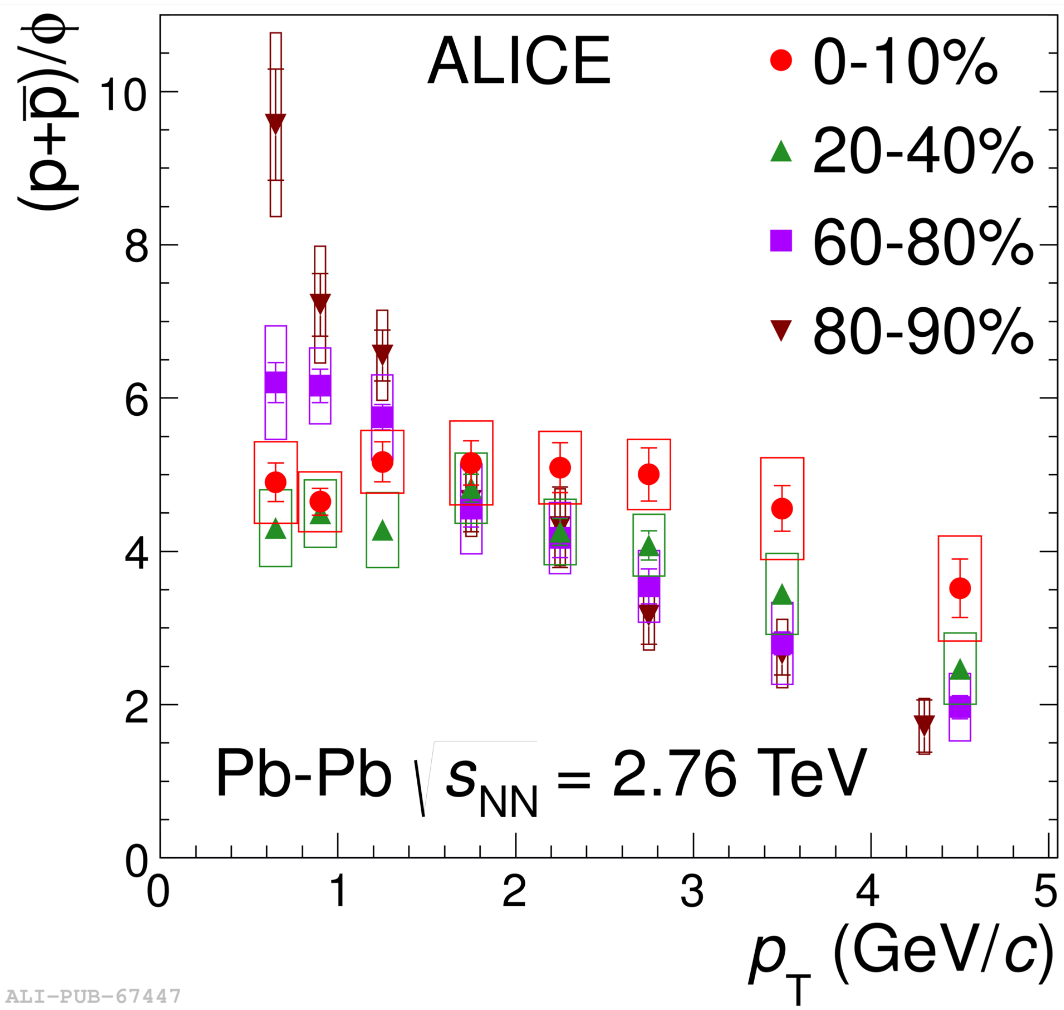

[1404.0495]

Baryon-to-meson and meson-to-meson have similar shapes in central Pb-Pb if the masses of the baryon and the meson are similar: p/Φ is flat as a function of p_T for $p_T < 3$-4 GeV/*c*.

This suggests a clean mass dependency (not number of valence quarks) at low p_T in central Pb-Pb, consistent with the hydrodynamic picture.

Blast-wave fits to p-Pb data

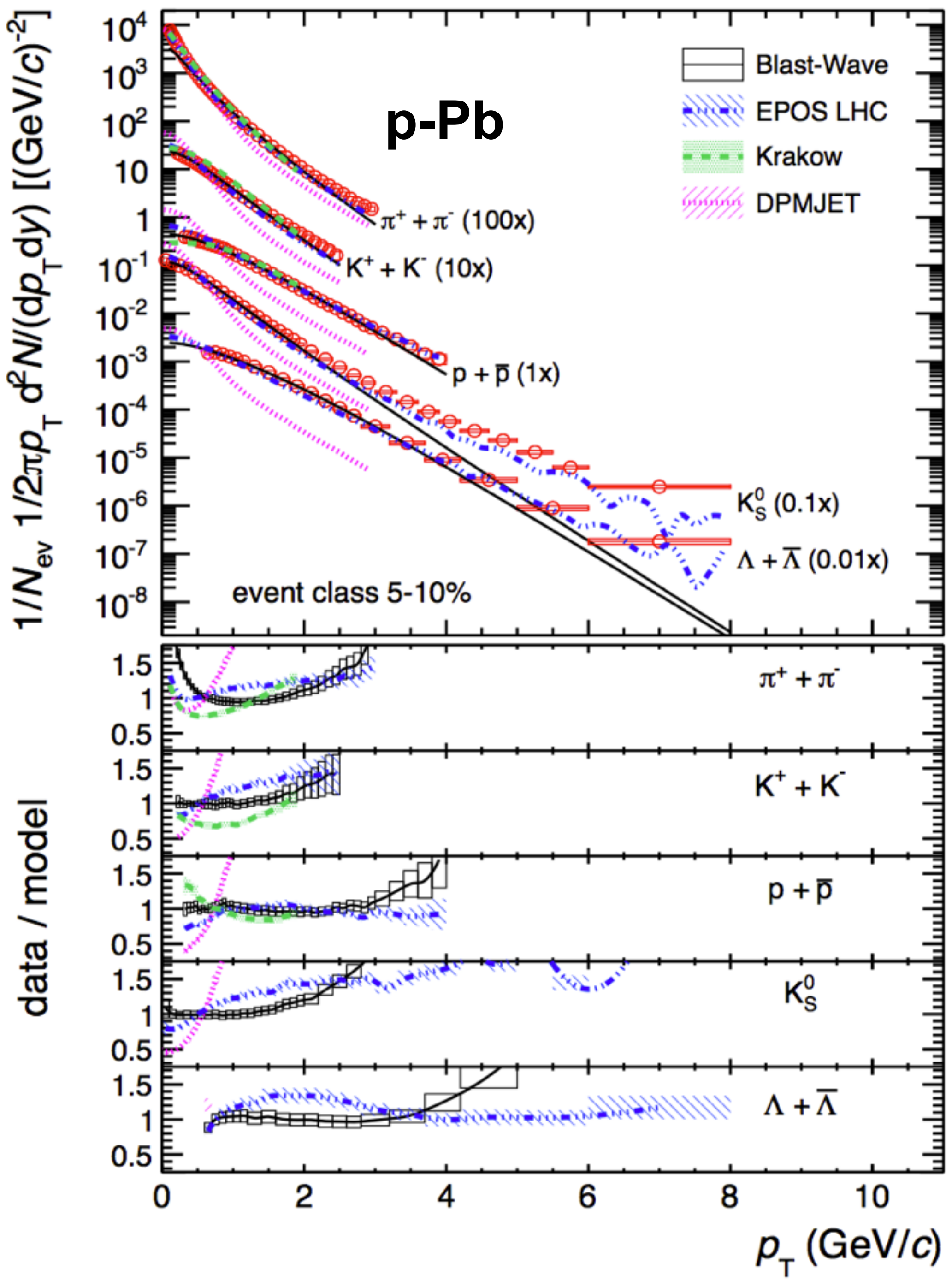

[Phys. Lett. B 728 (2014) 25-38]

Blast-wave fits to p-Pb data

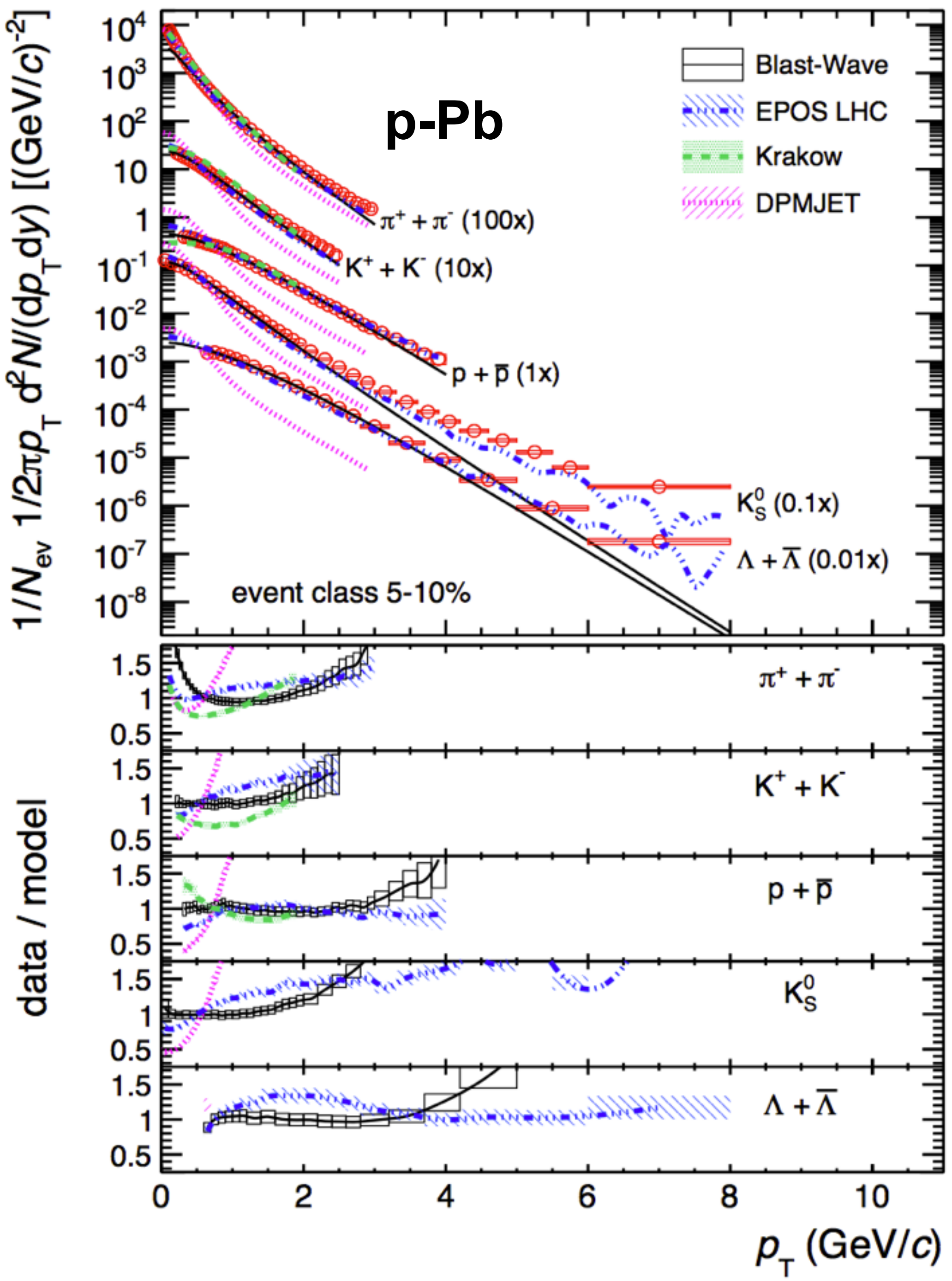

[Phys. Lett. B 728 (2014) 25-38]

Hydrodynamic models (EPOS, Krakow) show a better agreement than QCD inspired models (DPMJET).

Blast-wave fits to p-Pb data

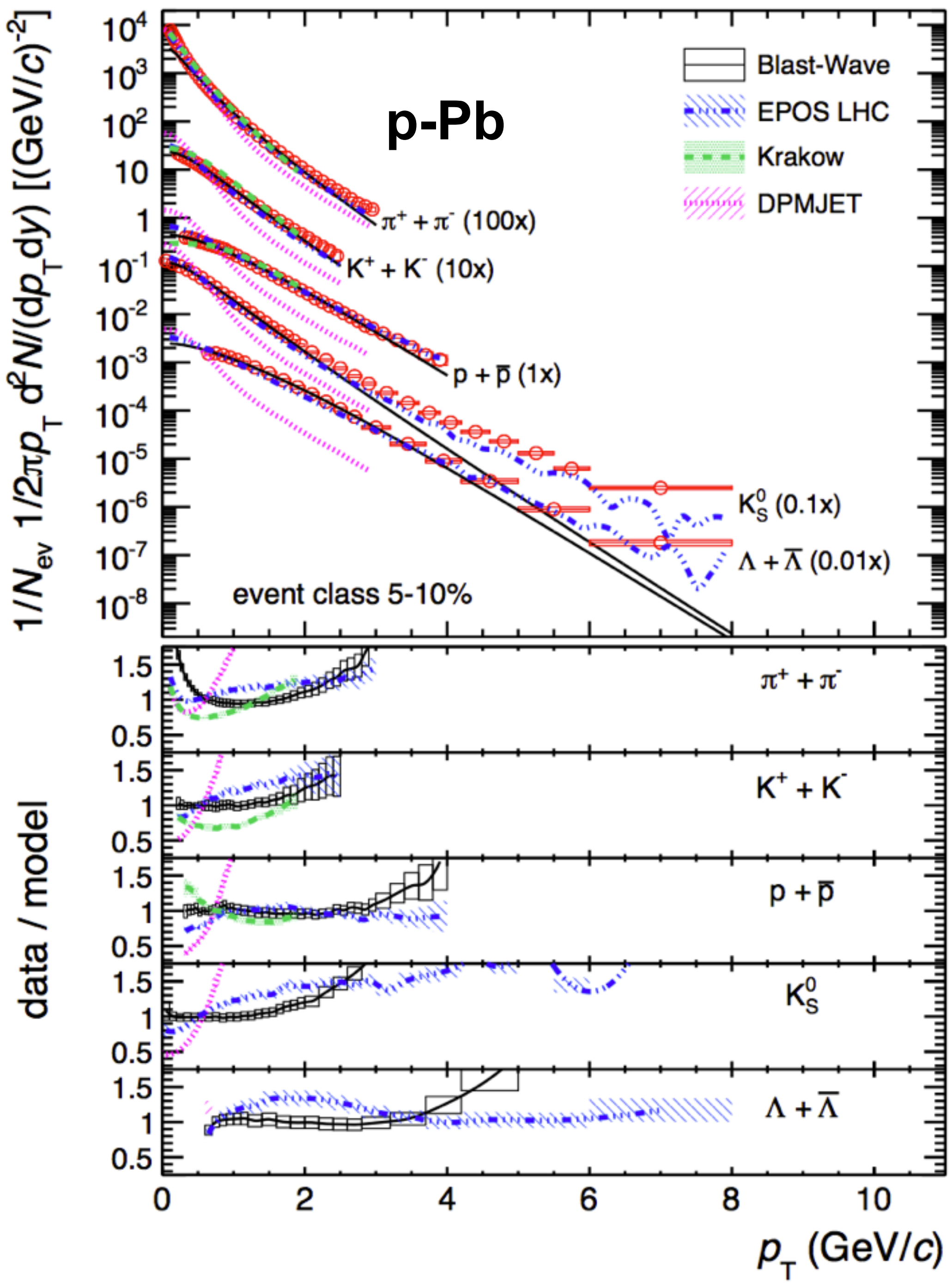

[Phys. Lett. B 728 (2014) 25-38]

Hydrodynamic models (EPOS, Krakow) show a better agreement than QCD inspired models (DPMJET).

A combined blast-wave fit to the data gives a reasonable description also here.

Blast-wave fits to p-Pb data

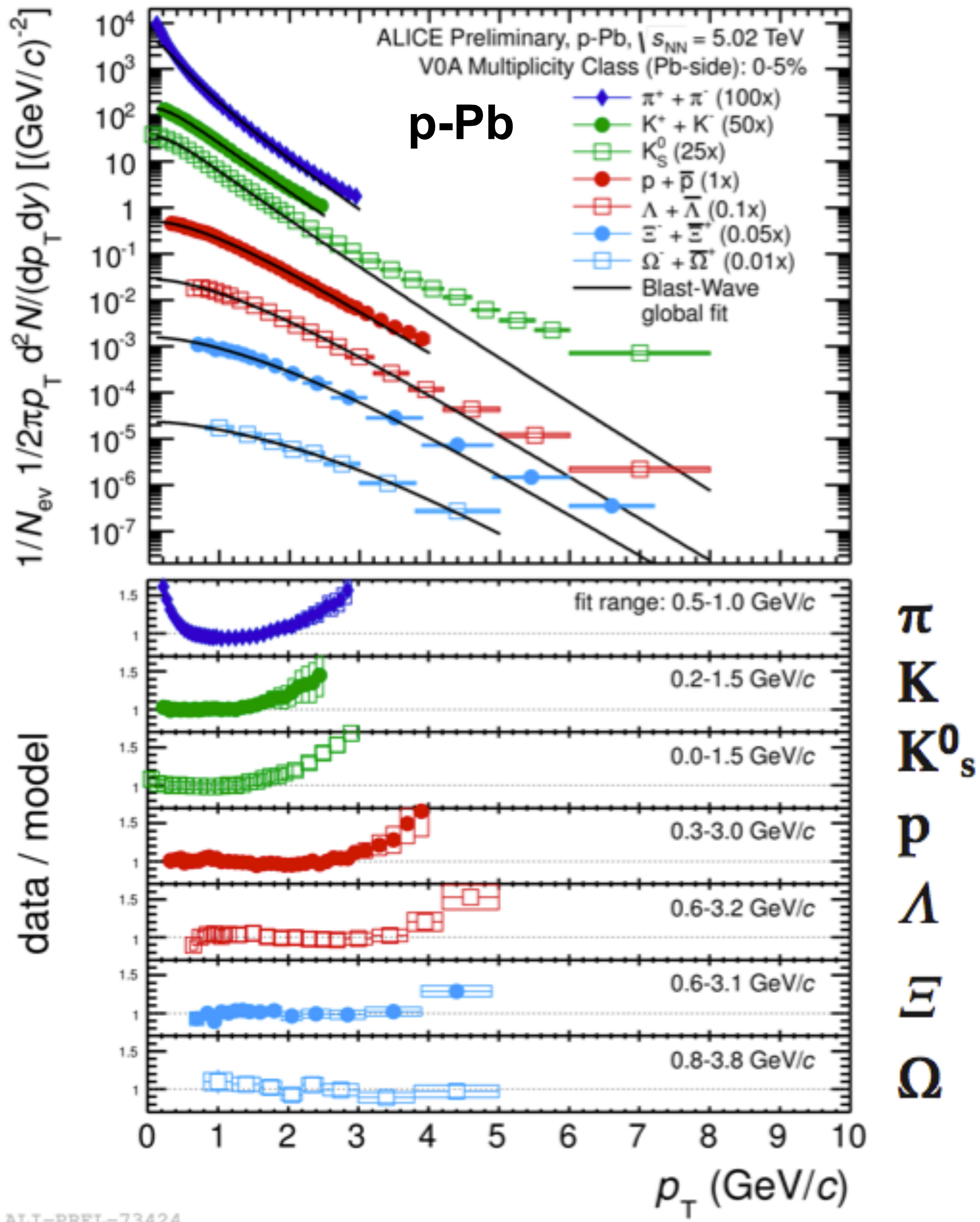

Hydrodynamic models (EPOS, Krakow) show a better agreement than QCD inspired models (DPMJET).

A combined blast-wave fit to the data gives a reasonable description also here.

Blast-wave fits to p-Pb data

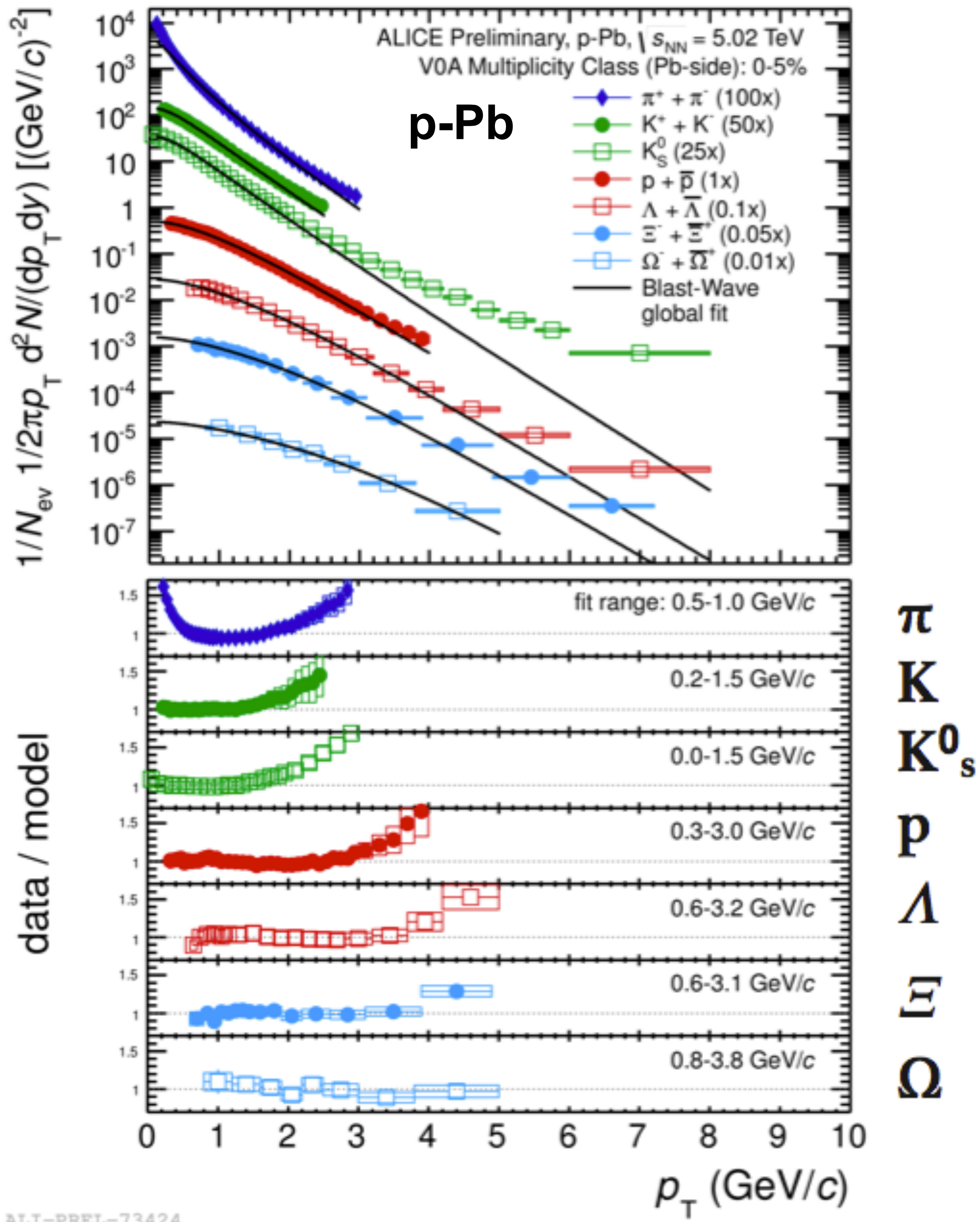

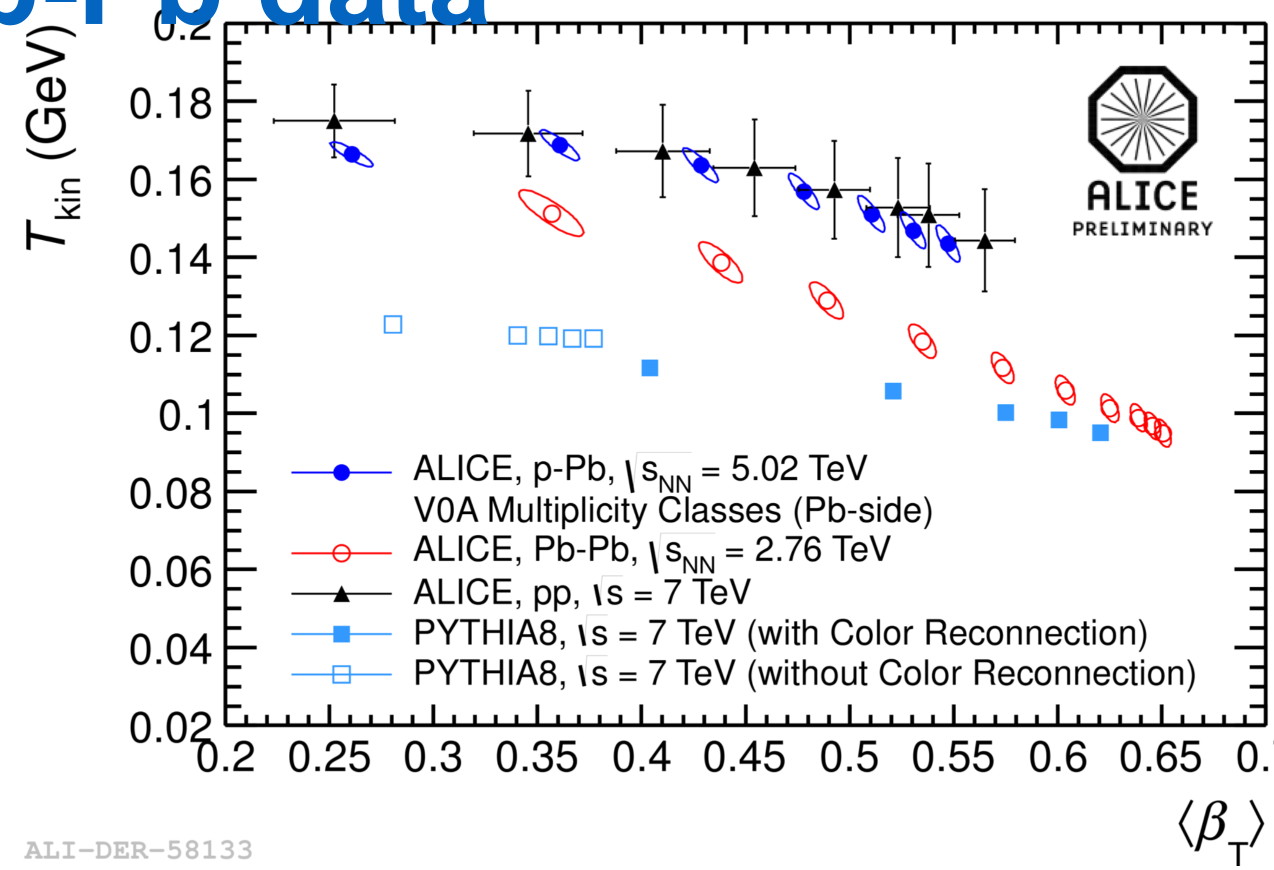

Hydrodynamic models (EPOS, Krakow) show a better agreement than QCD inspired models (DPMJET).

A combined blast-wave fit to the data gives a reasonable description also here.

Blast-wave fits to p-Pb data

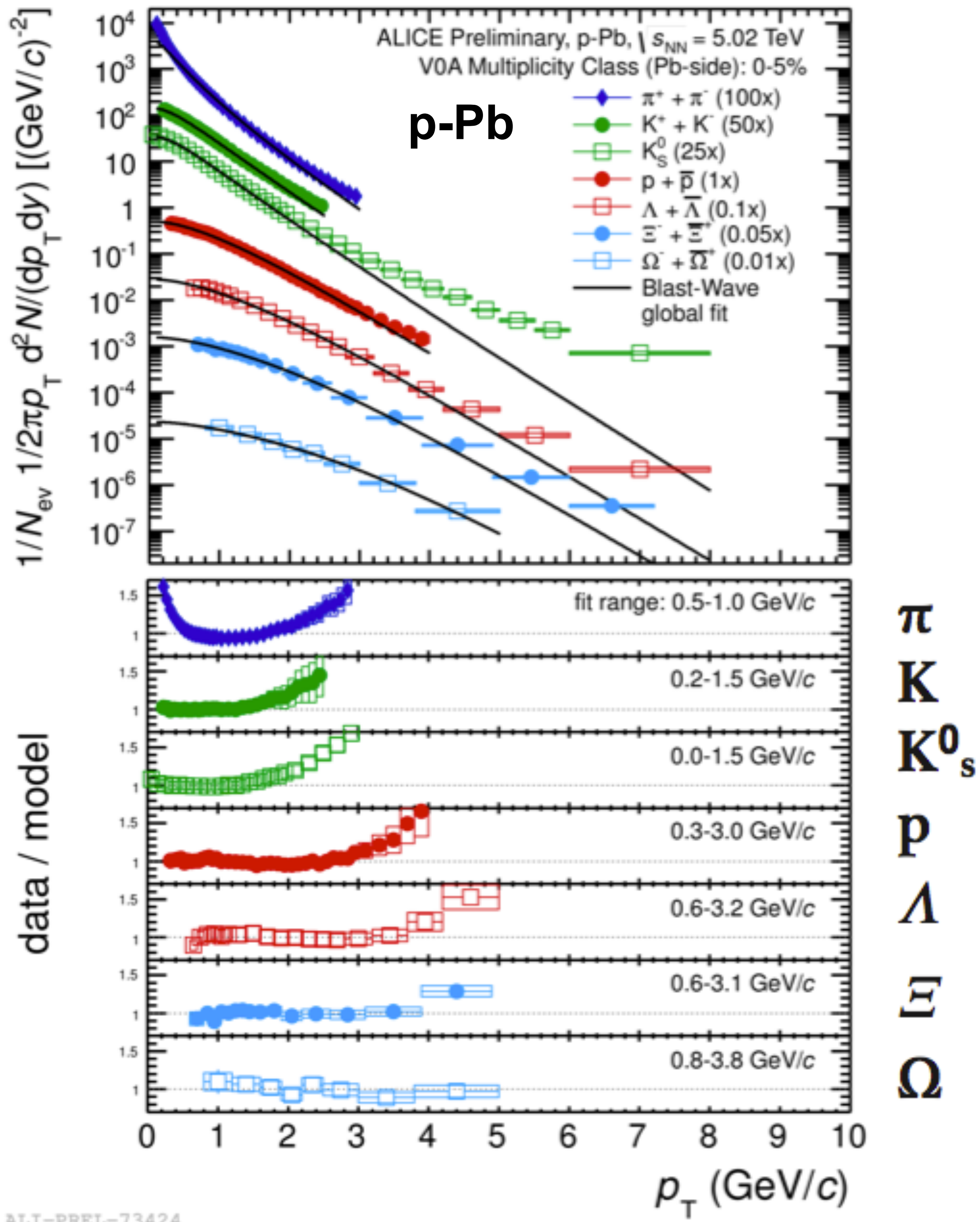

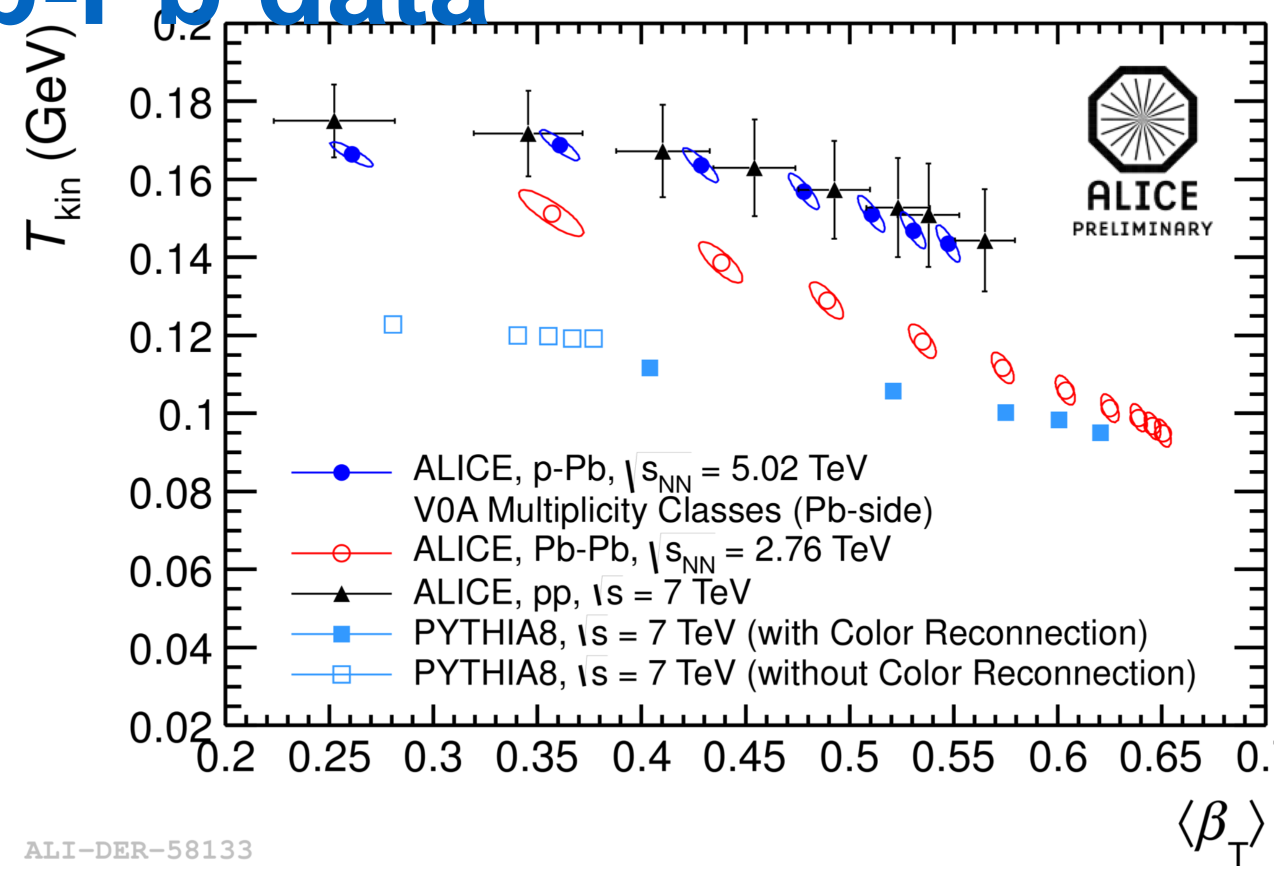

Hydrodynamic models (EPOS, Krakow) show a better agreement than QCD inspired models (DPMJET).

A combined blast-wave fit to the data gives a reasonable description also here.

p-Pb and Pb-Pb data follow the same trend → consistent with a collective expansion.

Blast-wave fits to p-Pb data

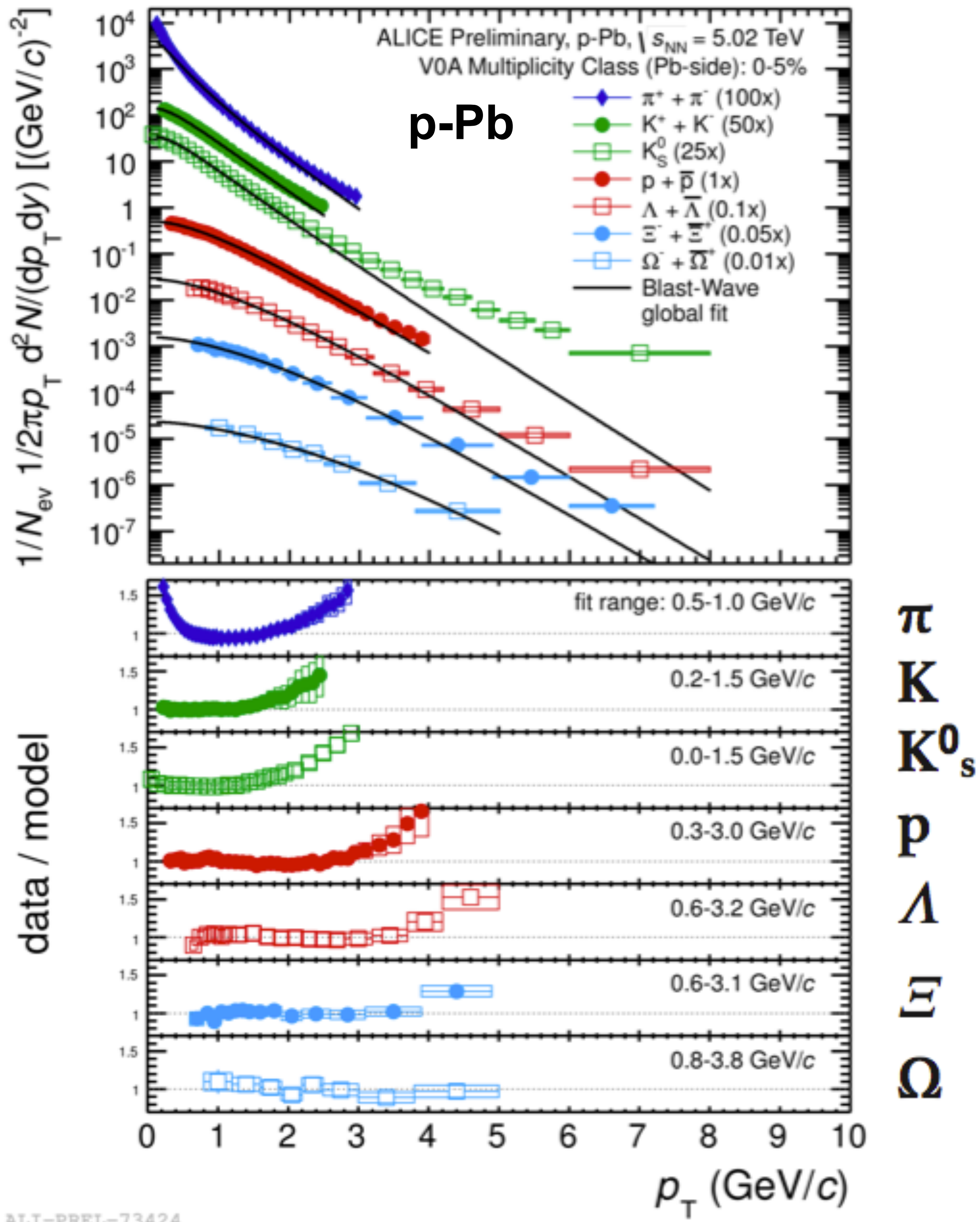

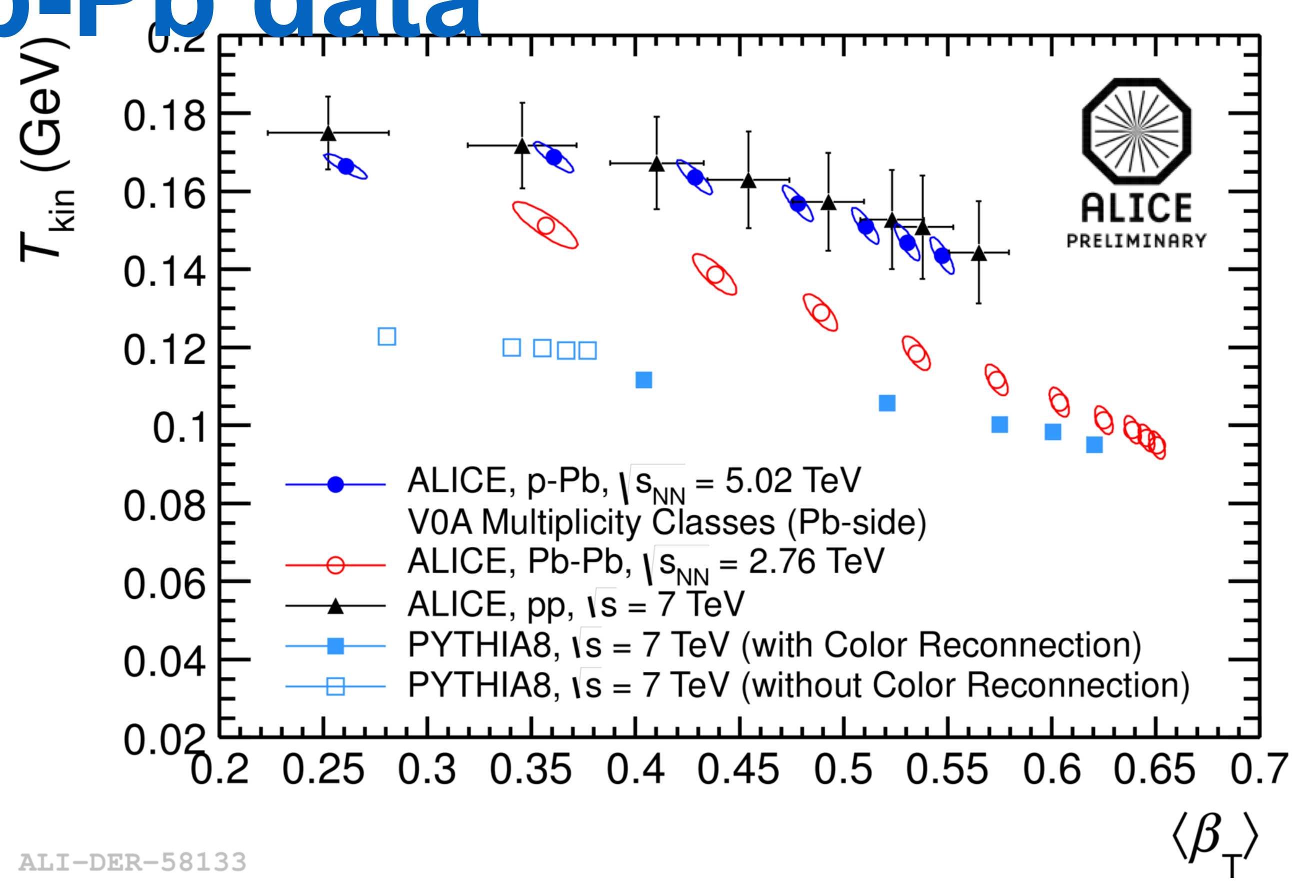

Hydrodynamic models (EPOS, Krakow) show a better agreement than QCD inspired models (DPMJET).

A combined blast-wave fit to the data gives a reasonable description also here.

p-Pb and Pb-Pb data follow the same trend → consistent with a collective expansion.

PYTHIA 8 with color reconnection shows a similar trend (without hydrodynamic flow).

Blast-wave fits to p-Pb data

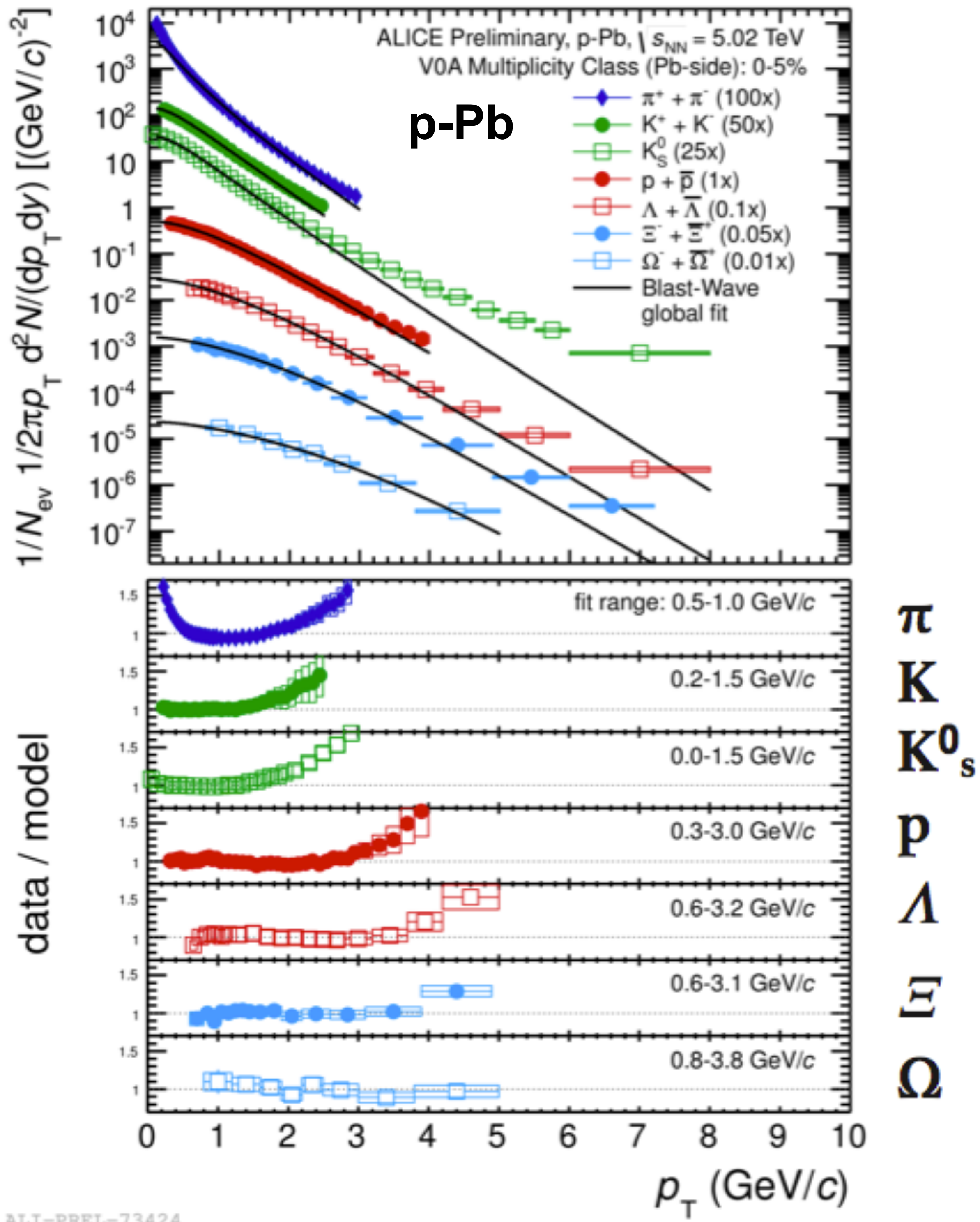

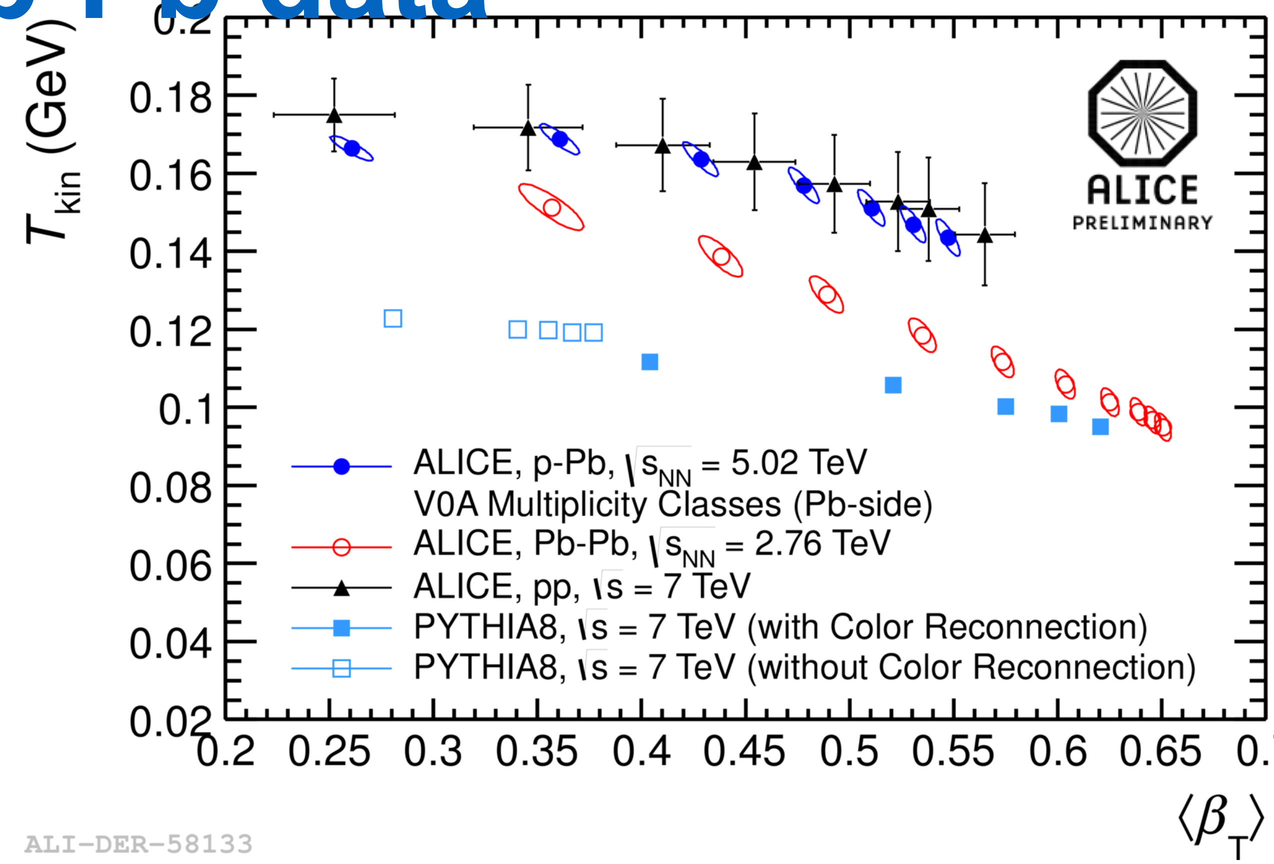

Hydrodynamic models (EPOS, Krakow) show a better agreement than QCD inspired models (DPMJET).

A combined blast-wave fit to the data gives a reasonable description also here.

p-Pb and Pb-Pb data follow the same trend → consistent with a collective expansion.

PYTHIA 8 with color reconnection shows a similar trend (without hydrodynamic flow).

Other effects can mimic flow-like patterns! And also pp data shows a similar trend..

Hyper-Triton

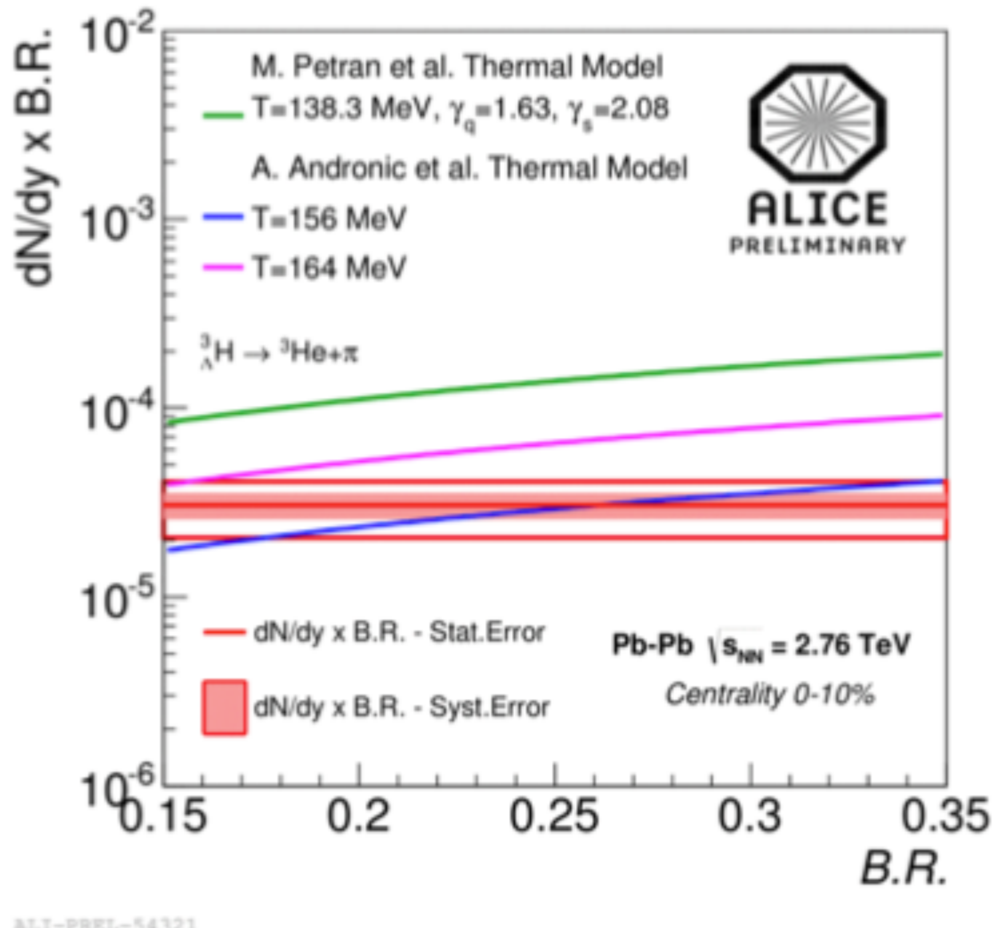

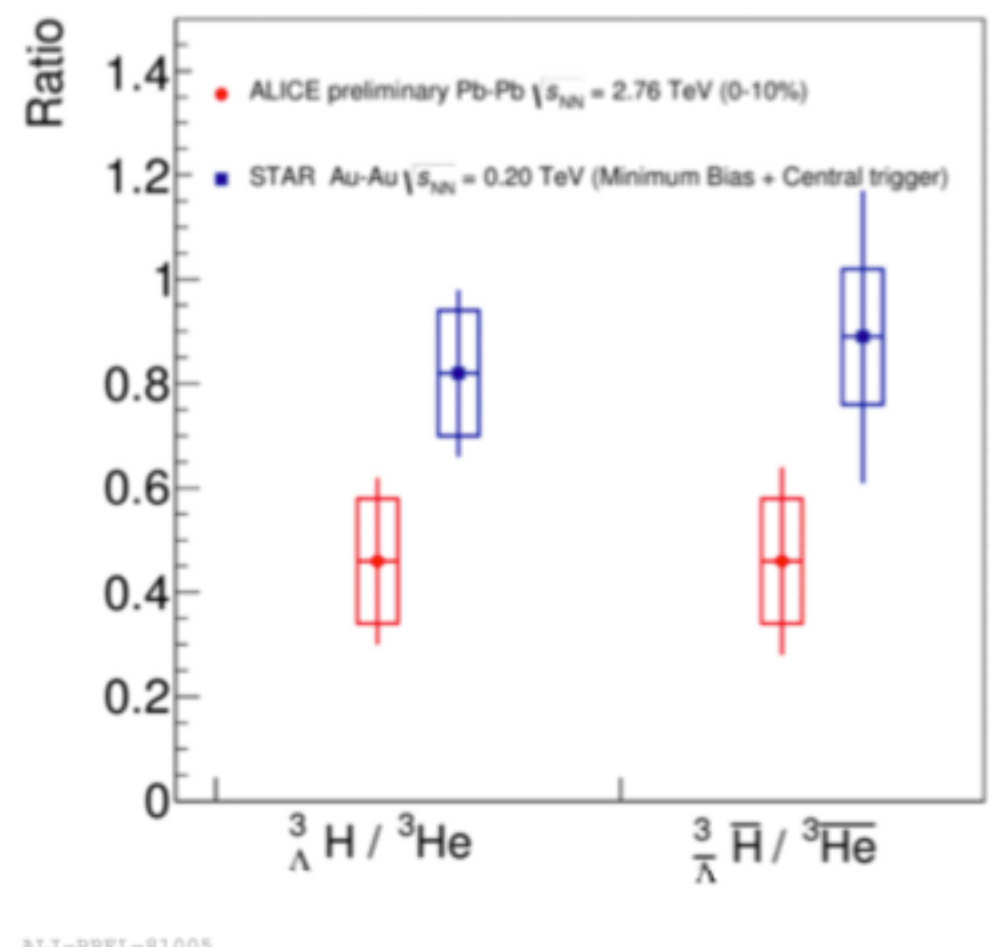

Hagedorn spectrum

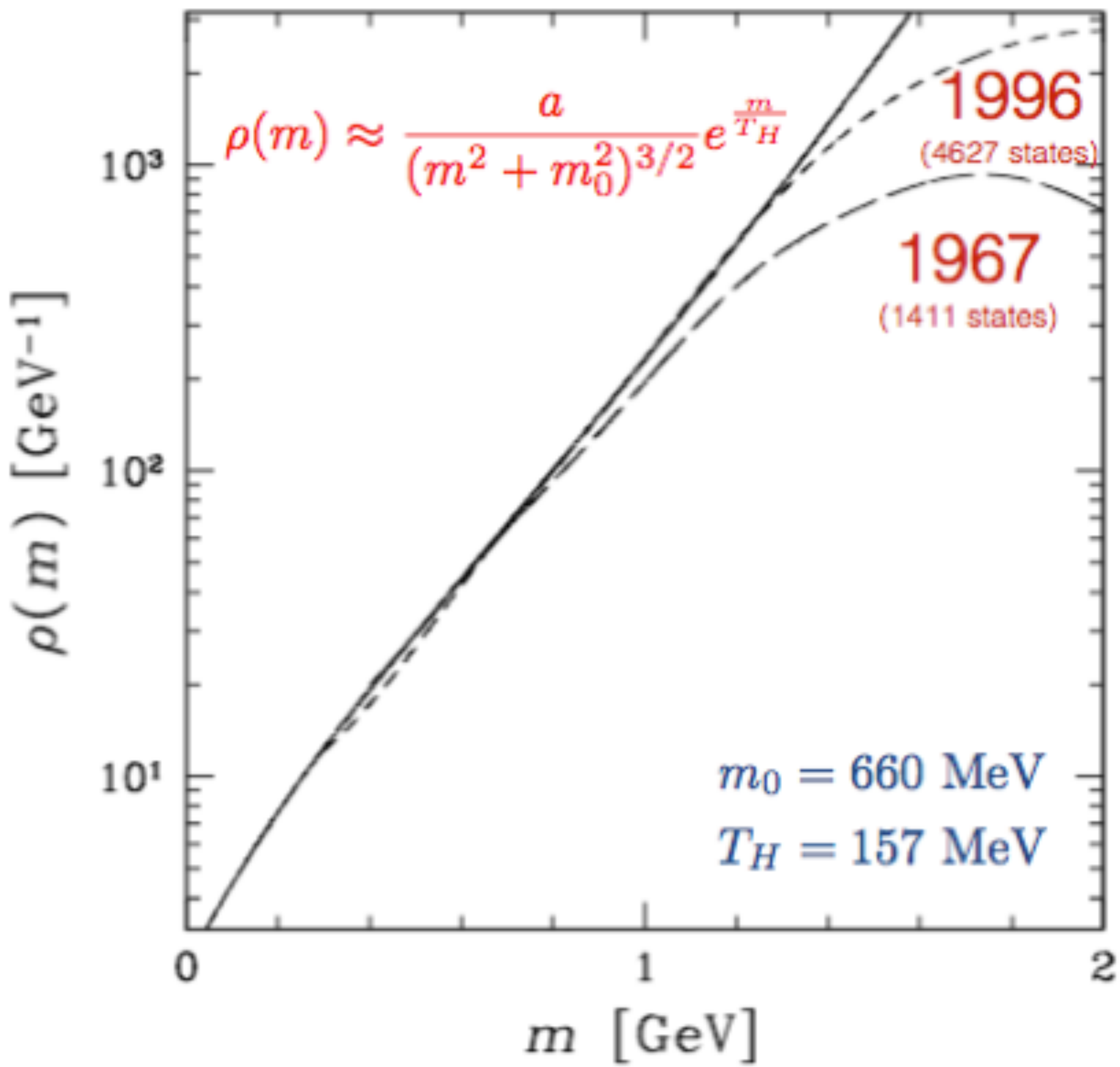

Protons

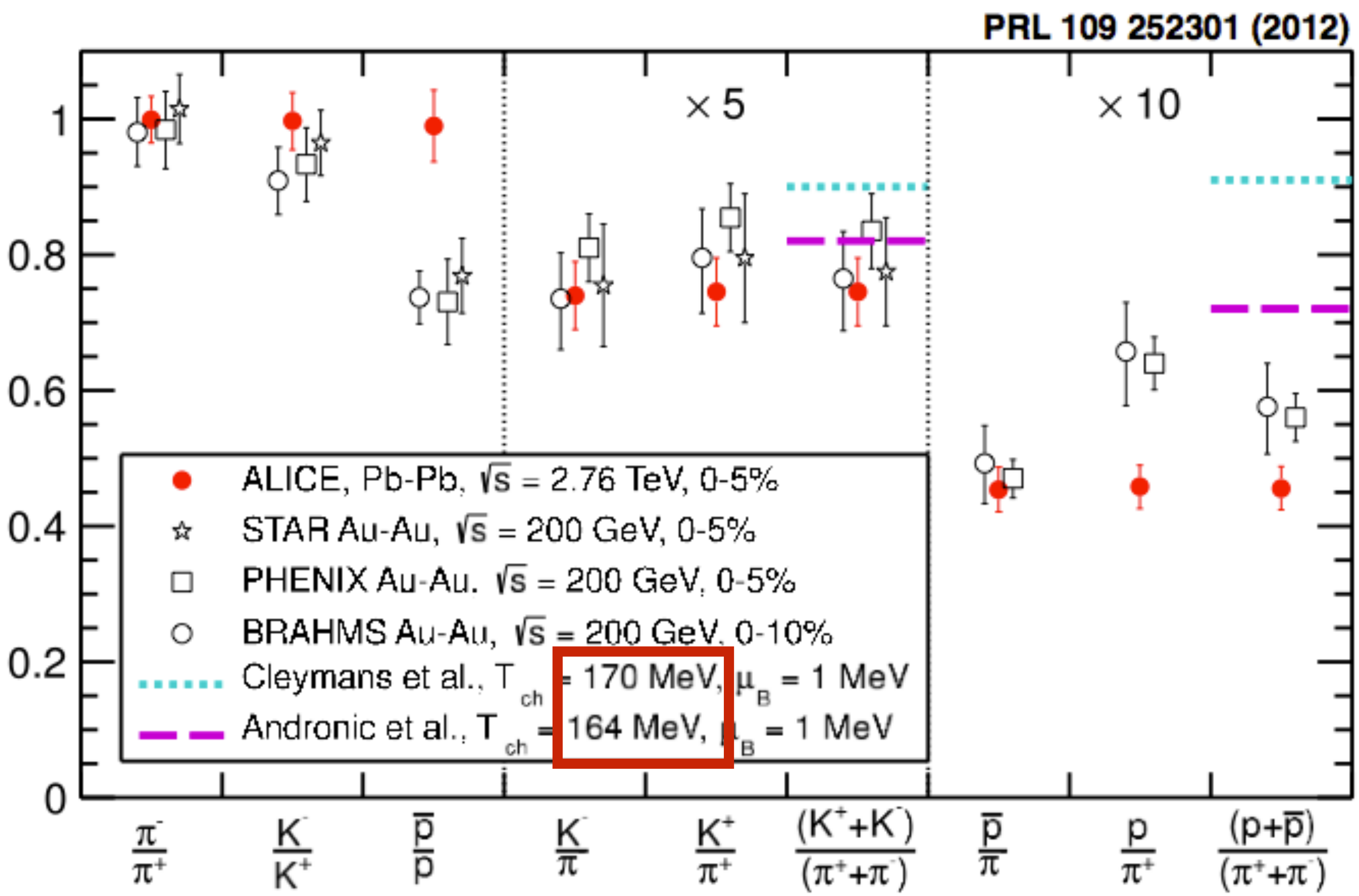

ALICE, QM11

p/π: 1.5 smaller than expectations

Thermodynamics and hadron chemistry

Short introduction to statistical thermodynamics (B)

- We therefore distinguish three different *statistical ensembles*:

(i) micro-canonical: *E*, *V*, *N* fix

Statistical model for e^+e^- collisions.

(ii) canonical: *T*, *V*, *N* fix
➔ given volume element is coupled to a heat bath

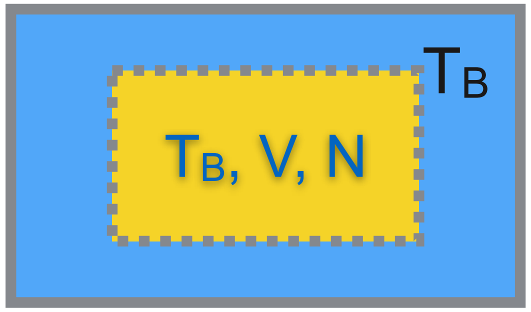

Strangeness conservation in peripheral HI collisions.

(iii) grand-canonical: *T*, *V*, *μ* fix
➔ given volume element can also exchange particles with its surrounding (heat bath and particle reservoir)

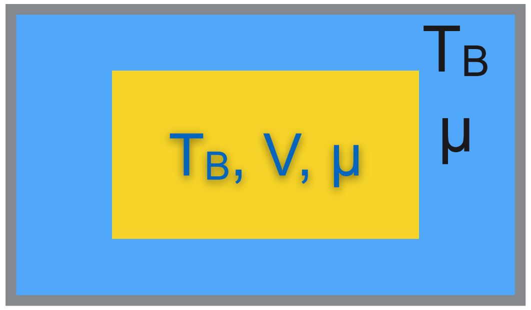

Central relativistic heavy-ion collisions.

Short introduction to statistical thermodynamics (C)

- A small example: barometric formula (density of the atmosphere at a fixed temperature).

- Probability to find a particle on a given energy level *j*:

$$P_j = \frac{e^{-\frac{E_j}{k_\mathrm{B}T}}}{Z}$$

Boltzmann factor

Partition function *Z*
(*Zustandssumme* = *“sum over states”*)

$$\frac{n(h_1)}{n(h_0)} = \frac{NP(h_1)}{NP(h_0)} = e^{-\frac{\Delta E_{pot}}{k_\mathrm{B}T}}$$

$$= e^{-\frac{Mg}{RT}\Delta h}$$

Thermal model for heavy-ion collisions (A)

- Starting point: grand-canonical partition function for an *relativistic ideal quantum gas of hadrons* of particle type i (i = pion, proton,… → full PDG!):

$$\ln Z_{GK_i} = \pm g_i \frac{V}{2\pi^2\hbar^3}\int_0^\infty dp\, p^2 \ln\left(1 \pm e^{-\beta(\epsilon(p)-\mu_i)}\right)$$

- Once the partition function is known, we can calculate all other thermodynamic quantities:

$$\boxed{n = \frac{1}{V}\frac{\partial(T\ln Z)}{\partial\mu}} \quad P = \frac{\partial(T\ln Z)}{\partial V} \quad s = \frac{1}{V}\frac{\partial(T\ln Z)}{\partial T}$$

Thermal model for heavy-ion collisions (A)

- Starting point: grand-canonical partition function for an *relativistic ideal quantum gas of hadrons* of particle type i (i = pion, proton,… → full PDG!):

$$\beta = \frac{1}{kT}$$

$$\ln Z_{GK_i} = \pm g_i \frac{V}{2\pi^2\hbar^3} \int_0^\infty dp\, p^2 \ln\left(1 \pm e^{-\beta(\epsilon(p)-\mu_i)}\right)$$

- Once the partition function is known, we can calculate all other thermodynamic quantities:

$$\boxed{n = \frac{1}{V}\frac{\partial(T\ln Z)}{\partial\mu}} \quad P = \frac{\partial(T\ln Z)}{\partial V} \quad s = \frac{1}{V}\frac{\partial(T\ln Z)}{\partial T}$$

Thermal model for heavy-ion collisions (A)

- Starting point: grand-canonical partition function for an *relativistic ideal quantum gas of hadrons* of particle type i (i = pion, proton,… → full PDG!):

(-) for bosons, (+) for fermions
(quantum gas)

$\beta = \frac{1}{kT}$

$$\ln Z_{GK_i} = \pm g_i \frac{V}{2\pi^2\hbar^3} \int_0^\infty dp\, p^2 \ln\left(1 \pm e^{-\beta(\epsilon(p)-\mu_i)}\right)$$

- Once the partition function is known, we can calculate all other thermodynamic quantities:

$$\boxed{n = \frac{1}{V}\frac{\partial(T\ln Z)}{\partial\mu}} \quad P = \frac{\partial(T\ln Z)}{\partial V} \quad s = \frac{1}{V}\frac{\partial(T\ln Z)}{\partial T}$$

Thermal model for heavy-ion collisions (A)

- Starting point: grand-canonical partition function for an *relativistic ideal quantum gas of hadrons* of particle type i (i = pion, proton,… → full PDG!):

(-) for bosons, (+) for fermions (quantum gas)

$\beta = \frac{1}{kT}$

$$\ln Z_{GK_i} = \pm g_i \frac{V}{2\pi^2\hbar^3} \int_0^\infty dp\, p^2 \ln\left(1 \pm e^{-\beta(\epsilon(p)-\mu_i)}\right)$$

spin degeneracy

- Once the partition function is known, we can calculate all other thermodynamic quantities:

$$\boxed{n = \frac{1}{V}\frac{\partial(T\ln Z)}{\partial\mu}} \quad P = \frac{\partial(T\ln Z)}{\partial V} \quad s = \frac{1}{V}\frac{\partial(T\ln Z)}{\partial T}$$

Thermal model for heavy-ion collisions (A)

- Starting point: grand-canonical partition function for an *relativistic ideal quantum gas of hadrons* of particle type i (i = pion, proton,… → full PDG!):

(-) for bosons, (+) for fermions (quantum gas)

$\beta = \frac{1}{kT}$

$E_i = \sqrt{p^2 + m_i^2}$ *dispersion relation (relativistic)*

$$\ln Z_{GK_i} = \pm g_i \frac{V}{2\pi^2\hbar^3} \int_0^\infty dp\, p^2 \ln\left(1 \pm e^{-\beta(\epsilon(p)-\mu_i)}\right)$$

spin degeneracy

- Once the partition function is known, we can calculate all other thermodynamic quantities:

$$\boxed{n = \frac{1}{V}\frac{\partial(T\ln Z)}{\partial\mu}} \quad P = \frac{\partial(T\ln Z)}{\partial V} \quad s = \frac{1}{V}\frac{\partial(T\ln Z)}{\partial T}$$

Thermal model for heavy-ion collisions (A)

- Starting point: grand-canonical partition function for an *relativistic ideal quantum gas of hadrons* of particle type i (i = pion, proton,… → full PDG!):

(-) for bosons, (+) for fermions (quantum gas)

$\beta = \frac{1}{kT}$

$E_i = \sqrt{p^2 + m_i^2}$ *dispersion relation (relativistic)*

$$\ln Z_{GK_i} = \pm g_i \frac{V}{2\pi^2\hbar^3} \int_0^\infty dp\, p^2 \ln\left(1 \pm e^{-\beta(\epsilon(p)-\mu_i)}\right)$$

spin degeneracy

$\mu_i = \mu_B B_i + \mu_S S_i + \mu_{I_3} I_{3_i} + \mu_C C_i$

chemical potential representing each conserved quantity

- Once the partition function is known, we can calculate all other thermodynamic quantities:

$$\boxed{n = \frac{1}{V}\frac{\partial(T\ln Z)}{\partial\mu}} \quad P = \frac{\partial(T\ln Z)}{\partial V} \quad s = \frac{1}{V}\frac{\partial(T\ln Z)}{\partial T}$$

Thermal model for heavy-ion collisions (A)

- Starting point: grand-canonical partition function for an *relativistic ideal quantum gas of hadrons* of particle type i (i = pion, proton,… → full PDG!):

(-) for bosons, (+) for fermions (quantum gas)

$\beta = \frac{1}{kT}$

$E_i = \sqrt{p^2 + m_i^2}$ *dispersion relation (relativistic)*

$$\ln Z_{GK_i} = \pm g_i \frac{V}{2\pi^2\hbar^3} \int_0^\infty dp\, p^2 \ln\left(1 \pm e^{-\beta(\epsilon(p)-\mu_i)}\right)$$

spin degeneracy

$\mu_i = \mu_B B_i + \mu_S S_i + \mu_{I_3} I_{3_i} + \mu_C C_i$

chemical potential representing each conserved quantity

- Once the partition function is known, we can calculate all other thermodynamic quantities:

$$\boxed{n = \frac{1}{V}\frac{\partial(T\ln Z)}{\partial\mu}} \quad P = \frac{\partial(T\ln Z)}{\partial V} \quad s = \frac{1}{V}\frac{\partial(T\ln Z)}{\partial T}$$

Only two free parameters are needed: **(T,μ_B)**. Volume cancels if particle ratios n_i/n_j are calculated. If yields are fitted, it acts as the third free parameter.

Thermal model for heavy-ion collisions (A)

- Starting point: grand-canonical partition function for an *relativistic ideal quantum gas of hadrons* of particle type i (i = pion, proton,… → full PDG!):

(-) for bosons, (+) for fermions (quantum gas)

$\beta = \frac{1}{kT}$

$E_i = \sqrt{p^2 + m_i^2}$ *dispersion relation (relativistic)*

$$\ln Z_{GK_i} = \pm g_i \frac{V}{2\pi^2\hbar^3} \int_0^\infty dp\, p^2 \ln\left(1 \pm e^{-\beta(\epsilon(p)-\mu_i)}\right)$$

spin degeneracy

$\mu_i = \mu_B B_i + \mu_S S_i + \mu_{I_3} I_{3_i} + \mu_C C_i$

chemical potential representing each conserved quantity

- Once the partition function is known, we can calculate all other thermodynamic quantities:

$$\boxed{n = \frac{1}{V}\frac{\partial(T\ln Z)}{\partial\mu}} \quad P = \frac{\partial(T\ln Z)}{\partial V} \quad s = \frac{1}{V}\frac{\partial(T\ln Z)}{\partial T}$$

Only two free parameters are needed: **(T,μ_B)**. Volume cancels if particle ratios n_i/n_j are calculated. If yields are fitted, it acts as the third free parameter.

Partition function shown here is only valid in the resonance gas limit (HRG), i.e. relevant interactions are mediated via resonances, and thus the non-interacting hadron resonance gas can be used as a good approximation for an interacting hadron gas.

Thermal model for heavy-ion collisions (B)

- We thus arrive at a set of formulas:

$$\begin{pmatrix} n_i \\ \varepsilon_i \\ s_i \\ P_i \end{pmatrix} = \frac{g_i}{2\pi^2} \begin{pmatrix} \int_0^\infty \frac{p^2 dp}{e^{(E_i(p)-\mu_i)/T} \pm 1} \\ \int_0^\infty \frac{p^2 dp}{e^{(E_i(p)-\mu_i)/T} \pm 1} E_i(p) \\ \pm \int_0^\infty dp\, p^2 \left(\ln\left(1 \pm e^{-(E_i(p)-\mu_i)/T}\right) \pm \frac{E_i(p)-\mu_i}{T(e^{(E_i(p)-\mu_i)/T} \pm 1)} \right) \\ \pm \int_0^\infty dp\, p^2 \ln\left(1 \pm e^{-(E_i(p)-\mu_i)/T}\right) \end{pmatrix}$$

$$\mu_i = \mu_B B_i + \mu_S S_i + \mu_{I_3} I_{3_i} + \mu_C C_i$$

$$E_i = \sqrt{p^2 + m_i^2}$$

Thermal model for heavy-ion collisions (C)

- Baryon number conservation: $$V \sum_i n_i B_i = Z + N$$
- Initial system has no charm or strangeness: $$\sum_i n_i(\mu_S) S_i = 0$$ $$\sum_i n_i(\mu_C) C_i = 0$$
- Third component of isospin: $$V \sum_i n_i(\mu_{I_3}) I_{3_i} = \frac{Z - N}{2}$$

Thermal model for heavy-ion collisions (C)

- Baryon number conservation: $$V \sum_i n_i B_i = Z + N$$
- Initial system has no charm or strangeness: $$\sum_i n_i(\mu_S) S_i = 0$$ $$\sum_i n_i(\mu_C) C_i = 0$$
- Third component of isospin: $$V \sum_i n_i(\mu_{I_3}) I_{3_i} = \frac{Z - N}{2}$$

Sum over all known states from the PDG!

Thermal model for heavy-ion collisions (C)

- Baryon number conservation: $$V \sum_i n_i B_i = Z + N$$
- Initial system has no charm or strangeness: $$\sum_i n_i(\mu_S) S_i = 0$$ $$\sum_i n_i(\mu_C) C_i = 0$$
- Third component of isospin: $$V \sum_i n_i(\mu_{I_3}) I_{3_i} = \frac{Z - N}{2}$$

Sum over all known states from the PDG!

Final results of a thermal model calculation depend on the used hadron list (resonance spectrum)!

Thermal fits and comparison to data

- Non-stable particles (resonances) are decayed and the result is compared to the experimentally accessible particles. The procedure is iterated for different sets of (T, μ_B, V) until the residuals between data and model are minimized.

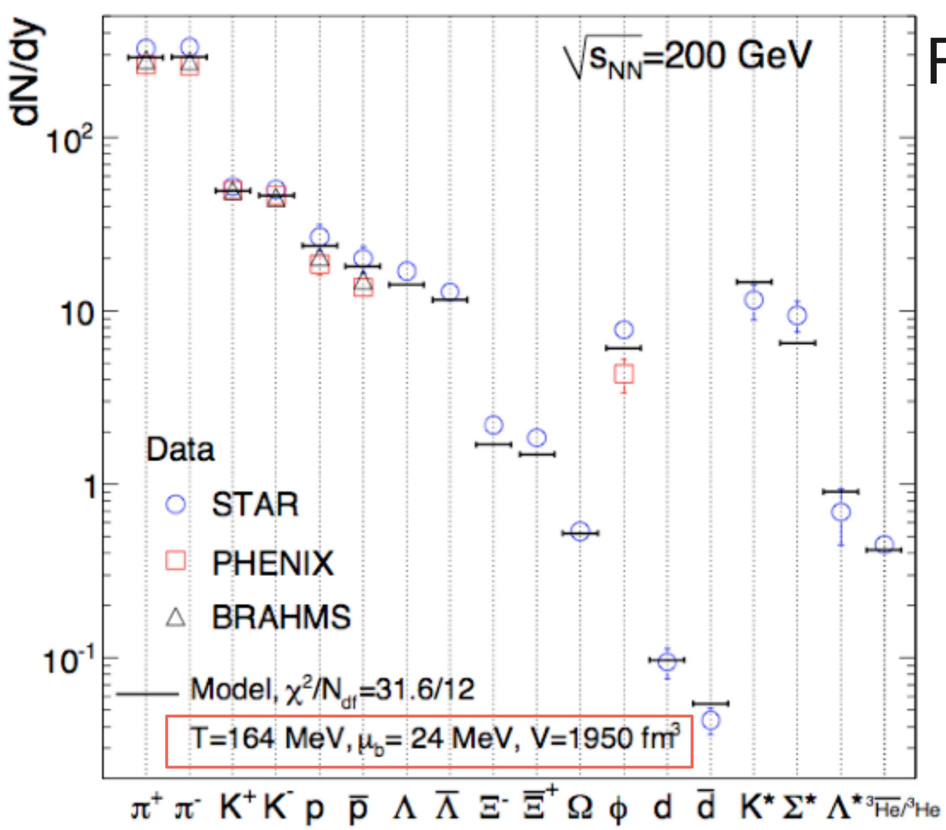

RHIC

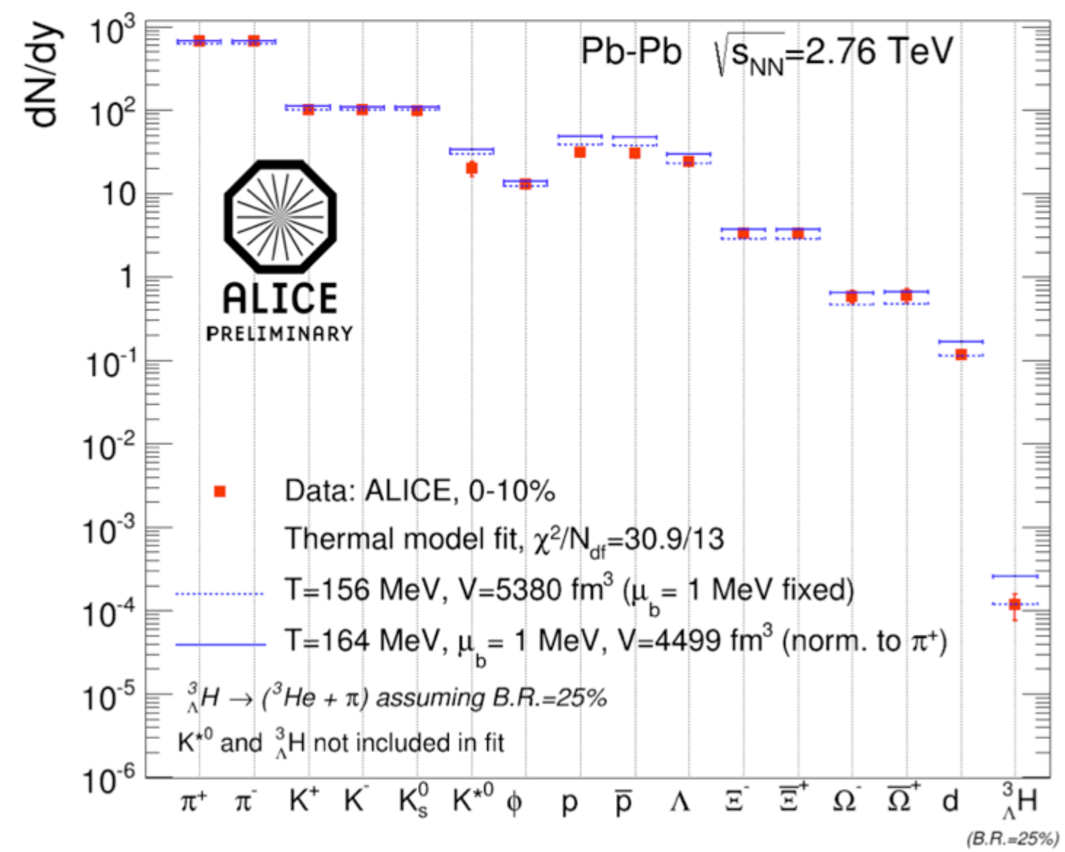

LHC

(1) A. Andronic et al., Phys.Lett.B673:142-145,2009

Thermal model from:
A.Andronic, P. Braun-Munzinger, J. Stachel, Nucl. Phys.A 772 (2006) 167

Implementations of statistical models

- Original ideas go back to Pomeranchuk (1950s) and Hagedorn (1970s).
- Precise implementations and also interpretations differ from group to group (no details in this lecture!):
  - K. Redlich
  - P. Braun-Munzinger, J. Stachel, A. Andronic (GSI)
    - Eigen-volume correction: ideal gas → Van-der-Waals gas
    - emphasis on complete hadron list
  - F. Becattini
    - non-equilibrium parameter γ_S^N
  - J. Rafelski (SHARE)
    - non-equilibrium parameter γ_S^N and γ_q^N
  - J. Cleymans (THERMUS)
    - Allows also canonical suppression in sub-volumes of the fireball
  - W. Broniowski, W. Florkowski (THERMINATOR)
    - space time evolution, p_T-spectra, HBT, fluctuations

Hypertriton branching ratio

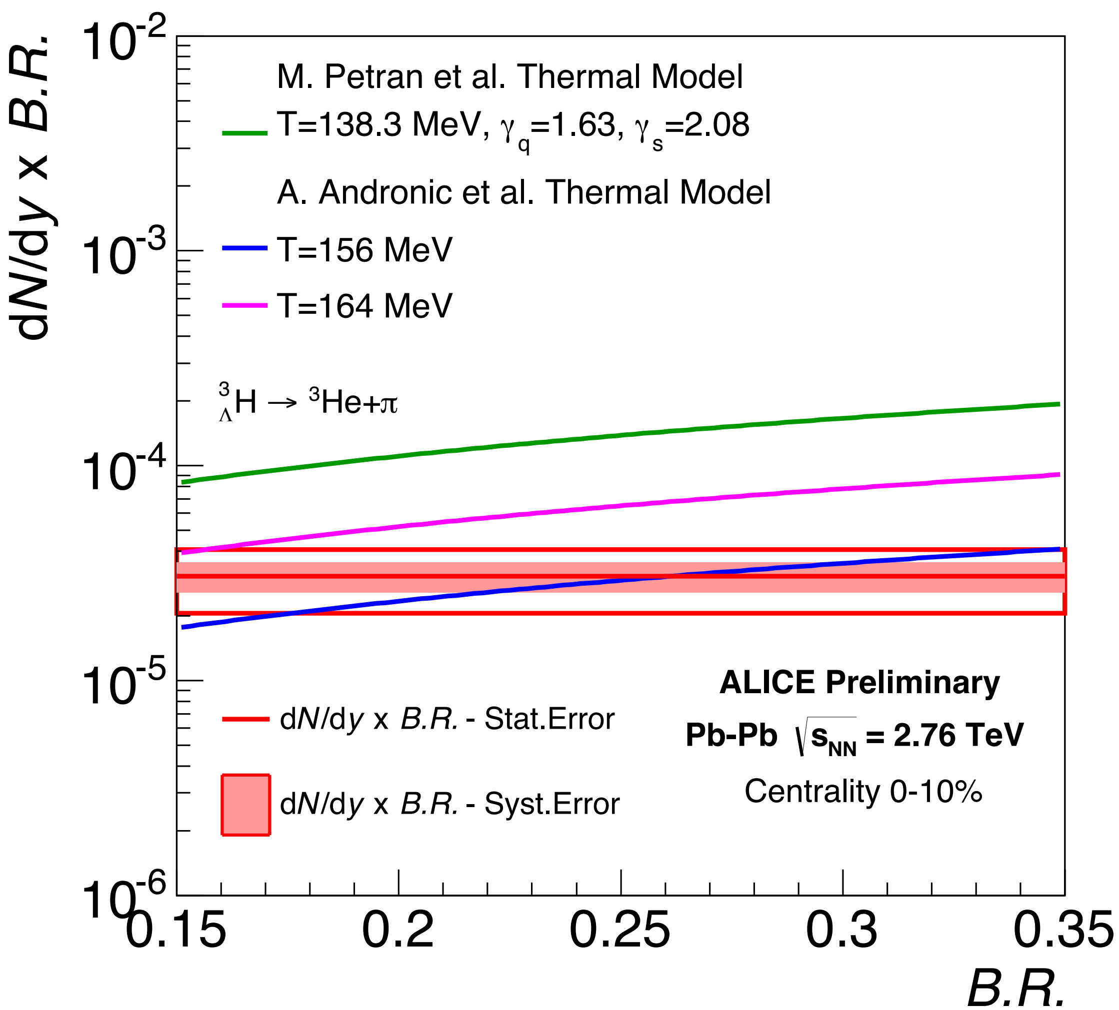

ALI-PREL-54321

PHYSICAL REVIEW D VOLUME 1, NUMBER 1 1 JANUARY 19

Properties of $_\Lambda H^3$†

G. Keyes
Argonne National Laboratory, Argonne, Illinois 60439 and Northwestern University, Evanston, Illinois 60201
AND
M. Derrick, T. Fields,* and L. G. Hyman
Argonne National Laboratory, Argonne, Illinois 60439
AND
J. G. Fetkovich, J. McKenzie, B. Riley, and I.-T. Wang
Carnegie-Mellon University, Pittsburgh, Pennsylvania 15213
(Received 29 September 1969)

The properties of the hypernucleus $_\Lambda H^3$ were measured in an analysis of helium-bubble-chamber pictures taken at the Argonne ZGS. Some 90 examples of the production reaction $K^- + He^4 \rightarrow {}_\Lambda H^3 + p + \pi^-$ were found in which the K^- stopped and the $_\Lambda H^3$ decayed via π^- emission. Twenty-seven events were observed to decay via the two-body mode $_\Lambda H^3 \rightarrow \pi^- He^3$, with the remaining events decaying to $\pi^- pd$ or $\pi^- ppn$. The production rate was measured to be $(1.8_{-0.6}^{+0.7}) \times 10^{-3}$ per stopping K^-. The mean life of the hyperfragment was measured from the two-body decay mode as $(2.64_{-0.52}^{+0.84}) \times 10^{-10}$ sec. The lifetime obtained from the three-body decays was consistent with this value, after the elimination of a serious source of background. The binding energy of $_\Lambda H^3$ was measured to be 0.25 ± 0.31 MeV. The decay ratio $R_3 = \Gamma({}_\Lambda H^3 \rightarrow \pi^- He^3)/\Gamma({}_\Lambda H^3 \rightarrow \text{all } \pi^-)$ was measured to be $0.36_{-0.06}^{+0.08}$, in agreement with values from previous experiments and with the value calculated for spin $\frac{1}{2}$ for the $_\Lambda H^3$ hypernucleus.

TABLE I. Partial and total mesonic and nonmesonic decay rates and corresponding lifetimes.

Channel	Γ [sec^{-1}]	Γ/Γ_Λ	$\tau=\Gamma^{-1}$ [sec]
$^3He + \pi^-$ and $^3H + \pi^0$	0.146×10^{10}	0.384	0.684×10^{-9}
$d+p+\pi^-$ and $d+n+\pi^0$	0.235×10^{10}	0.619	0.425×10^{-9}
$p+p+n+\pi^-$ and $p+n+n+\pi^0$	0.368×10^{8}	0.0097	0.271×10^{-7}
All mesonic channels	0.385×10^{10}	1.01	0.260×10^{-9}
$d+n$	0.67×10^{7}	0.0018	0.15×10^{-6}
$p+n+n$	0.57×10^{8}	0.015	0.18×10^{-7}
All nonmesonic channels	0.64×10^{8}	0.017	0.16×10^{-7}
All channels	0.391×10^{10}	1.03	2.56×10^{-10}
Expt. [6]			$2.64 +0.92 -0.54 \times 10^{-10}$
Expt. (averaged) [11]			$2.44 + 0.26 -0.22 \times 10^{-10}$

Phys. Rev. C **57**, 1595